EXPRESSION OF ENVELOPE PROTEINS BY PRE-S1/PRE-S2 DELETION MUTANTS OF HBV ISOLATED FROM SOUTHERN AFRICAN HIV-POSITIVE PATIENTS

Daniel Simelane

A Dissertation submitted to the Faculty of Health Sciences, University of the Witwatersrand, Johannesburg, in fulfilment of the requirements for the degree of Master of Science in Medicine

Johannesburg, 2018

DECLARATION

I, Daniel Simelane, declare that this dissertation is my own, unaided work. It is being submitted for the Degree of Master of Science in Medicine at the University of the Witwatersrand, Johannesburg. It has not been submitted before for any degree or examination at this or any other University.

_____

___20th___day of____September___2018

PRESENTATIONS

This work was orally presented in China-RSA Symposium on 'Hepatocellular Carcinoma related HBV mutation in people living with HIV/AIDS', held at the Guangxi Zhuang Autonomous region Centre for Disease Prevention and Control (8th – 12th May 2017).

Again presented in the *China-RSA joint research program* (Internal workshop) held at the Department of Internal Medicine, University of the Witwatersrand (3rd November 2015). As well as in the *Hepatitis in Africa: No room for complacency* (International Symposium), held at the Wits West Campus, University of the Witwatersrand (29th – 30th November 2016), both oral presentations.

ACKNOWLEDGEMENTS

I thank the most high God, for the gift of life, strength and the supportive family He chose for me.

To my family, every time I think of you, I get motivated to keep moving. All the support and guidance is appreciated. You are all one can ask for, in terms of a support structure.

My supervisor, teacher and a life coach, Professor A. Kramvis, I thank you for giving me the opportunity to be part of your research team. The knowledge of the Hepatitis virus shared and of life in general. Thanks for all the guidance and motivation.

Thanks to my co-supervisor, Dr Aurelie Deroubaix for the assistance and guidance with the Transfections, Immunofluorescence and patience on confocal microscopy lessons.

Ms Suzanne Wolhuter, your project gave birth to this project. I thank you for taking me through the stages of this project: Bacterial Transformations, DNA isolations, PCR, Transfections and more techniques. To every member of the HVDRU, you are an amazing team indeed. All you input and assistance is appreciated,

I would also like to acknowledge the National Research Foundation (NRF), Deutsche Forschungsgemeinschaft (DFG) and Poliomyelitis Research Foundation (PRF) for financial assistance received. Last but not least, I also would like to appreciate the permission to utilize the facilities of the University of the Witwatersrand and for the Merit Award funding I received for this project.

ABSTRACT

Hepatitis B Virus (HBV) pre-S deletion mutants of genotypes B and C have been shown to predispose to hepatocellular carcinoma (HCC). Studies have reported that envelope protein expression can be affected by the deletion mutants, leading to endoplasmic reticulum (ER) stress, apoptosis and hepatic injury. In South Africa, genotype A/subgenotype A1 prevails and it also has a relatively high hepatocarcinogenic potential compared to non-A genotypes. The aim of the study was to determine whether strains of HBV subgenotype A1, isolated from HIV-infected patients, affect envelope protein expression *in vitro.* The strains included pre-S deletion mutants (also frequently found in HCC patients) and the strain isolated from HBsAg negative HIV positive individual*.* Different 1.28 mer replication-competent constructs, generated previously, including two wild type subgenotype A1 strains from an HBsAg-positive infection (A12C15; A12C15 ALT9.3), a strain from an occult infection (SHH193A) and 3 different deletion mutants: SHH011A (with deletions in the pre-S1/pre-S2 regions), SHH045A and SHH167A (with deletions in the pre-S2 region) were used.

The plasmids were transfected into Huh7.5 cells and envelope protein expression followed by immunofluorescence using anti-HBs antibody and confocal microscopy on days 1, 3 and 5 post-transfection as well as quantification co-localization of the HBsAg using Zen software (Zeiss). Mean of fluorescence was quantified by Image J software.

All the constructs expressed HBsAg and the HBsAg was located mainly in the cytoplasm for 100% of the transfected cells with a diffuse staining for wild-type (A12C15_OL and A12C15 ALT 9.3) and the 3 deletion mutants (SHH011A, SHH045A & SHH167A). The strain from an occult infection (SHH193A) showed aggregates of HBsAg in the cytoplasm with more extensive accumulation at the perinuclear region of the cells, a finding that is suggestive of envelope protein retention in the cellular compartments,

which prevented secretion leading to the HBsAg-negative phenotype of the patient. In general, the deletion mutants (SHH011A, SHH045A & SHH167A), expressed envelope proteins at comparable amounts to that shown by the wild-type constructs (A12C15_OL and A12C15 ALT 9.3).

Although other groups have shown the expression of the envelope proteins by pre-S deletion mutants of different HBV genotypes, this study is the first to show the expression of the envelope proteins for subgenotype A1 constructs. Immunocytochemistry and high resolution confocal microscopy was successfully used to follow the expression of HBsAg in the secretory pathway. The accumulation of HBsAg in the perinuclear region following transfection with the strain from the occult infection could account for the HBsAg-negative phenotype seen in the patient.

TABLE OF CONTENTS

LIST OF ABBREVIATIONS

aa	amino acid
anti-HBe	anti-hepatitis B e antibodies
anti-HBs	anti-hepatitis B s antibodies
ART	anti-retroviral treatment/therapy
ASHV	Arctic Squirrel Hepatitis Virus
BCP	Basic core promoter
bp	base pairs
BQW	best-quality water
BSA	Bovine Serum Albumin
cccDNA	covalently closed circular DNA
CHB	chronic HBV in infection
DAPI	4’,6-Diamidino-2-Phenylindole, Dihydrocloride
DMEM	Dulbecco’s Modified Eagle’s Medium
DNA	Deoxyribonucleic acid
E.coli	*Escherichia coli*
ELISA	enzyme-linked immunosorbent assay
EnhI	Enhancer one
EnhII	Enhancer two
ER	endoplasmic reticulum
ERGIC	endoplasmic reticulum golgi intermediate compartment
FCS	Foetal Calf Serum
GFP	Green Fluorescent Protein
GGH	Ground Glass Hepatocytes
GSHV	Ground Squirrel hepatitis B virus
HBeAg	hepatitis B e antigen
HBsAg	hepatitis B surface antigen

HBV	hepatitis B virus
HBx	Hepatitis B X protein
HCC	hepatocellular carcinoma
HCV	hepatitis C virus
HIV	human immunodeficiency virus
Huh7.5	human hepatic cell line
IQR	Interquartile Range
kb	kilobase
LB	Luria-Bertini broth
LHBs	large hepatitis B surface protein
MHBs	middle hepatitis B surface protein
mRNA	messenger Ribonucleic acid
NTCP	sodium taurocholate cotransporting polypeptide
OBI	Occult hepatitis B virus infection
OCFL	Occult full-length
OD	Optical Density
ORF	Open reading frame
PBS	Phosphate Buffer Saline
PCR	polymerase chain reaction
pgRNA	pregenomic RNA
rcDNA	relaxed circular DNA
RFLP	Restriction Fragment Length Polymorphism
SHBs	small hepatitis B surface protein
WHV	Woodchuck hepatitis virus
WMHBV	Woolly Monkey Hepatitis B virus

CHAPTER 1: INTRODUCTION

1.1 A brief overview of the HBV History

The infectious nature of viral hepatitis disease was recognized as early as in the year 1885 during an icterus epidemic which occurred following a small pox vaccination campaign (Lürman, 1885). Hepatitis outbreaks, which occurred around the year 1942, were later confirmed to be a result of HBV through retrospective analysis (MacCallum, 1972, Seeff *et al*., 1987). In 1960s, Baruch Blumberg, who wanted to study genetic markers for susceptibility to certain illnesses, i.e. cancer, detected an antigen that was frequently found in haemophiliacs and leukaemia patients and not commonly found in the blood of healthy patients (Blumberg *et al*., 2000). The detected protein was named Australia antigen (Au) as it was isolated from an Australian aborigine (Blumberg *et al*., 2000). While the link between Au and hepatitis was unclear, Alfred Prince, reported the link between the two, identified the serum hepatitis (SH) antigen, also demonstrated that SH and Au were identical and that the antigen represented the HBsAg (Prince, 1968, Prince *et al*., 1970). These ground-breaking studies made possible the serologic diagnosis of hepatitis B and opened up the field to further investigations.

1.2 HBV Classification

The family *Hepadnaviridae* is divided into two genera namely: the *Orthohepadnavirus*, infecting mammals and the *Avihepadnavirus*, infecting birds. HBV is the prototype member of the mammalian hepadnaviruses. Other orthohepadnaviruses have been identified and based on the host animal were named as follows: Chimpanzee Hepatitis B Virus, infecting the Chimpanzee (*Pan troglodytes*) (Vaudin *et al*., 1988), Gibbon Hepatitis B Virus, infecting White handed gibbon (*Hylobates lar*) (NORDER *et al*., 1996), Gorilla Hepatitis B Virus, infecting Gorilla (*Gorilla gorilla*) (Grethe *et al*., 2000), Orangutan Hepatitis B Virus, infecting Orangutan (*Pongo*

pygmaeus Pygmaeus) (Warren *et al*., 1999), Woolly Monkey Hepatitis B virus (WMHBV) infecting the Woolley Monkey (*Lagothrix lagotricha*) (Lanford *et al*., 1998), Woodchuck Hepatitis Virus (WHV) infecting the Woodchuck (*Marmota monax*) (Summers *et al*., 1978), Arctic Squirrel Hepatitis Virus (ASHV) infecting the Arctic Squirrel (*Spermophylus parryi kennicotti*) (Testut *et al*., 1996) and the Ground Squirrel Hepatitis Virus (GSHV) infecting the Ground Squirrel (*Spermophilus beecheyi*) (Marion *et al*., 1980).

1.3 Epidemiology of the HBV: Globally, Africa and in the Southern Africa

HBV infection remains a serious global public health issue. An estimated 2 billion people worldwide have been infected with HBV (WHO, 2015) and above 350 million are chronic carriers of the HBV surface antigen (HBsAg) (Lavanchy, 2004, Yan *et al*., 2012). With underreporting and inefficient data collection in Africa, it is difficult to precisely quantify the burden of HBV infection in our continent. However, based on the available statistics, it can be estimated that about 65 million chronically infected people reside in Africa (Kramvis and Kew, 2007). An annual 1.5 million deaths are attributed to HBV-related diseases globally and about 250 000 of these are unfortunately occurring in Africa (Kramvis and Kew, 2007).

The HBV prevalence varies by geographical region and based on the prevalence of HBsAg carrier rates, the world can be divided into regions of high (>8%), intermediate (2-7%) and low (<2%) endemicity (Figure 1.1) (Hou *et al*., 2005). The virus is found to be hyperendemic in sub-Saharan Africa (>8%), except for Zambia, Kenya, Cote d'Ivoire, Liberia, Sierra Leone and Senegal, which are areas of intermediate endemicity (2–8%). The following northern African countries: Morocco, Algeria, Tunisia and Egypt are regarded low endemicity regions with the HBsAg prevalence as low as <2% (Kramvis and Kew, 2007).

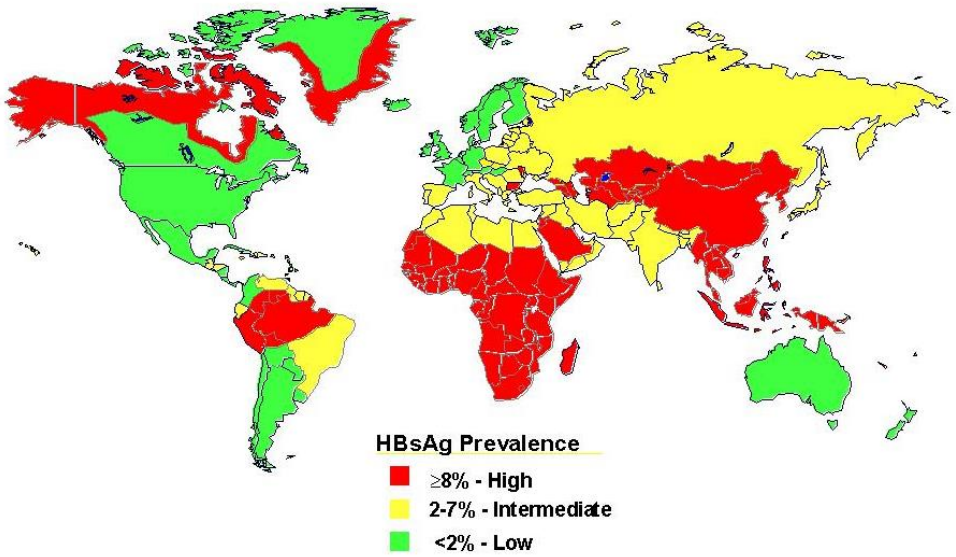

Figure 0.1: Geographical distribution of chronic HBV infection, in terms of the HBsAg prevalence (https://www.mrsa-today.com/blood-borne-pathogens/2/). (Accessed: December 2017)

1.4 HBV Transmission

Various modes of HBV transmission exist and include sexual, percutaneous, and perinatal transmission (Hou *et al*., 2005). The virus may also be transmitted through the use of inadequately sterilized syringes and needles; acupuncture; body piercing; tattooing; intravenous and percutaneous drug abuse; accidental inoculation of blood or fluid during medical, surgical and dental procedures, or from razors and similar objects contaminated with infected blood (Beasley *et al*., 1983). HBV is predominantly spread by percutaneous or mucosal exposure to infected blood and other body fluids like: saliva, seminal, vaginal, and menstrual fluids (Alter, 2003, Mast *et al*., 1999). Sexual transmission of HBV occurs in all parts of the world, it is however most common in unvaccinated homosexual men and heterosexual persons with multiple sex partners or those in contact with sex workers (Alter, 2003, Beasley *et al*., 1983). Perinatal transmission is regarded the major route of HBV transmission in many parts of the world, like South- East Asia and China where it has an important factor in maintaining the reservoir of the infection. There is high

risk of HBV transmission from viraemic mothers, who are seropositive for HBeAg to their infants at the time of, or shortly after birth (Beasley et al., 1983). The is a 90% risk of developing chronic infection, following perinatal infection (up to 6 months of age) about 20–60% between the ages of 6 months and 5 years (McMahon *et al*., 1985, Beasley *et al*., 1983). Horizontal transmission is another possible mode of HBV transmission, commonly occurring in Africa. It predominantly occurs in early childhood through child contact with either related or unrelated playmates as well as other family members (Hou *et al*., 2005, Kew, 1996).

1.5 Acute HBV infection

Acute HBV infection can either be asymptomatic or present with symptomatic acute hepatitis. Most HBV-infected adults recover, but between 5%–10% are unable to clear the virus and become chronically infected unfortunately (Liang, 2009). Acute HBV infection may be associated with highly variable clinical consequences and it has an incubation period that ranges between 6 weeks to 6 months, with the development of clinical manifestations that is highly age dependent. The risk of developing clinical hepatitis after acute infection with HBV is greater in adults than in children. Newborns generally do not show clinical symptoms, with about 5 to 15% of children aged 1 to 5 years tend to produce typical illness (McMahon *et al*., 1985). Symptomatic infections vary in severity from mild to fulminant forms. With an acute HBV infection, the following clinical signs and symptoms may be expected: nausea, malaise, anorexia, fever, vomiting, jaundice, clay coloured or pale stools, dark urine and abdominal pain. Extra-hepatic manifestations occasionally occur with the associated skin rashes, arthralgias, and arthritis and fulminant hepatitis occurs in about 1-2% of people with reported acute disease and has a case-fatality ratio of 63 to 93% (Mahoney, 1999).

1.6 Chronic HBV infection

Chronic HBV infection is defined by the persistence of HBsAg in the serum for more than 6 months. The risk of developing chronic infection differs with age and is highest for infants infected in the perinatal period (Hyams, 1995, Mahoney, 1999). The clinical consequences of chronic HBV infection include chronic carrier state, cirrhosis and hepatocellular carcinoma (HCC) (Lin *et al*., 2012, Chen *et al.*, 2006). The chronic HBV carriers are reported to have a >100-fold increase in relative risk of developing HCC compared to uninfected individuals and chronic infection is a major global cause of HCC (Hsieh *et al*., 2004). Studies have shown that up to 25% of those who acquire HBV infection as infants and young children develop either HCC or cirrhosis compared to 15% of adolescents and young adults who acquire chronic HBV infection (Hsieh *et al*., 1992, Hwang *et al*., 1991).

1.7 Hepatocellular carcinoma

HCC is a primary cancer of the hepatocytes and its development can be associated with the following major risk factors: liver cirrhosis, chronic infections with HBV or HCV, alcohol consumption, exposure to aflatoxin B1 and diabetes (El–Serag and Rudolph, 2007, Davis *et al.*, 2008). It can therefore be extrapolated that any cause of liver disease leading to cirrhosis should be considered a potential risk factor for HCC (Snowberger *et al*., 2007). In 2016, HCC was recorded as the second leading cause of cancer-related mortality, with about 745 000 deaths annually (White *et al*., 2016).

Subgenotypes C1, C2 are reported to be associated with an increased risk of cirrhosis and HCC in elderly patients. Contrastingly, subgenotype B2 also associated with an increased risk of HCC or HCC recurrence has mostly been seen in young and non-cirrhotic patients (Norder *et al*., 2004). Various mutations of different regions of the HBV genome have also been

found to be independently predisposing to HCC, as for examples mutations at the pre-S, EnhII, BCP, and pre-core (EnhII/ BCP/Pre-core) (Sung *et al*., 2008, Tanaka *et al*., 2006). Disturbingly, more than 80% of the HCC cases occur in either Eastern Asia or sub-Saharan Africa (El–Serag and Rudolph, 2007).

1.8 Occult hepatitis B virus infection (OBI)

OBI is regarded as one of the most challenging topics in the field of viral hepatitis and it was initially described in the late 1970s. The experts meeting on OBI, held in Taormina (Italy) on March 2008, has led to OBI defined as the presence of the HBV DNA in the liver of individuals testing HBsAg negative by current available assays and if HBV DNA is detectable in serum it is basically 200 IU/ml (Raimondo *et al*., 2008). A seropositive OBI exists when the patient is positive for anti-hepatitis B core (anti-HBc) and/or anti-HBs, while a seronegative OBI exist when the patient is negative for anti-HBc and anti-HBs (Raimondo *et al.*, 2008). Cases of false OBI occur when the serum HBV DNA levels are comparable to those usually detected in different phases of serologically evident HBV infection and are usually due to infection by HBV variants with mutations in the surface gene (escape mutants) producing a modified HBsAg that is not recognized by some or all commercially available detection assays (Torbenson and Thomas, 2002). Majority of the OBI cases are infected with replication competent HBV, with a strong suppression of overall replication activity and gene expression resulting in a significant reduced yield of HBV (Torbenson and Thomas, 2002, Raimondo *et al*., 2008). OBI has a potential risk for HBV transmission through haemodialysis, blood transfusion and organ transplant. It also has been reported that OBI can cause cryptogenic liver disease, acute exacerbation of chronic hepatitis B, or fulminant hepatitis and development of HCC (Hu, 2002). HBV DNA remains the only reliable diagnostic marker of OBI, it can however be recommended that if HBV DNA testing is not feasible, anti-HBc can be

used as a less than ideal surrogate marker for identifying potential seropositive OBI individuals (Raimondo *et al*., 2008).

1.9 HBV-HIV Co-infection: Epidemiology and Characteristics

HBV and HIV share common transmission routes, and a concurrent infection with these viruses usually leads to a more severe and progressive liver disease, a higher incidence of cirrhosis, HCC and mortality (Koziel and Peters, 2007). An estimated 5-15% of the HIV-infected persons worldwide are co-infected with HBV, with the South-East Asia and sub-Saharan Africa having the greatest burden of the co-infection (Alter, 2006) .

Following HBV infection, an HIV-infected individual is reported to have up to a six-fold risk of developing CHB than those who are HIV negative (Bodsworth *et al.*, 1991). Due to liver related diseases, HBV-HIV co-infected individuals have an increased mortality rate of up to 19-fold higher than in individuals infected with HBV only. Anti-HBs-positive individuals, who are HIV-infected, are most likely to lose the anti-HBs antibody and thus resulting in reactivation of the HBV infection (Thio, 2009). Among the negative consequences of HBV-HIV co-infection, is the fact that HIV decreases the rate of seroconversion of HBeAg to anti-HBe, and this increases HBV DNA replication (Colin *et al*., 1999).

1.10 HBV Biology and Viral structure

The Dane particle (HBV virion) is double-shelled particle of about 40 to 42 nm in diameter (Figure 1.2**A**), consists of an outer lipoprotein envelope and the inner nucleocapsid (Dane *et al.*, 1970). The envelope consists of the large (LHBs), middle (MHBs) and small (SHBs) surface proteins (Ganem, 1991, Heermann *et al*., 1984). The icosahedral nucleocapsid is made up of core proteins (HBcAg) and encloses a partially double

stranded relaxed circular DNA that is covalently linked to a polymerase enzyme (Summers *et al*., 1975). In addition to the virions, HBV-infected hepatocytes produce two subviral lipoprotein particles in large surplus as filamentous (Figure 1.2**B**) or round (Figure 1.2**C**) non-infectious particles of about 20 nm in diameter (Greenberg *et al*., 1976). These HBsAg particles contain only envelope glycoproteins and host-derived lipids, typically outnumber virions by 1000:1 to 10000:1 and in their purified form are used as a vaccine against HBV (Heermann *et al*., 1984).

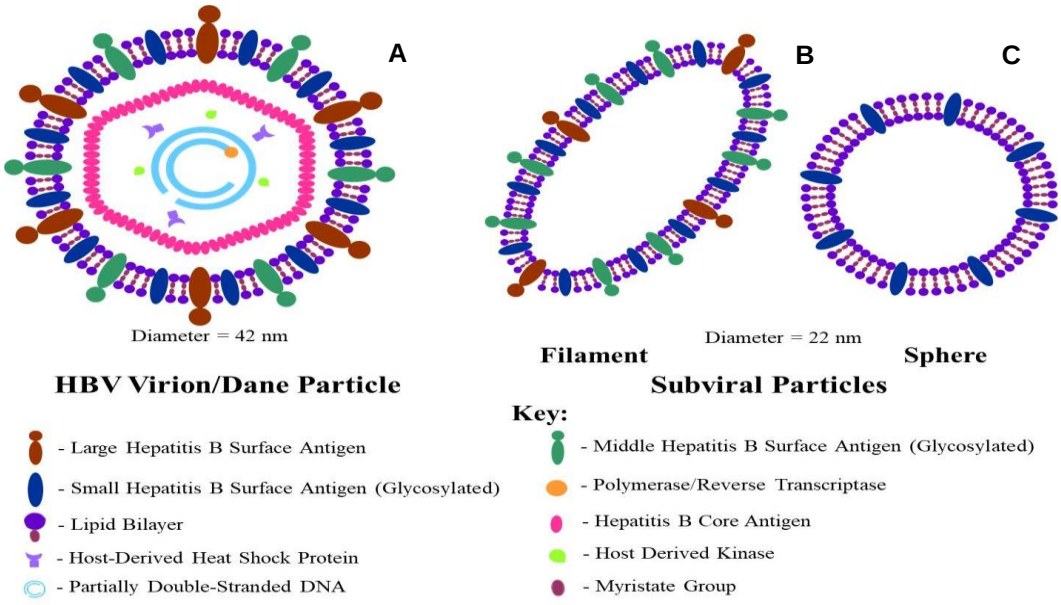

Figure 1.2: Schematic illustration of the HBV virion structure, and its subviral Particles (Bhoola *et al*., 2014). Reproduced with permission of Dr. N.H. Bhoola (PhD: University of the Witwatersrand).

1.11 HBV Genome Organisation

The HBV genome size is genotype dependent, varying from 3182 to 3248 nucleotides (nt) (Kramvis *et al.*, 2005) and it is the smallest known animal virus (Pollicino *et al.*, 2014). The HBV genome comprises a relaxed circular, partially double stranded DNA (rcDNA), with the genome structure maintained by base pairing between the 5' ends of both strands (Tiollais *et al*., 1985). The genome comprise a complete minus DNA strand (3.2 kb)

and an incomplete plus DNA strand that varies in length (~1.6-2.8 kb) (Ganem and Varmus, 1987). Attached to the 5' end of the minus strand DNA is the HBV polymerase (Seeger *et al*., 1986, Gerlich and Robinson, 1980) with the capped oligonucleotide covalently linked to the 5' end of the plus strand DNA. The 5' cap prevents phosphorylation of the plus strand (Figure 1.3) (Seeger *et al*., 1986, Gerlich and Robinson, 1980).

The genome is organized into four partially overlapping ORFs, namely the polymerase (P), X, core (C) and surface (S) (Pollicino *et al*., 2014, Utama *et al*., 2011). The above mentioned ORFs encodes the polymerase (P), X protein, structural protein of the viral nucleocapsid, HBcAg, and the non-structural secreted hepatitis B e antigen (HBeAg) and surface proteins (LHBs, MHBs &SHBs), respectively (Locarnini, 2004, Pollicino *et al*., 2014, Yeung *et al*., 2011). Four mRNA transcripts of different sizes, with known function have been identified as being involved in HBV transcription and translation (Figure 1.3). According to the reports by Mahoney et al, Su et al, Moolla et al and Cattaneo et al, the following transcripts can be listed:

(1) The 3.5 kb transcript, for genome replication and the expression pre-C/C and P proteins.
(2) The 0.7/0.8 kb X mRNA transcript translated to form the X protein.
(3) The 2.1 kb transcript encodes the pre-S and the HBsAg.
(4) The 2.4 kb transcript encodes pre-S1/S2 and HBsAg (Cattaneo *et al*., 1984, Mahoney, 1999, Moolla *et al*., 2002, Su *et al*., 1989).

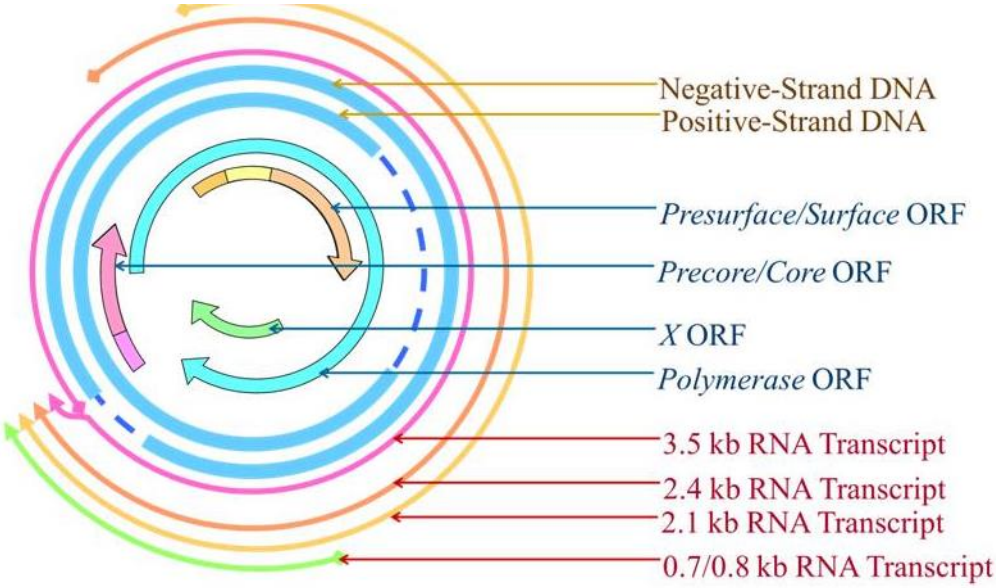

Figure 1.3: Schematic illustration of the structure, and genetic organization of the HBV genome.

The figure represents a partially double-stranded rcDNA HBV genome. The dashed line in blue represents where the HBV genome is repaired to form the cccDNA. The four arrows within the HBV genome represent the four ORFs while the four arrows on the outside of the HBV genome represent the four RNA species (Bhoola *et al.*, 2014). Reproduced with permission of Dr. N.H. Bhoola (PhD: University of the Witwatersrand).

1.12 HBV Life Cycle

The receptor responsible for the attachment of the viral particle to the cell remained a mystery until recently when it was identified as the Sodium taurocholate cotransporting polypeptide (NTCP) (Yan *et al*., 2012). The attachment of the HBV to the hepatocytes has been characterized by a reversible, low affinity bond and the virus particle is transferred to the NTCP. After membrane fusion, the capsid is released into the cytosol and actively transported to the nucleus (Tuttleman *et al.*, 1986). At the nuclear pore complex, the capsid is dissociated and the viral genome is released into the nucleus (Tuttleman *et al*., 1986, Beck and Nassal, 2007). The partially double stranded rcDNA genome is converted to covalently closed circular DNA (cccDNA) by cellular repair factors (Tuttleman *et al*., 1986). The cccDNA serves as the transcriptional template for host RNA polymerase II enzyme which generates a series of pre-genomic RNA

(pgRNA) and sub-genomic mRNAs (Will *et al*., 1987). The pgRNA has two major roles in viral life cycle: as both the translation and reverse transcription template. Generated viral RNAs are translocated into the cytoplasm, followed by a translation step to yield the viral envelope, core, polymerase proteins, pre-C and the X polypeptides occurring in the ER. The nucleocapsids are assembled within the cytoplasm, and then a genomic RNA is incorporated into the assembling viral core and followed by reverse transcription (Seeger and Mason, 2000, Pollack and Ganem, 1994). Sequentially, the reverse transcriptase will mediate the synthesis of the two viral DNA strands, with the minus DNA strand made from the encapsidated RNA template. During or after the synthesis of the first strand, the RNA template is degraded and the synthesis of the plus DNA strand proceeds, with the newly synthesized minus DNA strand used as a template (Wang and Seeger, 1993, Will *et al*., 1987). The mature nucleocapsid containing the newly synthesised rcDNA can either be re-directed into the nucleus to build up a cccDNA pool within the nucleus (Tuttleman *et al*., 1986, Zhang *et al.*, 2003), or they can interact with the envelope proteins in the ER, forming a mature infectious virion which is secreted and further infect other cells and thus all the above steps mark a complete HBV life cycle (Figure 1.4) (Lambert *et al*., 2007, Watanabe *et al*., 2007).

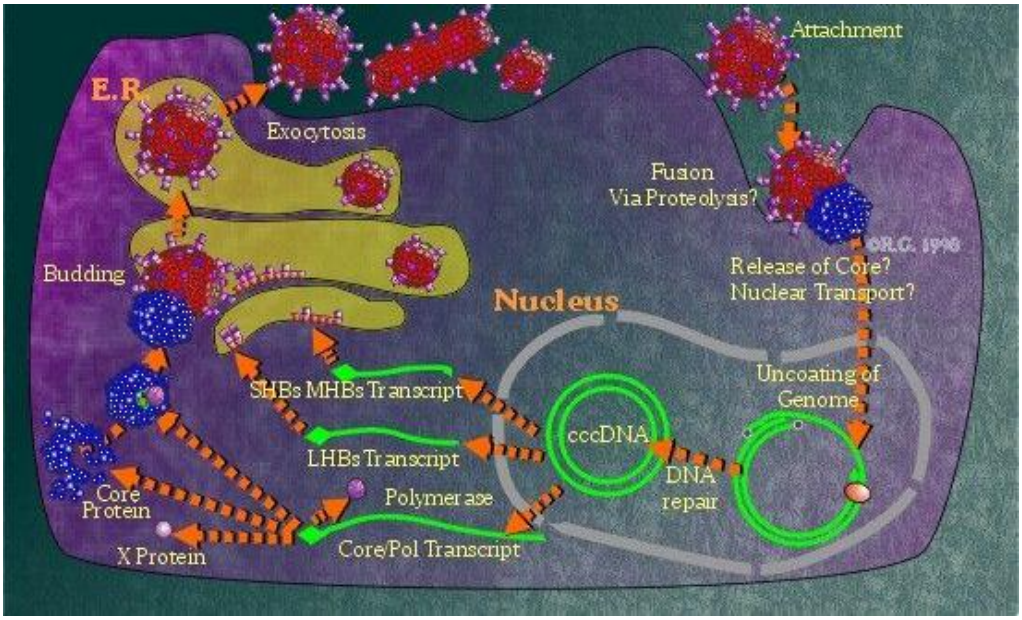

Figure 1.4: HBV life cycle
https://web.stanford.edu/group/virus/1999/tchang/replication.jpg (Accessed: March 2018).

As mentioned in the HBV life cycle, the translation steps yield a number of viral gene products namely: viral polymerase, HBx protein, core proteins (HBeAg and HBcAg) and the surface proteins: large hepatitis B surface antigen (LHBs), medium hepatitis B surface antigen (MHBs) and small hepatitis B surface antigen (SHBs). In the present study, we investigated deletion mutants in the S open reading frame (ORF).

1.13 Envelope proteins

The S ORF can be divided into three coding regions, the pre-S1, pre-S2 and the S regions (Seeger and Mason, 2000, Pollack and Ganem, 1994). The S ORF has three *in-frame* initiation codons, where the LHBs is translated from the first initiation codon, the MHBs and SHBs translated from the subsequent initiation codons, respectively (Xu *et al*., 1997). The 2.4 kb pre-S1 mRNA transcript encodes for the LHBs and the shorter 2.1 kb pre-S2 transcript for both the MHBs and HBsAg (Seeger and Mason, 2000). SHBs is the major surface protein that is 226 amino acid (aa) long and it is produced in excess amongst the three surface proteins. It is the

major constituent of both the HBV virion and sub-viral particles. HBV has a common immunodominant and immunoprotective determinant, the 'a' determinant, located between 124 - 147 aa of the SHBs (Chen *et al*., 1996). The MHBs is 281 aa long, it consists of the SHBs with the additional 55 aa upstream encoded by the pre-S2 region. The pre-S2 domain is assumed to play a role in virus-host hepatocyte attachment as a secondary mechanism (Bruss, 2007). LHBs is the largest of the three surface proteins, about 389 or 400 aa long and it contains the pre-S1, pre-S2 and S domains (figure 1.5). Synthesis of the surface protein occurs in the ER, an overexpression of the this protein, leads to its retention in the ER, which can result in ER stress and prevent maturation of the virus (Xu *et al*., 1997). It can also be noted that the surface proteins exist in two forms, the glycosylated and unglycosylated form and are covalently linked to the other viral proteins by disulphide bridges formed by cysteine residues (Seeger and Mason, 2000). Its pre-S1 domain becomes myristylated at the N-terminus in order to anchor the N-terminus to the membrane, a step that is essential for infectivity (Chouteau *et al*., 2001).

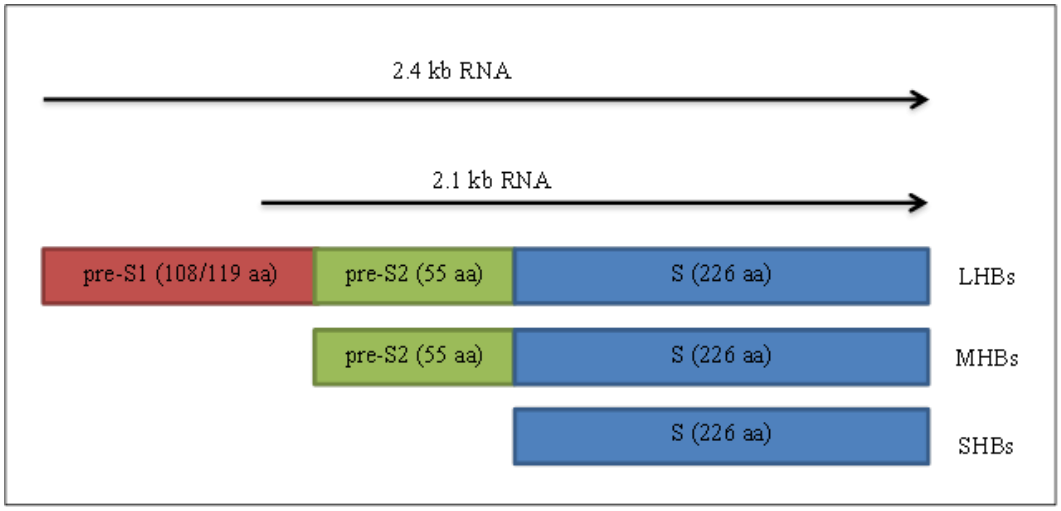

Figure 1.5: The three domains of the complete surface gene. The 2.4 kb mRNA translates into the LHBs, while the shorter 2.1 kb mRNA is used for the translation of both the MHBs and SHBs proteins.

1.14 HBV Genotypes and Subgenotypes

The term genotype can generally be referred to as a genetic constitution of an organism or cell (Pownall, 1999). However, with regard to viruses, it applies to the form into which the genomic sequence has stabilized after a prolonged period of time (François *et al*., 2001). HBV genotypes have been classified into nine genotypes: A to D (Norder *et al*., 1994, Okamoto *et al*., 1988); E to F (Naumann *et al*., 1993, Norder *et al*., 1994, Norder *et al*., 1992); G (Stuyver *et al*., 2000), H (Arauz-Ruiz *et al*., 2002); and I (Huy *et al.*, 2008, Olinger *et al*., 2008). The classification was based on an intergroup divergence of more than 8 % in the complete genome sequence of the HBV (Kramvis *et al*., 2008, Norder *et al*., 1994, Stuyver *et al*., 2000) and more than 4 % divergence at the S gene level (Kramvis *et al*., 2005, Norder *et al*., 1992). Recently a tenth genotype J was proposed based on an isolate from one individual (Tatematsu *et al*., 2009).

HBV genotypes have a distinct geographic distribution (Figure 1.6) (Kramvis, 2014, Kramvis *et al*., 2005, Norder *et al*., 2004, Norder *et al*., 1993). Genotype A is mainly found in North-western Europe, North America, and Africa (Bowyer *et al*., 1997, Norder *et al*., 1993). Genotype B and C are predominantly found in the Asian and Oceania populations (Arankalle *et al*., 2010, Lindh *et al*., 1997, Okamoto *et al.*, 1988). Genotype D has a worldwide distribution, however predominates in the Mediterranean area with genotype E mainly found in West Africa and Madagascar (Arauz-Ruiz *et al*., 1997, Kramvis *et al*., 2005, Norder *et al*., 1993). Genotype F has been reported the most divergent amongst the HBV genotypes and prevail in the aboriginal populations of the South America (Arauz-Ruiz *et al*., 1997, Norder *et al*., 1993). Genotype G predominates in Europe and USA (Arauz-Ruiz *et al*., 1997, Stuyver *et al*., 2000), while genotype H is mostly found in the Amerindian populations of Central America (Kramvis *et al*., 2005). Genotype I is reported to be mainly found in Laos, Vietnam, South East Asia and India (Arankalle *et al*., 2010, Hannoun *et al*., 2000, Huy *et al*., 2008, Olinger *et al*., 2008, Yu *et al*.,

2010). Lastly, genotype J was isolated from a Japanese man with HCC (Tatematsu *et al*., 2009). Genotypes A, D, and E predominates the African continent, Genotype A is the most common genotype in the central, eastern and the southern part of the continent. Genotype D dominates the northern part, while genotype E is predominantly found in the western and central parts of the continent (Kramvis and Kew, 2007). Genotypes are further divided into subgenotypes as follows: A (A1-A6), B (B1-B9), C (C1-C16), D (D1-D6), F (F1-F4) and I (I1-I2) (Kramvis, 2013, Okamoto *et al*., 1988). There is increasing evidence that the heterogeneity in the global distribution of the HBV genotypes may be responsible for differences in the clinical outcomes of HBV infections and the response to antiviral treatment and vaccination (Kramvis and Kew, 2005).

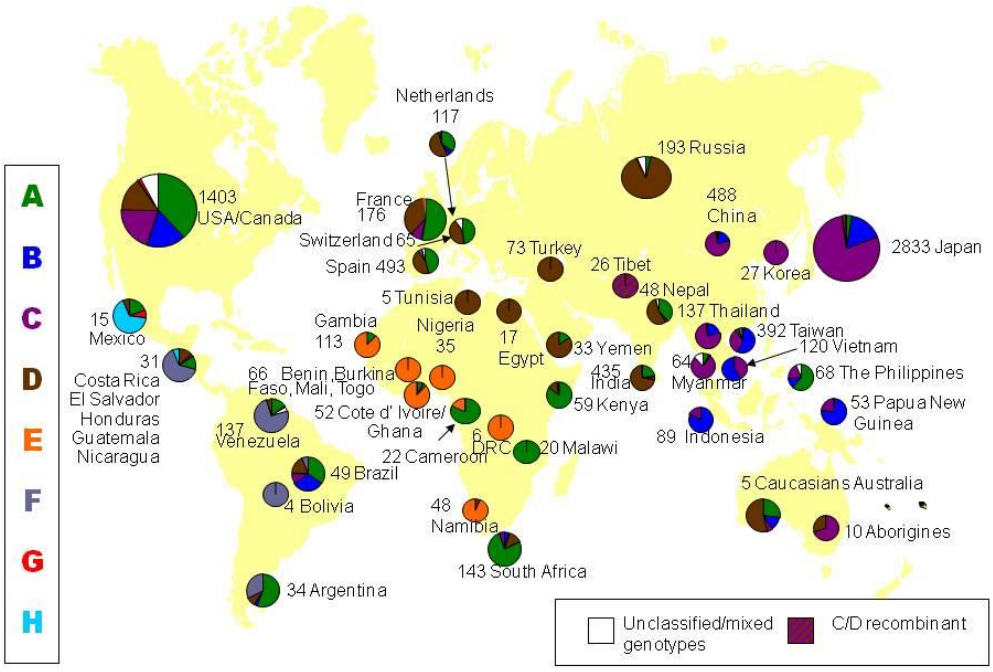

Figure 1.6: Global distribution of the eight genotypes of HBV. The numbers next to the pie charts are the number of isolates genotyped (Kramvis *et al*., 2005). Image used with copyright permission from Elsevier (2018).

Subgenotype A1 is the strain prevailing in southern sub-Saharan Africa, including South Africa.

1.15 Subgenotype A1 of HBV

HBV subgenotype A1 is a unique segment of the genotype A and it was first identified in isolates from South Africa using phylogenetic analysis of pre-S2/S sequences (Bowyer *et al*., 1997, Kramvis *et al*., 2002, Kramvis *et al*., 2005). It was the first subgenotype to be recognized and has been reported to be the dominant genotype A strain in Africa, consisting of unique molecular characteristics that differentiate it from subgenotype A2 (Kramvis *et al*., 2002, Kramvis and Paraskevis, 2013, Bowyer *et al*., 1997). Some studies have suggested that the molecular characteristics of subgenotype A1 are associated with the higher risk of HCC in patients infected with this subgenotype than their non-A counterparts (Baptista *et al*., 1999, Kew *et al*., 2005). A study on sub-Saharan Africans on HCC and asymptomatic carriers of the HBV, reported a 4.5 relative risk of HCC in genotype A carriers compared to participants infected with non-A genotypes. As well, those infected with genotype A developed cancer 6.5 years younger than those infected with non-A genotypes (Kramvis and Kew, 2007, Kew et al., 2005). Phylogenetic analyses of subgenotype A1 can be used to trace human migrations in and out of Africa (Kramvis and Paraskevis, 2013).

1.16 HBV pre-S1/S2 associated mutations

HBV mutants may be associated with alteration of epitopes important in the host immune recognition, enhanced virulence with increased replication of HBV, resistance to antiviral therapies, or facilitated cell attachment or penetration (Chen *et al*., 2006). Naturally occurring pre-S mutations have been frequently identified during the course of chronic infection, especially at the later stage of the disease, with the most commonly found being the: deletions at the 3’ terminus of pre S1 region, the 5’ terminus of pre-S2 region, the pre-S2 start codon, and point mutations at the pre-S2 start codon (Yeung *et al*., 2011, Chen *et al*., 2006). The pre-S mutants cause oxidative stress-induced DNA damage

and mutation, suggesting that the pre-S mutants are associated with genomic instability in HBV-infected hepatocytes (Hsieh *et al*., 2004). Liu and co-workers carried out a meta-analysis study, which investigated the association between the mutations and the risk of HCC. The study found pre-S mutations, C1653T, T1753V, and A1762T/G1764A to be associated with an increased risk of HCC. Also, the frequencies of the mentioned mutations increased as chronic HBV infection progresses from the asymptomatic HBsAg carrier state to liver cirrhosis and HCC (Liu *et al*., 2009). The study carried out by Skelton and co-workers reported a HBV-induced HCC patient with five subgenotype A1 distinct mutant HBV genomes, and mutations in all four ORFs which were not reported before. The study reported a 93bp deletion mutation in the S ORF (nt 3184-55), which resulted in a 31 amino acid deletion, covering the carboxyl end of the pre-S1 and the amino end of the pre-S2 region (Skelton *et al*., 2012). According to the same authors, the complex nature of the mutations in the investigated patient is likely to have contributed towards the early onset of the hepatocarcinogenesis (Skelton *et al*., 2012).

Studies have shown that accumulation of a number of pre-S1/S2 rearrangements, deletions and start codon mutations are common during fulminant hepatitis and at the later stage of chronic HBV infection (Pollicino *et al*., 1997, Fan *et al*., 2001). A Chinese study, reported that pre-S deletion mutations are independently associated with the development of HCC (Qu *et al*., 2014). Studies carried out in Taiwan, also reported the pre-S deletion mutants to be associated with the development of HCC (Yeung *et al*., 2011, Chen *et al*., 2006). Although pre-S deletion mutants are shown to be a risk factor for HCC, the studies were carried out for genotypes B and C. In South Africa, subgenotype A1 prevails which also has a hepatocarcinogenic potential compared to patients who are infected with genotype non-A (Kew *et al*., 2005). Studies carried out on genotypes B and C showed that HBV deletion mutants can affect the expression of the HBsAg, which can then lead to ER stress, apoptosis and hepatic

injury. We would like to determine whether this holds true for deletion mutants in subgenotype A1.

1.17 Study Rationale

The sub-Saharan Africa is classified as a hyperendemicity region, in terms of the HBsAg prevalence (greater than 8%) (WHO, 2015). HCC is a major cause of cancer death in black Africans living in sub-Saharan Africa, with 46 000 new HCC cases diagnosed each year in the sub-continent and the village dwellers tends to be the most burdened (Kew, 2013). Due to cases not properly diagnosed and/or cases not recorded in the cancer registry, the impact HCC causes tend to be underestimated in the region (Kew, 2013). Frequencies of the pre-S mutations are reported to increase as chronic HBV infection progresses from the asymptomatic HBsAg carrier state to liver cirrhosis and HCC (Liu *et al*., 2009). In HIV infected individuals, reports are showing an increase in the detection of deletion mutants as well as a high frequency of OBI (Hofer *et al*., 1998, Laure *et al*., 1985, Grob *et al*., 2000). The finding is supported by a report showing an increased risk of OBI in HBV-HIV co-infected South African individuals (Mphahlele *et al*., 2006). In regions where genotypes B and C predominate, a link between pre-S deletion mutants and risk factor for HCC has been strongly emphasized (Chen *et al*., 2006, Qu *et al*., 2014, Yeung *et al*., 2011). In Africa, HBV genotypes A, D and E are the most common and in South Africa, subgenotype A1 predominates with a hepatocarcinogenic potential when compared to non-A genotypes (Kew et al., 2005). Although the expression of pre-S deletion mutants had been followed *in vitro* using isolates belonging to other genotypes, this had not been done for subgenotype A1, which is the strain prevailing in South Africa.

1.18 Study aim:

The aim of this study was to determine whether HBV subgenotype A1 from HIV-infected patients affect envelope protein expression *in vitro.* The strains included pre-S deletion mutants (also frequently found in HCC patients) and the strain isolated from HBsAg negative HIV positive individual.

1.19 Study Objectives:

- To prepare recombinant plasmid constructs for transfection
- To transfect Huh7.5 liver cells with wild-type and deletion mutant clones
- To follow envelope protein expression of the pre-S deletion mutants using Confocal microscopy
- To compare the HBsAg expression and intracellular localization of the deletion mutant relative to the wild-type from an overt infection (HBsAg-positive), as well as
- To compare the HBsAg expression and intracellular localization of the deletion mutant relative to an HBV isolated from an occult infection (HBsAg-negative)

CHAPTER 2: MATERIALS AND METHODS

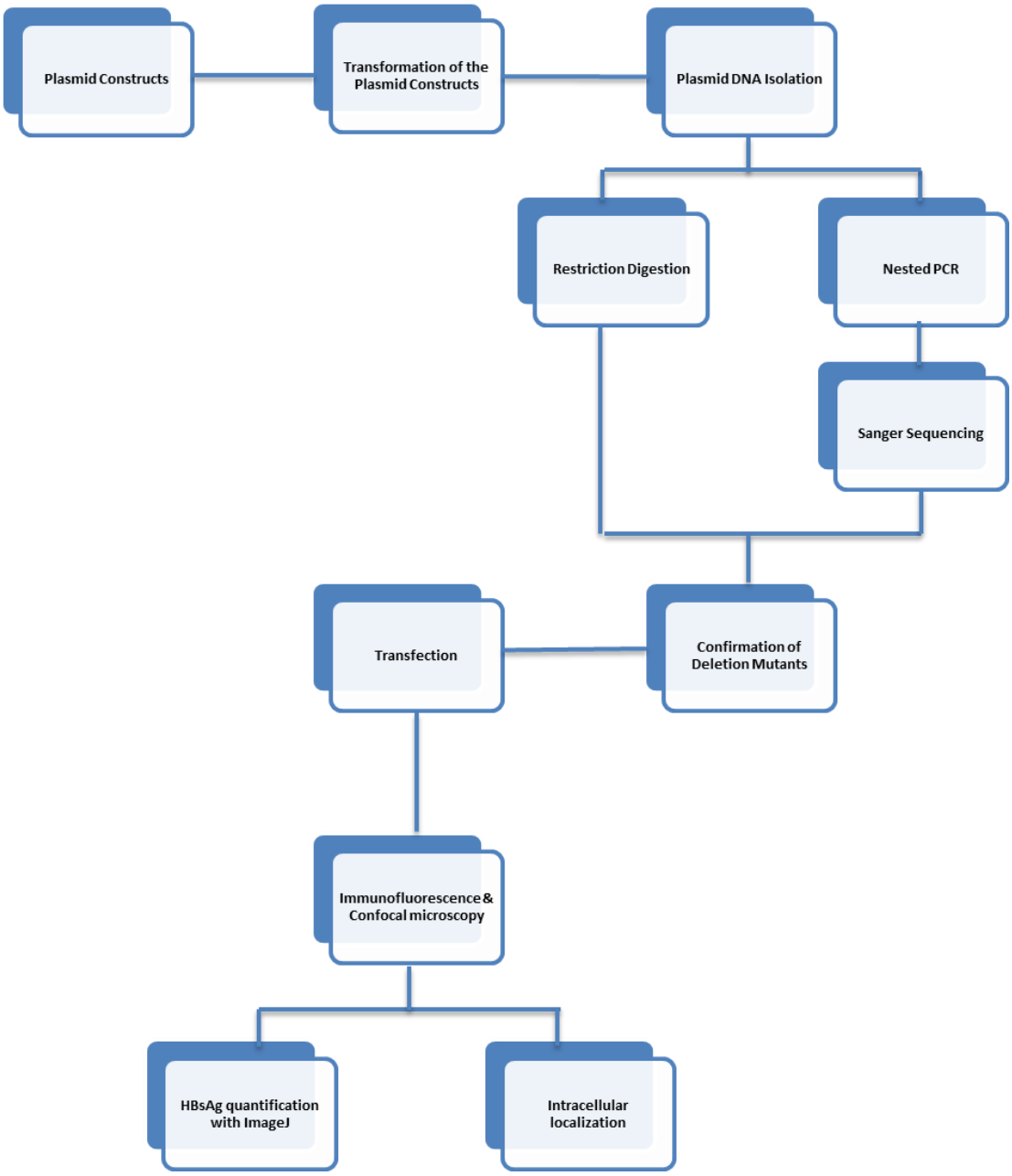

Figure 2.1 Overview and organization of the study

2.1 Plasmid Construct Clones and Ethical Clearance

The Recombinant HBV DNA containing Plasmids investigated in this study were prepared from isolates acquired from the HIV infected treatment naive patients in the Shongwe rural cohort study. The rural cohort was established at the Shongwe Hospital, in Malelane area, Mpumalanga Province of South Africa (Bell *et al*., 2012). In the same study, five of the participants (SHH011, SHH045, SHH167, SHH274 and SHH300) were found to be co-infected with HBV, with deletions in the pre-S1 and pre-S2 regions of the virus (Makondo *et al*., 2012). Three of these five isolates (SHH011, SHH045 and SHH167) together with a wild-type isolate from an occult infection (SHH193) (Makondo *et al*., 2012) were used to prepare recombinant HBV plasmid constructs by (Wolhuter S. unpublished). These plasmid constructs were concurrently assayed with two other Subgenotype A1 wild-type constructs (A12C15) (Bhoola *et al*., 2014) and (A12C15 ALT 9.3) (Wolhuter S. unpublished) from an overt infection and found to be replication competent *in vitro* (Wolhuter S. unpublished). The three deletion mutants (SHH011A, SHH045A, & SHH167A), one occult wild-type (SHH193A) and two overt wild-type (A12C15, & A12C15 ALT 9.3) Recombinant HBV DNA containing Plasmid constructs were used for this current study. Ethics clearance certificate for the current study was obtained unconditionally from the Human Research Ethics Committee (Medical) of the University of the Witwatersrand on the 09th of October 2015, certificate number M150983 (appendix B2).

2.2 Escherichia coli (E.coli) SCS 110 cell preparation

The *E.coli* SCS 110 cell stocks were plated on Luria Agar (LA) plates and grown overnight (14 - 16 hours) at 37°C to form colonies. Colonies were picked, inoculated into 5 ml of Luria Broth (LB) medium and incubated overnight with shaking (120 RPM) at 37°C. The overnight cultures were transferred into separate 250 ml flasks with 50 ml fresh LB medium and

incubated with shaking (120 RPM) at 37°C for 90 min until bacteria were in mid-log phase, Optical Density at 600nm (OD600) of 0.3-0.5. To test for OD, 100 µl of the bacterial culture, diluted with 900 µl of fresh LB medium was aliquoted into a cuvette, mixed and absorbance was read on the Spectrophotometer (with LB medium used as a blank solution). The bacterial culture with OD between 0.3 - 0.5 was used for competent cell preparation. Ten millilitres of bacterial culture (OD of 0.3 - 0.5) was aliquoted into the 15 ml Falcon tubes and spun at 4 500 RPM for 15 min at 4°C and the supernatant was discarded. The pellet in each 15 ml tube was gently resuspended in 1 ml PIPES buffer and incubated on ice for 20 min. The tubes were centrifuged at 4 500 RPM for 10 min at 4°C and the supernatant was discarded. The pellet was then resuspended in 200 µl of fresh PIPES buffer, aliquoted into 2 ml capped sterile tubes and stored at -70°C until further use.

2.3 Transformation of the plasmid constructs into the *E.coli* cells

Falcon polypropylene tubes were pre-chilled on ice. The SCS 110 cells were thawed on ice, gently mixed and 200 µl aliquoted into each of the pre-chilled tubes. 1.5 µl of the β-mercaptoethanol was added into each tube with the cells, tubes were gently swirled and incubated on ice for 10 min with a gentle swirl every 2 min. 50 ng of the plasmid DNA (SHH011A, SHH045A, SHH167A, SHH193A, A12C15 OL 1.28MER, A12C15 Altered 9.3 (ALT 9.3), pEGFP-C3 and pTZ57R/T), respectively was aliquoted into eight of the ten pre-chilled tubes. No DNA was added into the tubes that served as negative controls. All tubes were swirled, gently incubated on ice for 30 min and then incubated at 42°C in a heating bock for 45 seconds (A critical step for the protocol, the stage where the DNA is

inserted into the SCS110 cells if carried out properly). The tubes were incubated on ice for two min and 100 µl transformation mixture plated on LB agar plates containing the appropriate antibiotic (Ampicillin for the positive control, one negative and the six experimental samples other than the pEGFP-C3 of which Kanamycin antibiotic was used). The plates were then incubated at 37°C overnight and observed on the following day.

2.4 Small scale plasmid DNA isolation (Qiagen Mini prep protocol)

A colony was picked from the LA agar plates with the SCS110 cells (transformed with the following plasmid constructs: SHH011A, SHH045A, SHH167A, SHH193A, A12C15 OL 1.28MER, A12C15 ALT 9.3 and pEGFP-C3), inoculated into 7 ml of fresh LB medium in 15 ml tubes with 7 µl of ampicillin (or kanamycin for pEGFP-C3 tube). The cultures were grown overnight with shaking at 37°C. A day after the incubation, 2 ml of the bacterial culture was stored at 4°C to be used for large scale plasmid DNA isolation and the remaining 5 ml from all the respective cultures was centrifuged at 13 000 RPM for 5 min with the supernatant was discarded afterwards. The pellet was resuspended in 250 µl Buffer P1 and transferred into the 1.5 Eppendorff tubes. 250 µl Buffer P2 was added into the mixtures and the tubes were thoroughly mixed 4–6 times by inversion. 350 µl N3 was as well added and the tubes were thoroughly mixed by inversion, immediately. Tubes were then centrifuged at 13 000 RPM for 10 min. The supernatants were aliquoted into the respective QIAprep spin columns and centrifuged at 13 000 RPM for 1 min. The flow-through was discarded. The columns were washed by 0.5 ml Buffer PB, centrifuging for 1 min and the flow-through was discarded. Then 0.75 ml Buffer PE was aliquoted into the respective columns, centrifuged at 13 000 RPM for 1

min and the flow-through was discarded. The columns were centrifuge at 13 000 RPM for an additional min to remove residual wash buffer. The columns were then placed in respective sterile 1.5 ml Eppendorff tubes. Then 50 µl of Sabax water for injection was added on the centre of each respective column, which were allowed to stand for 1 min and centrifuged at 13 000 RPM for 1 min to elute the plasmid DNA into the 1.5 tubes. The DNA concentration was then estimated by the NanoDrop spectrophotometer.

2.5 Restriction digestion

Restriction digestion protocol for the respective plasmids constructs was carried out to confirm the correct sequence of the plasmids, using the restriction maps for the respective construct.

Table 2.3: Restriction digestion, typical reaction

Content	Quantity
Enzyme	1 µl
Buffer	1 µl
Sabax water for injection	2 µl or X µl
DNA	6 µl or X µl
Total	10 µl

All reactions were set up as indicated above, where X is variable. The reaction tubes were incubated at 37°C for 1 hour. The reactions were halted by the addition of 2 µl of loading dye and the reaction contents were ran on 1% agarose gel electrophoresis for 2 hours at 80 V.

2.6 Large scale plasmid DNA isolation (Qiagen Maxi prep protocol) and Restriction digestion

When the isolated plasmid DNA was confirmed to be correct, the stored bacterial cultures were then used for the large scale isolation.

The remainder from each bacterial culture (stored 2 ml) used for the low scale plasmid DNA isolation was aliquoted into a 1 L flasks with 450 ml fresh LB medium and 450 µl ampicillin (with Kanamycin for the pEGFP-C3 flask). The bacterial cultures were incubated overnight with shaking at 37°C. The overnight culture for each respective plasmid construct was aliquoted into nine 50 ml tubes (8 for DNA isolation and 1 for glycerol stock preparation). The tubes were centrifuged at 5 500 RPM for 15 min at 4°C and the supernatant was discarded. The pellet was resuspended (all 8 tubes per sample) in 10 ml of Buffer P1 and mixed thoroughly by pipetting up and down, followed by lysing of the cells by the addition of 10 ml of Buffer P2, gently mixed by inversion and incubated at room temperature for 5 min. 10 µl of Buffer P3 was aliquoted into the mixture and incubated on ice for 15 min. The lysates were centrifuged at 11 000 RPM for 30 min at 4ºC, the supernatant was transferred into a sterile tube and centrifuged at 11 000 RPM for 15 min at 4ºC. Each Qiagen column was equilibrated with 4 ml of Buffer QBT and the flow through was discarded. The cleared lysate was then loaded onto the column and the flow through was discarded. The column was then washed twice with 30 ml of Buffer QC and the flow through was discarded. The plasmid DNA was eluted into a sterile 50 ml tube using 15 ml of buffer QN. Then 10.5 ml of isopropanol was added to the eluted DNA, carefully mixed, centrifuged at 12 000 RPM for 30 min at 4ºC and the supernatant was carefully discarded. Then 5 ml of 70% ethanol was added to each tube, carefully mixed, centrifuged at 12 000 RPM for 15 min at room temperature and the supernatant was carefully discarded. The pellet was air dried and then resuspended in 50 µl of sterile preheated Sabax water. Each tube was tapped vigorously, incubated at 60ºC for a few min and then again at 37ºC for a few min. The

DNA concentration was then estimated by the NanoDrop spectrophotometer.

2.7 Restriction Digestion

Because the isolated plasmid DNA was highly concentrated, the samples were diluted before a restriction digestion reaction was carried out. The reactions were set up in the same way as in the previous reactions for the small scale plasmid DNA isolation products.

2.8 Polymerase Chain Reaction (PCR)

The complete S region of the HBV (pre-S1/S2/S region) was amplified using the nested PCR method and the specific primers (Vermeulen *et al*., 2012), shown in table 2.4 were used.

Table 2.4: First and second round PCR primers used, their respective sequence, binding site and amplicon size

	Primer Name	Primer sequence	Nucleotide Position in HBV Genome	Amplicon size
1st round	S1F	5' -TCA ATC GCC GCG TCG CAG AAG ATC TCA ATC- 3'	2401 - 2439	2113
	S1R	5' -TCC AGA CCK GCT GCG AGC AAA ACA- 3'	1314 – 1291	2113
2nd round	S2F	5' -AAT GTT AGT ATT CCT TGG ACT CAT AAG GTG GG- 3'	2451 – 2482	2055
	S2R	5' -AGT TCC GCA GTA TGG ATC GGC AGA GGA- 3'	1286 - 1254	2055

Note: The *EcoR*I restriction site is considered as position one; F=forward and R=reverse

The PCR was carried out on the BioRad T100™ Thermal Cycler PCR machine. The first round PCR consisted of 45 µl of reaction mixture containing 9.25 µl Best Quality Water (BQW), 12.5 µl Qiagen Hot Start master mix, 0.375 µl of each of the primers (S1F and S1R) (table 2.5), respectively in a 0.2 ml Eppendorff tube. Then 2.5 µl of the DNA was added to bring the total reaction mixture to 25 µl. The positive control consisted of DNA isolated from HBV-positive serum sample and for the negative control sample, BQW was used instead.

Table 2.5: First round PCR

PCR Reaction Content	Quantity (µl)	X	Reaction Mixture
Best Quality Water (BQW)	9.25	9	83.25
Qiagen Hot (QH) Start master mix	12.5	9	112.5
20 mM Primer F (S1F)	0.375	9	3.375
20 mM Primer R (S1R)	0.375	9	3.375
DNA	2.5	-	-
Total	25		

The first round PCR cycling involved 40 cycles of initial denaturation at 95 °C for 15 min, denaturation at 94 °C for 1 min, Annealing at 66 °C for 1 min and extension at 72 °C for 3 min (table 2.6). The second round PCR consisted of 45 µl of reaction mixture containing 18.25 µl BQW, 25 µl QH Start master mix, 0.75 µl of each of the primers (S1F and S1R) (table 2.7), respectively in a 0.2 ml Eppendorff tube. Then 5 µl of the first round PCR product was added to make it up to 50 µl and second round PCR then carried out. The second round PCR cycling was carried out the same way as the first round cycling which involved 40 cycles of initial denaturation at

95 °C for 15 min, denaturation at 94 °C for 1 min, annealing at 66 °C for 1 min and Extension at 72 °C for 3 min (table 2.6)

Table 2.6: First and Second round PCR cycling conditions

Step	Temperature	Duration
Initial	95 °C	15:00 min
Denature	94 °C	1:00 min
Anneal	66°C	1:00 min
Extend	72°C	3:00 min
Final extend	72°C	10:00 min
Hold	4°C	-

Table 2.7: Second round PCR

PCR Reaction Content	Quantity (µl)	X	Reaction Mixture
BQW	18.5	6	111
QH Master mix	25	6	150
20 Mm Primer F	0.75	6	4.5
20 Mm Primer R	0.75	6	4.5
DNA	5.0	-	-
Total	50		

2.9 Detection and confirmation of the amplified PCR product

To confirm the size of the PCR product, 5 µl of the PCR product was run on a 1% agarose gel stained with Ethidium Bromide via electrophoresis at 170 V for 1 h 30 min to allow for separation of the PCR products by size. The size of the PCR products were estimated relative to the migration pattern of the 1 kb Gene ruler. PCR products on the gel were visualized and images captured using the GelDoc system (BioRad, US).

2.10 Gel purification and Sanger sequencing of the PCR product

The PCR products confirmed to be correct size were carefully excised from the gel and sent to Inqaba Biotech Sequencing Unit for purification and Sanger sequencing. The S gene forward sequencing primers (table 2.8) were used for the direct Sanger sequencing of the PCR products. The sequence chromatograms were edited for any wobble bases using the Finch TV software and the DNA Fragment Merger Tool (Bell and Kramvis, 2013) was used to merge the three overlapping sequences to form a complete S sequence.

Table 2.8: Surface gene primer sequences

Complete S Primers	Primer sequence	Nucleotide Position in HBV Genome
2497F	5’ -TTC CTT GGA CTC ATA AGG TG- 3’	2461 – 2480
3188F	5’ -AG TCA GGA AGG CAG CCT AC- 3’	3152 – 3170
591F	5’ -ATT GCA CCT GTA TTC CCA TCC- 3’	591 – 611

Note: The *EcoR*I restriction site is considered as position one

2.11 Bioinformatic analysis

The complete S DNA merged sequences were assembled and aligned manually against a consensus sequence of the HBV subgenotype A, with the accession number: AY233274 using GeneDoc. The aligned sequences were compared to the then aligned sequences (Makondo *et al*., 2012) to confirm if the deletions on the current clones were identical to the original isolates from the rural cohort.

2.12 Huh7.5 Cell Culture

Huh7.5 cells were maintained in complete growth Dulbecco's Modified Eagle's Medium (DMEM) supplemented with 10% Foetal Calf Serum (FCS) and 1 % Penicillin-Streptomycin-Glutamine. The cells were grown in a 75 cm^2 culture flask and incubated at 37 °C in a humid incubator containing 5% carbon dioxide (CO_2). The cells were either frozen for stocks, passaged, or seeded for transfections when they were allowed to grow 80 and 100% confluency. A haemocytometer was used to determine the number of cells for transient transfection, which was kept constant for all the samples.

2.13 Transient transfection of Recombinant HBV DNA containing Plasmids into the Human hepatoma Cells (Huh7.5)

Twenty-four hours prior to transfection, 1.8 x 10^5 of the Huh7.5 cells were seeded into 12-well plates with 16 MM round coverslips in each well and incubated overnight at 37 °C in a humid incubator containing 5% CO_2. On the following day, the cells were transfected with 800 ng Recombinant HBV DNA containing Plasmids, and pEGFP-C3 plasmid clones, complexed with 3 µl *Trans*IT®-LT1 Transfection reagent and incubated at 37 °C in a humid incubator containing 5% CO_2. The experiments were carried out in triplicate (with 7 quantifications per replicate) and the coverslips with the transfected cells were harvested on days 1, 3, and 5 post-transfection. A more detailed protocol is attached as appendix B3.

2.14 Measure of Transfection Efficiency in Transfected Cells

Transfection efficiency was measured on day 1 post-transfection by determining the number of cells that were successfully transfected with the pEGFP-C3 plasmid relative to the total number of cells under an Olympus IX71 fluorescence microscope (Olympus Soft Imaging Solutions GmbH, Münster, Germany). The pEGFP-C3 plasmid contains a green fluorescent protein (GFP), which emits fluorescence with a peak at 509 nm after excitation at 395 nm.

2.15 Indirect Immunofluorescence (Mono- and Double-Staining)

Immunofluorescence was carried out on Huh7.5 cells that were grown on cover slips and successfully transfected with the recombinant HBV DNA containing plasmids. Staining with both the primary and secondary antibodies was carried out on days 1, 3, and 5 post-transfection. The cells were fixed with 4% Formaldehyde, permeabilized with 0.5% Triton, and blocked with 1% Bovine Serum Albumin (BSA). Phosphate Buffer Saline (PBS) was used as a wash buffer between each step of the procedure. Cells were stained with Rabbit Polyclonal HBsAg antibody and with cell compartment primary antibody markers (Mouse anti-Calnexin; Mouse anti-ERGIC-C3; Mouse anti-Giantin) in the case of a double staining protocol and incubated for an hour at 37^0C. Cells were stained with Donkey anti-Rabbit IgG (H+L), AlexaFluor®488 conjugate, as well as Goat anti-Mouse, AlexaFluor®546 secondary antibodies in the case of double staining protocol and incubated for an hour at 37^0C. Cells were then stained with 4',6-Diamidino-2-Phenylindole, Dihydrocloride (DAPI) and incubated for 10 min at room temperature. Cells were mounted into the microscope slides with a drop of mounting medium. Slides were allowed to dry overnight in the dark and images were taken at the Confocal Microscope. A more detailed protocol is attached as appendix B4.

2.16 Quantification of the expressed HBsAg using ImageJ software

The brightness of the image opened on the software was first adjusted back to its original state through clicking on ‘Image’ button on the software (figure 2.2). A freehand selection of the brush was used to encircle the region showing the expressed envelope proteins with the exclusion of the nuclear region (images A & B). The ‘analyse’ button was clicked, with ‘measure’ selected afterwards. The result table appeared on the result window and when all quantifications were carried out, the table was imported to Microsoft Excel spread sheet and further analysis carried out. To eliminate background, quantification at a region with less to no HBsAg expression (images C & D) was carried out on 7 cells in each replicate and the mean of the quantification per replicate was recorded. The mean quantification of each replicate was subtracted from the HBsAg quantification of the same replicate to give us the actual intensity of the expressed HBsAg for that specific replicate for all the Constructs for all the time points.

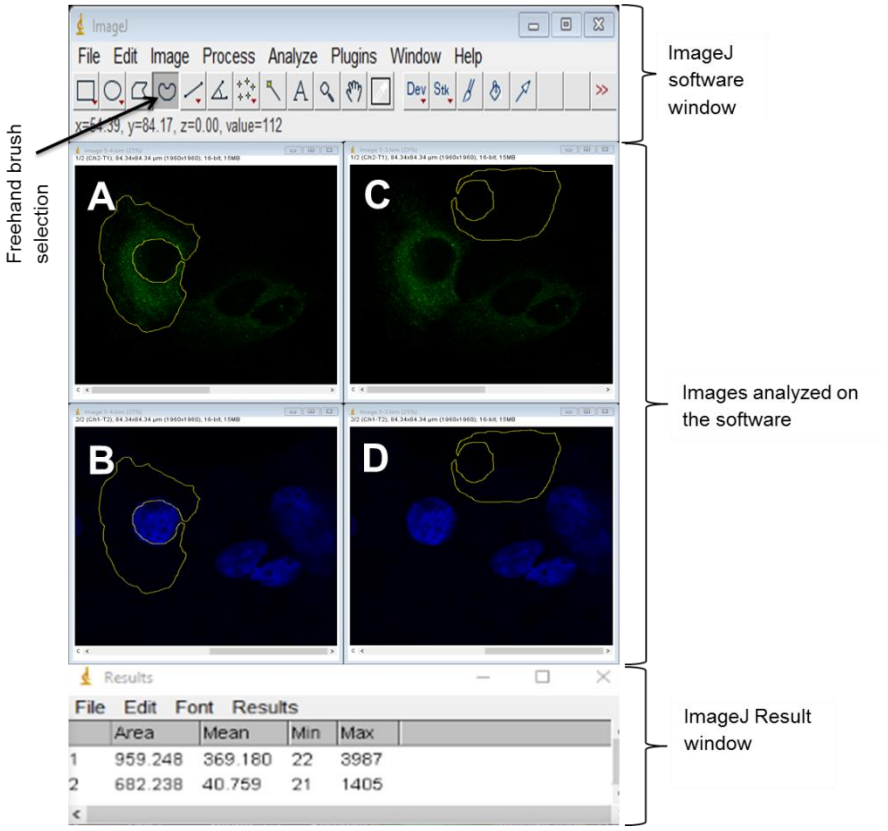

Figure 2.2: Quantification of the expressed HBsAg on ImageJ software

This figure shows how HBsAg was quantified using the software. As indicated on the figure, the software window, with all features necessary for the analysis. The middle part is showing the images viewed on the software and the result window showing the intensities for the expressed HBsAg.

CHAPTER 3: RESULTS

3.1 Confirmation of Plasmid Construct Sequences

3.1.1 Genotyping using Restriction Fragment Length Polymorphism (RFLP) assay

Following transformation of the recombinant HBV DNA containing plasmid constructs into the *E.coli* cells and plasmid DNA isolation, a restriction digestion/RFLP assay was also carried out to confirm the correct sequences of the constructs. Different restriction enzymes were used for the different constructs. Tables 3.1-3.6 show a list of restriction enzymes used, number of cuts expected and the sizes of the resulting fragments expected when RFLP was completed. Figures 3.1-3.6 below show the corresponding restriction digestion reaction products following electrophoresis on a 1% agarose gel stained with ethidium bromide.

A12C15_OL A1WTSA1.281MER Construct

Table 3.1: Restriction enzymes used and the expected band sizes, adapted from Ms. S. Wolhuter (MSc: University of the Witwatersrand)

Enzyme	Number of cuts	Size of the expected fragments for correct orientation
*Xba*I	3	5769 bp, 1658 bp and 784 bp
*BamH*I	1	8211 bp linear
*Stu*I	7	3257 bp, 2607 bp, 1119 bp, 587bp, 587 bp. 27 bp and 27 bp
*Sal*I	2	6026 bp and 2185 bp
*Bgl*II	3	5411 bp, 2776 bp and 24 bp

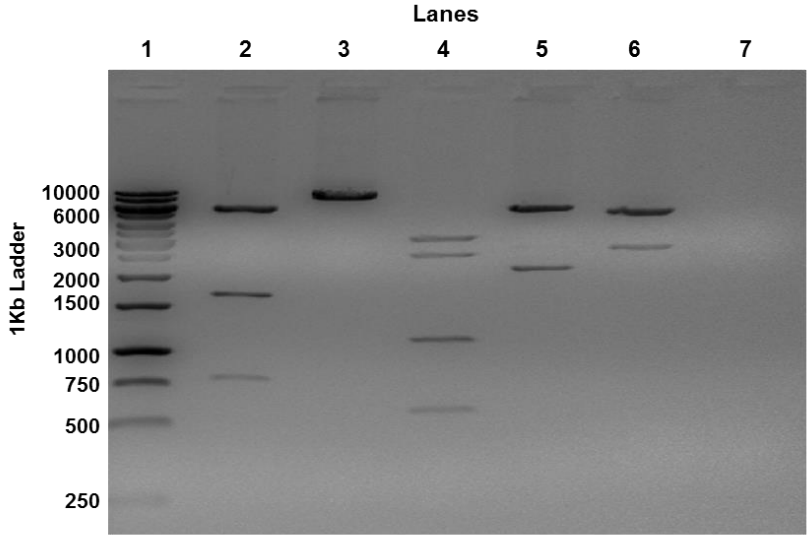

Lanes:

1. GeneRuler™ 1kb DNA Ladder
2. A12C15_OL A1WTSA 1.28 MER + *Xba*I
3. A12C15_OL A1WTSA 1.28 MER + *BamH*I
4. A12C15_OL A1WTSA 1.28 MER + *Stu*I
5. A12C15_OL A1WTSA 1.28 MER + *Sal*I
6. A12C15_OL A1WTSA 1.28 MER + *Bgl*II
7. No DNA + *Pst*I

Figure 3.1: Restriction mapping of A12C15_OL A1WTSA1.281MER Construct

The construct is considered correct as the restriction digestion products, run against a molecular weight marker, showed all the expected and correct size bands as per the restriction map for the same construct, table 3.1. The no DNA control was included. 1% Agarose gel, stained with ethidium bromide was used.

A12C15_OL A1WTSA1.281MER Altered 9.3 Construct

Table 3.2: Restriction enzymes used and the expected band sizes, adapted from Ms. S. Wolhuter (MSc: University of the Witwatersrand)

Enzyme	Number of cuts	Size of the expected fragments for correct orientation
BamH	1	8189 bp linear
*Sal*I	2	6004 bp and 2185 bp
*EcoR*I	1	8189 bp linear
*Bgl*II	3	5389 bp, 2776 bp and 24 bp
*Xba*I	2	7427 bp, 784 bp
*Stu*I	7	3257 bp, 2607 bp, 1097 bp, 587bp, 587 bp. 27 bp and 27 bp

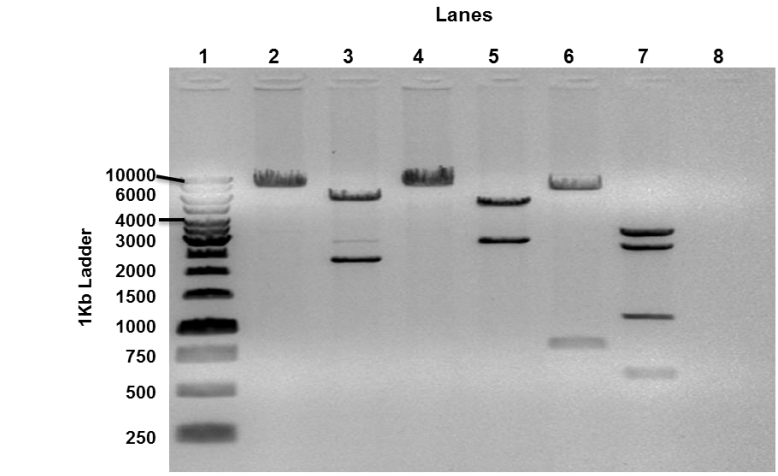

Lanes:

1. GeneRuler™ 1kb DNA Ladder
2. A12C15_OL A1WTSA 1.28 MER Alt 9.3 + *BamH*I
3. A12C15_OL A1WTSA 1.28 MER Alt 9.3 + *Sal*I
4. A12C15_OL A1WTSA 1.28 MER Alt 9.3 + *EcoR*I
5. A12C15_OL A1WTSA 1.28 MER Alt 9.3 + *Bgl*II
6. A12C15_OL A1WTSA 1.28 MER Alt 9.3 + *Xba*I
7. A12C15_OL A1WTSA 1.28 MER Alt 9.3 + *Stu*I
8. No DNA + *Xba*I

Figure 3.2: Restriction mapping of A12C15_OL A1WTSA1.281MER Altered 9.3 Construct

The construct is considered correct as the restriction digestion products, run against a molecular weight marker, showed all the expected and correct size bands as per the restriction map for the same construct, table 3.2. The no DNA control was included. 1% Agarose gel, stained with ethidium bromide was used.

OL_OCFL SHH193A-F Construct

Table 3.3: Restriction enzymes used and the expected band sizes, adapted from Ms. S. Wolhuter (MSc: University of the Witwatersrand)

Enzyme	Number of cuts	Size of the expected fragments for correct orientation
*Pst*I	0	8188 bp circular
*Xba*I	2	7405 bp and 783 bp
*BamH*I	1	8188 bp linear
*Sal*I	2	6003 bp and 2185 bp
*EcoR*I	1	8188 bp linear

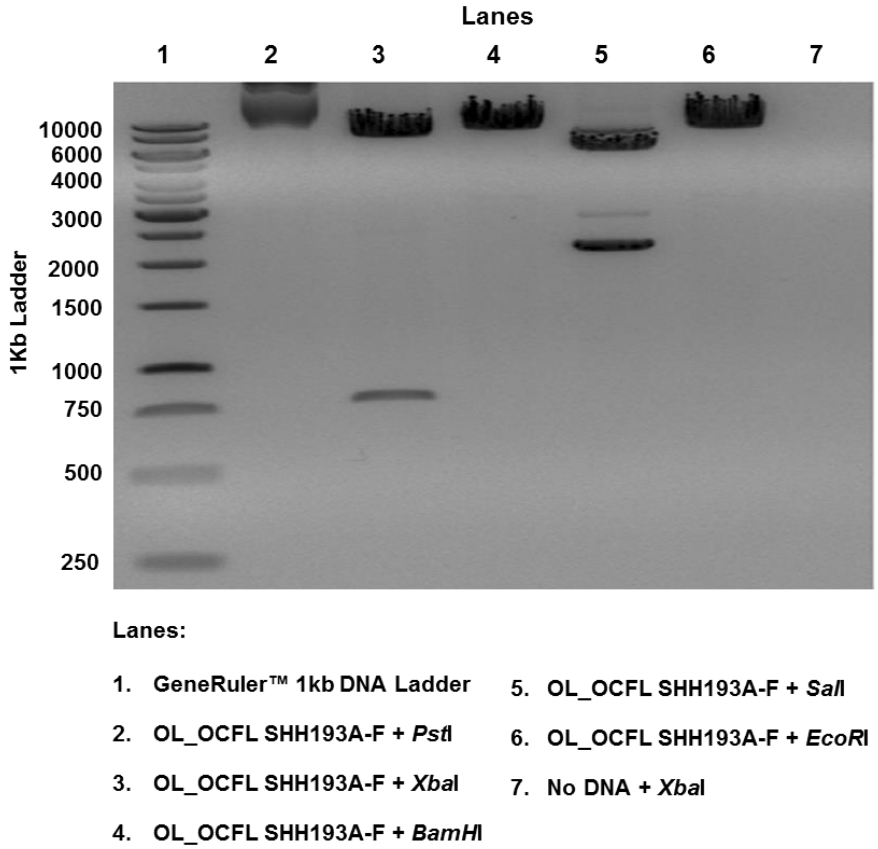

Figure 3.3: Restriction mapping of OL_OCFL SHH193A-F Construct

The construct is considered correct as the restriction digestion products, run against a molecular weight marker, showed all the expected and correct size bands as per the restriction map for the same construct, table 3.3. The no DNA control and sometimes an additional uncut plasmid were included to show that the enzyme activity was as expected. 1% Agarose gel, stained with ethidium bromide was used.

OL_DELMUT SHH045A-F Construct

Table 3.4: Restriction enzymes used and the expected band sizes, adapted from Ms. S. Wolhuter (MSc: University of the Witwatersrand)

Enzyme	Number of cuts	Size of the expected fragments for correct orientation
*Bgl*II	3	5419 bp, 2743 and 24 bp
*Xba*I	2	7405 bp and 688 bp
*Sal*I	2	6001 bp and 2185 bp
*Pst*I	0	8156 bp circular
*Xho*I	0	8156 bp circular
*EcoR*I	1	8156 bp linear
*BamH*I	2	7256 bp and 751 bp

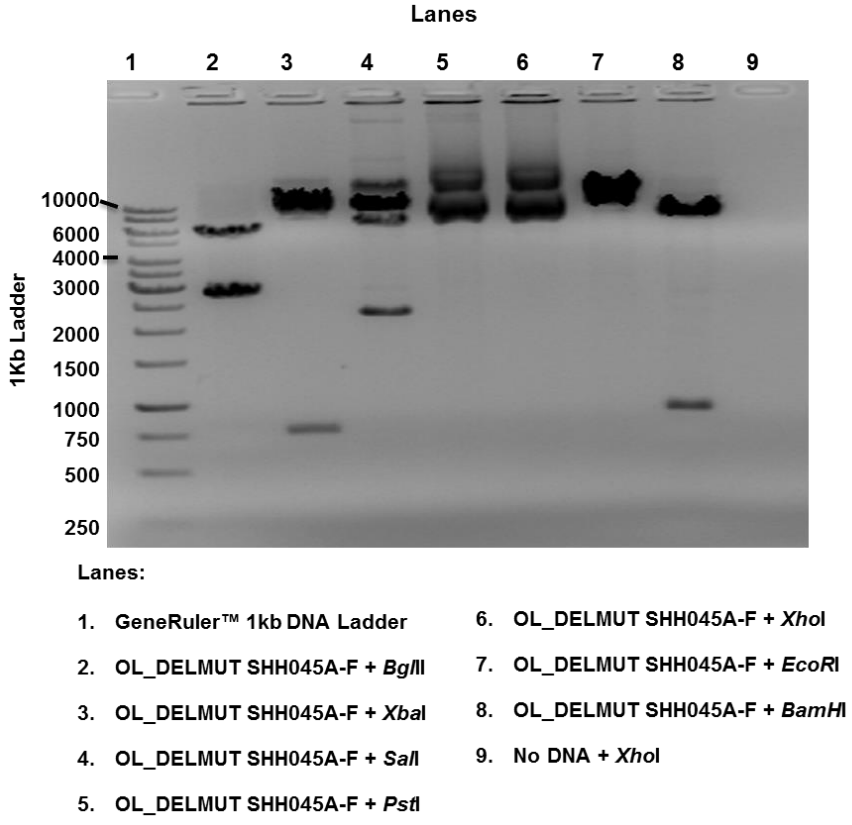

Figure 3.4: Restriction mapping of OL_DELMUT SHH045A-F Construct

The construct is considered correct as the restriction digestion products, run against a molecular weight marker, showed all the expected and correct size bands as per the restriction map for the same construct, table 3.4. The no DNA control and sometimes an additional uncut plasmid were included to show that the enzyme activity was as expected. 1% Agarose gel, stained with ethidium bromide was used.

OL_DELMUT SHH011A-F Construct

Table 3.5: Restriction enzymes used and the expected band sizes, adapted from Ms. S. Wolhuter (MSc: University of the Witwatersrand)

Enzyme	Number of cuts	Size of the expected fragments for correct orientation
*EcoR*I	0	8093 bp circular
*Bgl*II	3	5389 bp, 2680 and 24 bp
*BamH*I	2	7256 bp and 837 bp
*Sal*I	2	5908 bp and 2185 bp
*Xba*I	2	7405 bp and 688 bp

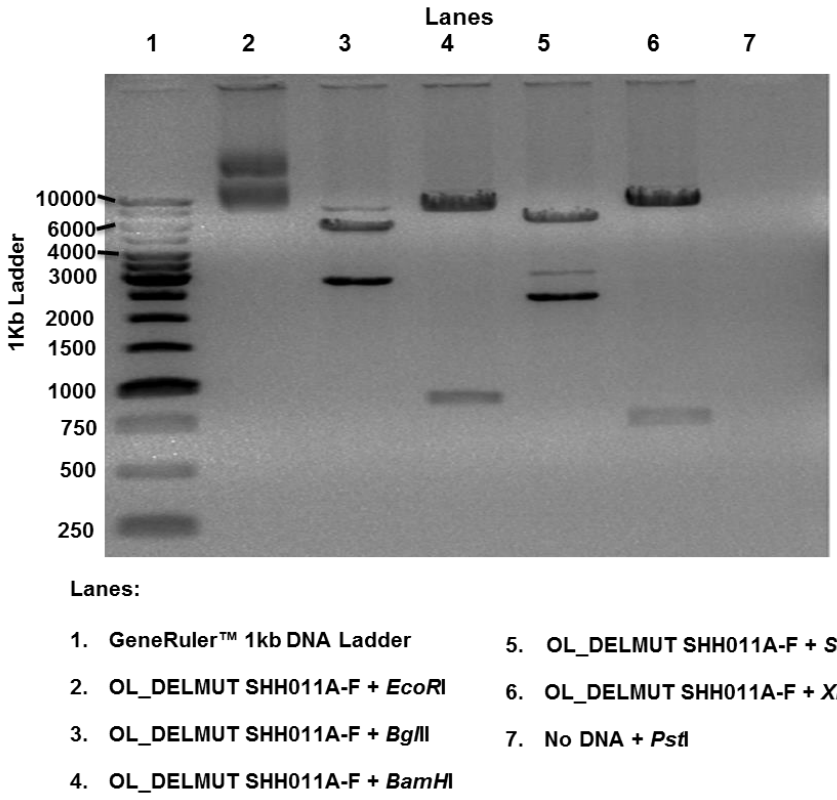

Figure 3.5: Restriction mapping of OL_DELMUT SHH011A-F Construct

The construct is considered correct as the restriction digestion products, run against a molecular weight marker, showed all the expected and correct size bands as per the restriction map for the same construct, table 3.5. The no DNA control and sometimes an additional uncut plasmid were included to show that the enzyme activity was as expected. 1% Agarose gel, stained with ethidium bromide was used.

OL_DELMUT SHH167A-F Construct

Table 3.6: Restriction enzymes used and the expected band sizes, adapted from Ms. S. Wolhuter (MSc: University of the Witwatersrand)

Enzyme	Number of cuts	Size of the expected fragments for correct orientation
*Xba*I	2	7405 bp and 739 bp
*BamH*I	1	8144 bp linear
*Sal*I	2	5959 bp and 2185 bp
*Bgl*II	3	5389 bp, 2731 and 24 bp
*Pst*I	0	8144 bp circular

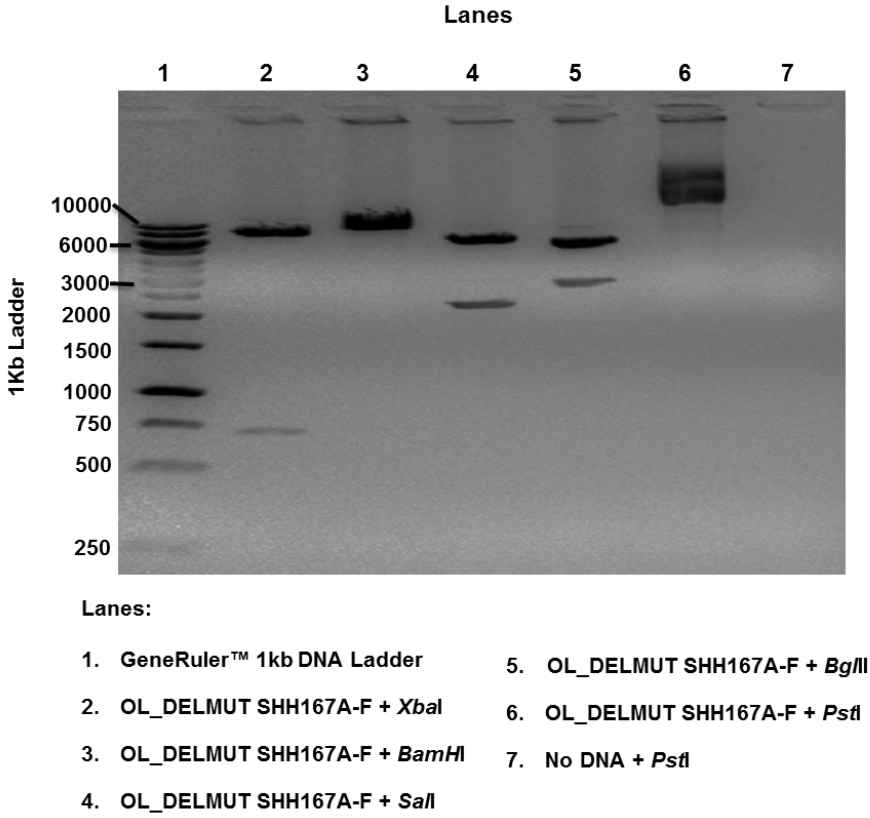

Figure 3.6: Restriction mapping of OL_DELMUT SHH167A-F Construct

The construct is considered correct as the restriction digestion products, run against a molecular weight marker, showed all the expected and correct size bands as per the restriction map for the same construct, table 3.6. The no DNA control and sometimes an additional uncut plasmid were included to show that the enzyme activity was as expected. 1% Agarose gel, stained with ethidium bromide was used.

3.2 Complete surface gene analysis

The plasmid constructs were further analysed using PCR of the complete surface gene in order to confirm the correct deletions. Nested PCR was carried out when a product was not obtained from a single PCR. A successful amplification of the HBV complete surface region was shown by the presence of a DNA band on a 1% agarose gel. The expected amplicon sizes of ~2113 bp during first round PCR (figure 3.7) and ~2055 bp for second round PCR (figure 3.8) DNA bands were detected for the first and second round PCR, respectively.

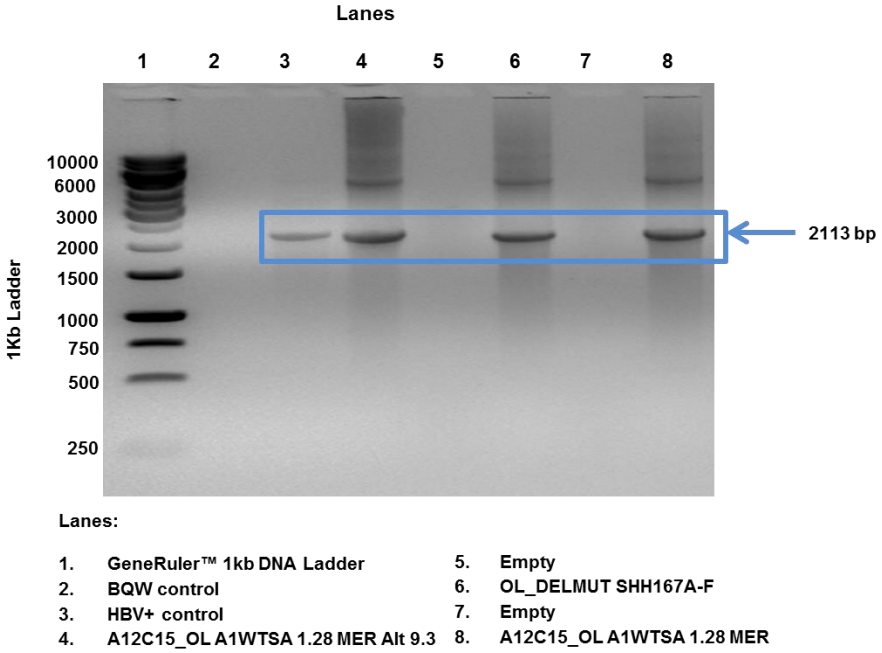

Figure 3.7: PCR of the HBV complete S Region

The figure shows the results for the first round PCR of the HBV complete S region. The PCR products were run in 1% agarose gel stained with ethidium bromide and ~2113 bp was the expected fragment size for the amplicons. BQW and HBV positive DNA were used as a negative and positive control, respectively.

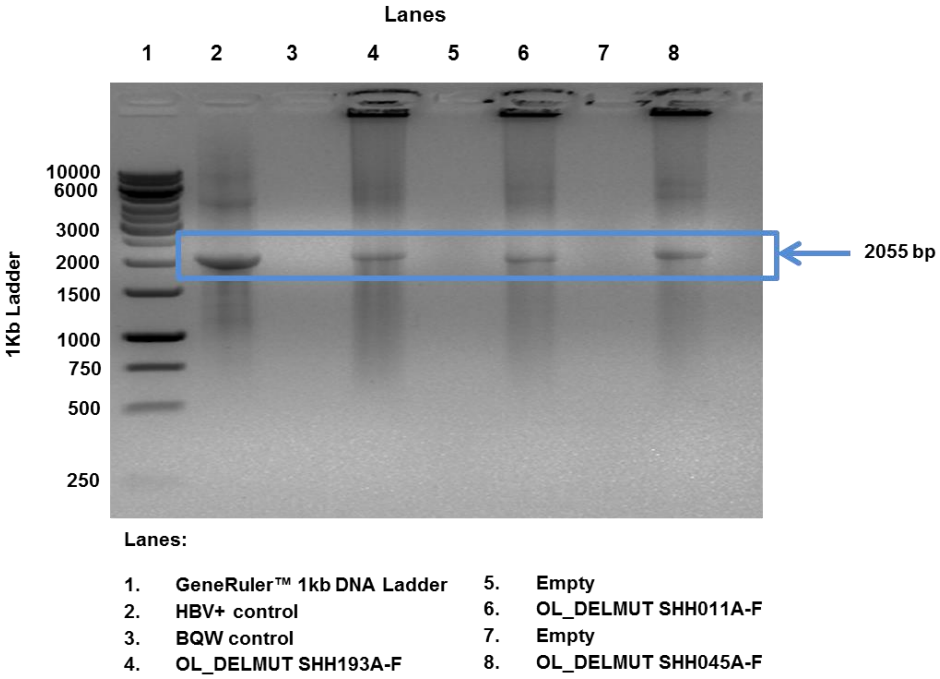

Figure 3.8: Nested PCR of the HBV complete S Region

The figure shows the results for the second round nested PCR of the HBV complete S region. The PCR products were run in 1% Agarose gel stained with ethidium bromide and ~2055 bp was the expected fragment size for the amplicons. BQW and HBV positive DNA were used as a negative and positive control, respectively.

3.3 Sequencing of the amplified complete surface gene products

The PCR products of the HBV complete surface region for all the plasmid constructs were sent for direct sequencing at Inqaba Biotech sequencing unit. The successfully sequenced PCR products were manually aligned against a sequence of the HBV subgenotype A1 (AY2332274) using GeneDoc. Even though the complete S region was aligned, the figure only shows the pre-S1 and some part of pre-S2 regions, which are the regions with the deletions. The top sequence is the sequence of the HBV subgenotype A1 (AY2332274), the next three are the deletion mutants: SHH011A, SHH045A, SHH167A and the last one is sequence of the wild-type clone from an occult infection, SHH193A. The consensus sequence is

shown on the bottom. The deletions in SHH011A are located in both the pre-S1 and pre-S2 regions (pre-S2 initiation codon also deleted), while SHH045A and SHH167A only have deletions in the pre-S2 region (figure 3.9).

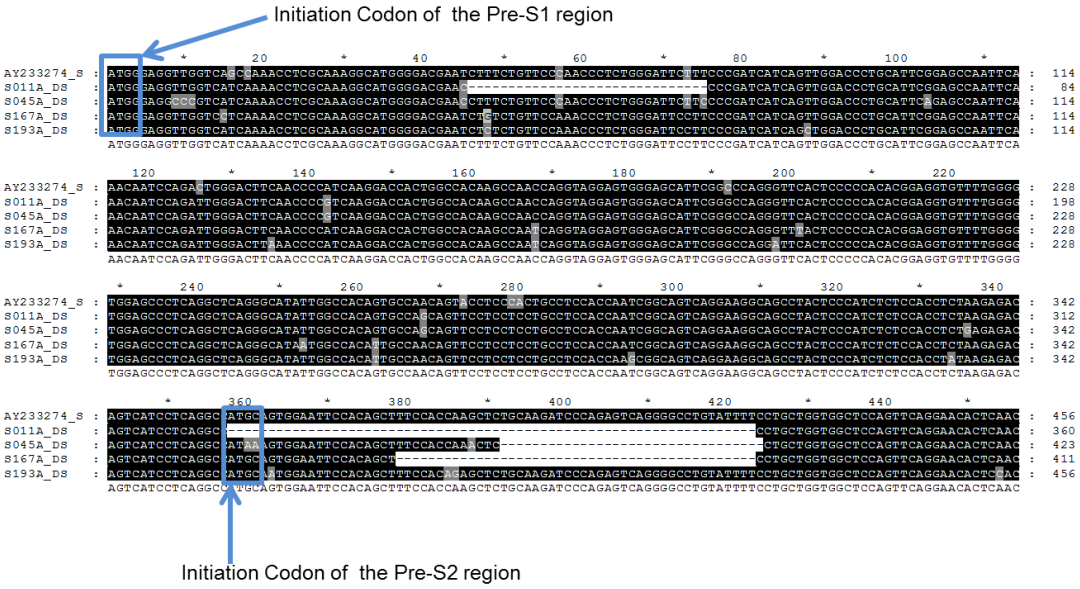

Figure 3.9: Deletion mutation confirmation from the constructs

Multiple sequence alignment of HBV subgenotype A1, showing deletions in the pre-S1/pre-S2 region. The deletion mutant constructs (SHH011A, SHH045A, & SHH167A) and a wild-type from an occult infection (SHH193A) are aligned against a sequence of the HBV subgenotype A1 (AY2332274) (Row 1). The consensus sequence of the HBV subgenotype A1 is shown in the last row. Boxed in blue are the initiation codons of the pre-S1 and the pre-S2 regions.

3.4 Transfection of Huh7.5 cells

3.4.1 Measurement of Transfection efficiency with eGFP expression

Transfection of the Huh7.5 cells with pEGFP-C3 was used to check if the transfection was successful and to measure the transfection efficiency (Fig.3.10A). A mock transfection (cell transfection with no DNA), was stained with a primary antibody against S region of HBV envelope proteins (rabbit anti-HBsAg) and a secondary antibody labelled with AlexaFluor 488 (Donkey anti-Rabbit). This is a control to determine the background for

immunofluorescence analysis (Figure 3.10B). The first column in figure 3.10A, represents the enhanced green fluorescent protein (eGFP), expressed by the cells transfected with pEGFP-C3, while the second column represents the nuclei (stained with DAPI staining) and the rows represent the different time points (days 1,3 & 5) post-transfection, respectively. The efficiency of transfection was 80% with the positive control (Huh7.5 cells transfected with pEGFP-C3), the experiment was considered successful.

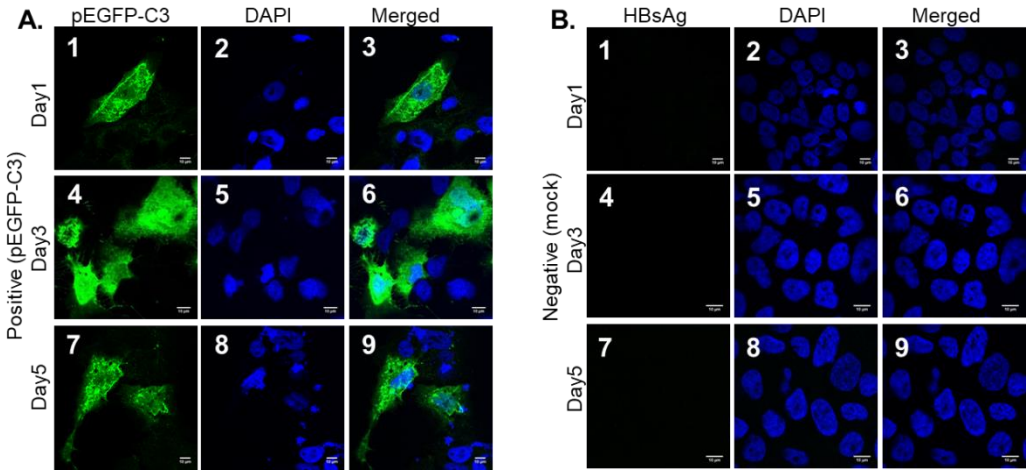

Figure 3.10: Transfection efficiency measurement using expression of eGFP and a mock transfection for the experimental control

A. Transfection of Huh7.5 cells with pEGFP-C3. The eGFP, is shown in green (**A.**1, 4, & 7)**.** Transfection efficiency in Huh7.5 cells was determined at day 1 (A1-3), days 3 (A4-6) and 5 post-transfection (A7-9). **B.** Mock transfection: transfection of cells with no DNA, cells stained with both primary antibody against S region of HBV envelope proteins (rabbit anti-HBsAg) and a secondary antibody labelled with AlexaFluor 488 (Donkey anti-Rabbit) on days 1 (B1-3), 3 (B4-6), and 5 post-transfection (B7-9). Both **A.** and **B.** 2, 5 and 8 show DAPI staining (blue) and images 3, 6 and 9 show merged images (Scale bar: 10 µm).

3.5 Detection of the expressed envelope proteins using mono-staining immunofluorescence technique

Plasmid constructs: A12C15 OL 1.28MER, A12C15 Altered 9.3 (ALT 9.3), SHH193A, SHH011A, SHH045A, and SHH167A, that were confirmed to be correct sequence, were transfected into the Huh7.5 cells. The expressed envelope proteins of the deletion mutants were compared to those expressed by the wild-type construct clones, and that was achieved by carrying out mono-staining immunofluorescence, with images captured on days 1, 3, and 5 post-transfection. Figure 3.11, A-B, show the two wild-type constructs (A12C15_OL A1WTSA1.281MER; A12C15_OL A1WTSA1.281MER Altered 9.3), C, occult full-length (OL_OCFL SHH193**)**; and D-F, deletion mutant constructs (OL_DELMUT SHH011/SHH045/SHH167). Successfully transfected Huh7.5 cells were stained with a rabbit anti-HBsAg primary antibody (against S region of HBV envelope proteins) and a donkey anti-rabbit conjugated to AlexaFluor 488 fluorochrome, which is shown in green colour on the first column for all the constructs A-F (figure 3.11. images 1, 4, & 7). Nuclei were counterstained with DAPI, shown in blue on the second column on all the Constructs A-F (figure 3.11. images 2, 5, & 8).

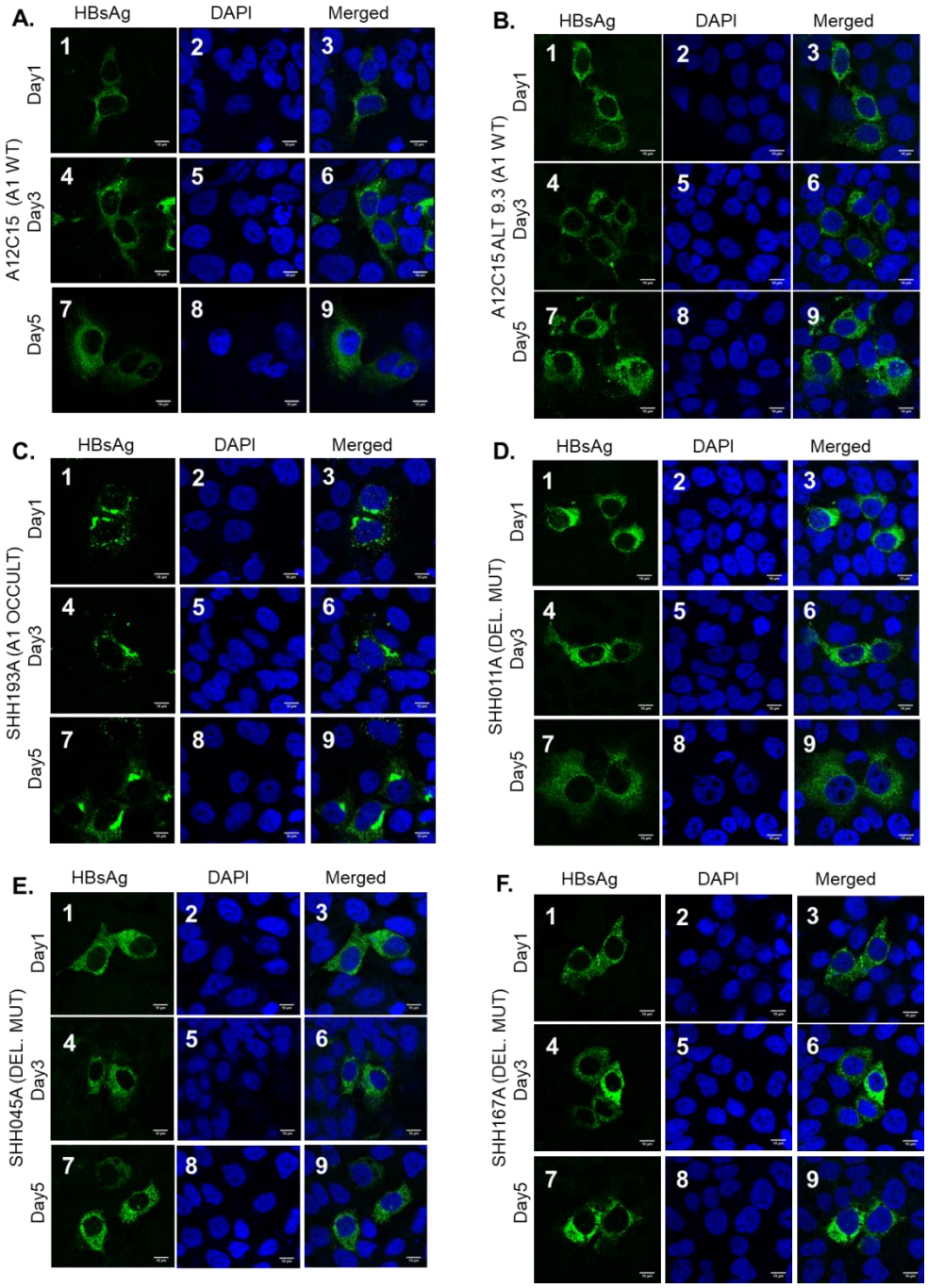

Figure 3.11: Expression of the HBV envelope proteins by the plasmid constructs on days 1, 3, and 5 post-transfection

Huh7.5 cells were transfected with plasmid constructs (Wild-type, Deletion mutant and occult), fixed subjected to indirect immunofluorescence on days 1, 3, and 5 post-transfection and viewed under a confocal microscope. Cells were treated with a primary antibody against S region of HBV envelope proteins (rabbit anti-HBsAg) and a secondary antibody labelled with AlexaFluor 488 detected in green (Constructs A-F, Images 1, 4, & 7). Nuclei were counterstained with DAPI, blue (Samples A-F, Images 2, 5, & 8). Scale bar, 10 µm.

The aim of the mono-staining immunofluorescence was to follow the expression of the envelope proteins after transfection of Huh7.5 cells with either the wild-type or the deletion mutant constructs, on days 1, 3, and 5 post-transfection. All plasmid constructs expressed envelope proteins at all the three time points post-transfection. With the exception of the construct from the occult infection (SHH193A), transfection of the cells with all other wild-type and deletion mutant constructs showed the expressed envelope proteins distributed throughout the cytoplasm throughout the time points (figure 3.11). No differences of expression and localization were noticed between the constructs. The occult infection construct, on the other hand, expressed envelope proteins as aggregates at the periphery of the nucleus, suggesting retention in the cellular compartments, which prevented secretion leading to the HBsAg-negative phenotype of the patient. Moreover, although the surface proteins were detected mainly in the cytoplasm, a small portion was found in the nucleus for all the constructs.

3.6 Quantification of the expressed envelope proteins

The quantification of the expressed HBsAg was carried out using ImageJ software as explained in Chapter 2. Tables 3.7-3.9 (Appendix C1-C3), show the mean of fluorescence of the expressed envelope proteins by all constructs for the three replicates for time points day 1, 3, and 5 post-transfection. The mean of fluorescence for each construct was quantified in the cytoplasm of 7 transfected cells for three replicates (21 quantifications for each sample per time point). For elimination of the background, the average of the means of fluorescence for a replicate was determined from non-transfected cells (Tables 3.10-3.12, Appendix C4-C6). The average mean of fluorescence of a replicate was subtracted from each quantification for each transfected cell of the same replicate (Tables 3.7-3.9, Appendix C1-C3). The resulting mean of fluorescence shown by tables 3.13-3.15, Appendix C7-C9 represent the actual fluorescence of the

expressed envelope proteins, with median, lower quartile, upper quartile and interquartile range (IQR) included (data rearranged from smallest to largest). Table 3.16 (Appendix C10) summarizes the medians of the mean of fluorescence of the expressed HBsAg in the cytoplasm as show in tables 3.13-3.15, Appendix C7-C9.

Histograms on SPSS statistical software with the use of either means or medians of the expressed HBsAg, showed a non-normally distributed data. In this current study, we followed HBsAg expression when by the same construct clones over time, a Wilcoxon signed-rank test was found to be the most appropriate test as it is a non-parametric test, meaning it does not assume normality in the data. Medians and IQRs of the mean of fluorescence were analysed to describe the outcomes of this study. The test showed no statistical significant difference in the HBsAg expression when cells were transfected with either the wild-type, occult or deletion mutant construct clones over time (Z = -1.572, p = 0.116 for day 1 against 3; Z = -1.153, p = 0.249 for day 1 against 5 and Z = -0.524, p = 0.600 for day 3 against 5 post-transfection) ($p > 0.05$ for all comparisons). The median HBsAg expression was 244.81 on day 1, 346.26 on day 3 and 364.94 on day 5 post-transfection as shown by the descriptive statistics table from the SPSS software (Appendix C11).

Figure 3.12(**A-D**) below, graphically represent the medians and IQRs of the mean of fluorescence of the expressed envelope proteins, as shown in tables 3.13-16 (Appendix C7-10). The error bars in figure 3.12**A**, represent the standard error amount for the HBsAg mean of fluorescence quantifications. The wild-type constructs (A12C15_OL and A12C15 ALT 9.3) and the deletion mutant construct (SHH011A) showed the same pattern of expression, the expression reached a peak on day 3 and decreased over time, on day 5 post-transfection. The wild-type from an occult infection (SHH193A) and the deletion mutant (SHH167A), showed a slow envelope protein expression for day 1, increasing with time. The expressed envelope proteins of deletion mutant (SHH045A), showed a

decrease on day 3 and the expression of proteins increased on day 5. This finding differs from that of the other two deletion mutants (SHH011A and SHH167A) as explained above. The deletion mutants expressed envelope proteins at comparable amounts to both wild-type clones with a different pattern of expression over time. This is consistent to our previous finding from the ELISA meaurements (Ms. S. Wolhuter, Unpublished).

The box and whisker diagrams (figure 3.12**B**-**D**) drawn using tables 3.13-3.15 (Appendix C7-C9), show the same medians with IQRs of the HBsAg mean of fluorescence for the investigated construct clones for the different time points, day 1, 3 and 5 after transfection. When cells were transfected with wild-type construct A12C15 OL 1,28MER, the envelope protein expression (shown as medians) was as follows: 239.04 (IQR= 317.71-145.31), 257.78 (IQR= 457.49-162.96) and 222.92 (IQR= 326.29-148.96) for days 1, 3 & 5 after transfection, respectively. Medians of 210.52 (IQR= 441.82-123.82), 448.70 (IQR= 615.34-239.01) and 235.61 (IQR= 405.02-112.66) were recorded for wild-type construct A12C15 ALT 9.3, while 236.66 (IQR= 306.86-98.59), 408.43 (IQR= 590.29-344.73) and 468.74 (IQR= 619.01-305.78) were recorded for the occult strain (SHH193A). For the deletion mutant construct (SHH011A), medians were recorded as follows: 340.66 (IQR= 479.09-258.37), 417.50 (IQR= 718.92-275.31) and 267.36 (IQR= 463.30-142.72) for the three time points. The second deletion mutant (SHH045A) was observed the only construct with decreased HBsAg expression on day 3 and increased on day 5, which occurred in this manner: 253.18 (IQR= 419.54-180.93), 204.87 (IQR= 381.88-152.39) and 330.34 (IQR= 534.51-212.12). Lastly, deletion mutant SHH167A, was the only mutant to show HBsAg expression which increased over time, 250.57 (IQR= 321.32-164.01), 284.08 (IQR= 335.96-159.80) and 296.22 (IQR= 434.24-211.50) for the three time points, respectively.

(A)

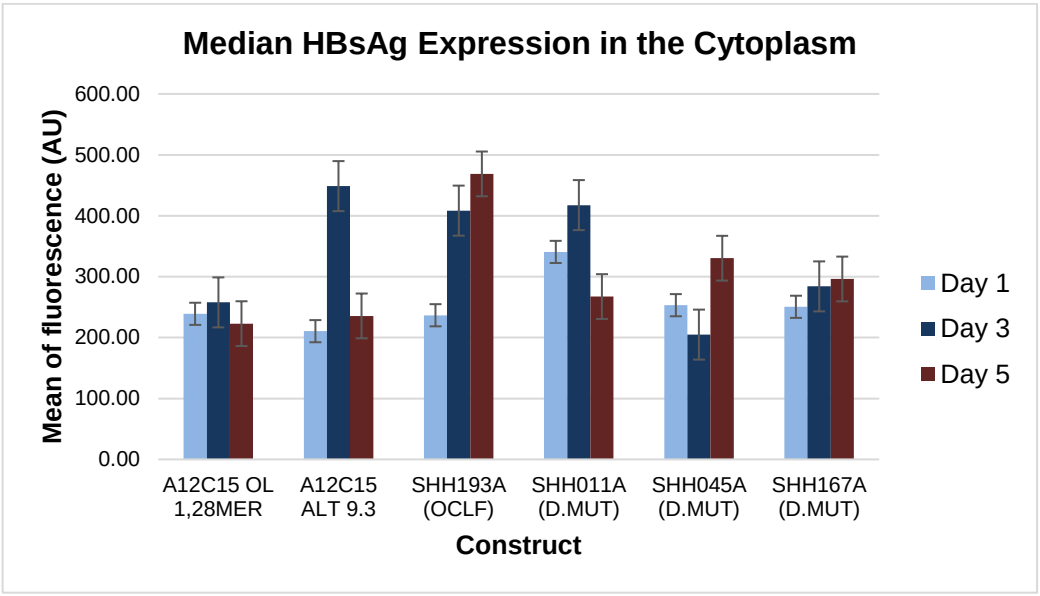
Median HBsAg Expression in the Cytoplasm
Mean of fluorescence (AU)
600.00
500.00
400.00
300.00
200.00
100.00
0.00
A12C15 OL 1,28MER
A12C15 ALT 9.3
SHH193A (OCLF)
SHH011A (D.MUT)
SHH045A (D.MUT)
SHH167A (D.MUT)
Construct
Day 1
Day 3
Day 5

(B)

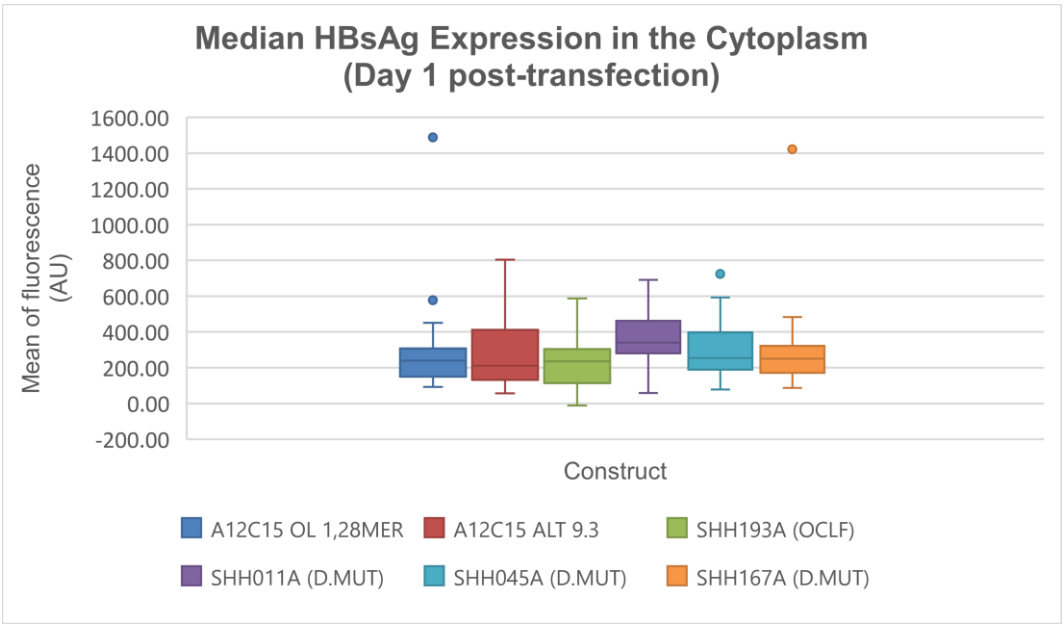
Median HBsAg Expression in the Cytoplasm
(Day 1 post-transfection)
Mean of fluorescence (AU)
1600.00
1400.00
1200.00
1000.00
800.00
600.00
400.00
200.00
0.00
-200.00
Construct
A12C15 OL 1,28MER
A12C15 ALT 9.3
SHH193A (OCLF)
SHH011A (D.MUT)
SHH045A (D.MUT)
SHH167A (D.MUT)

(C)

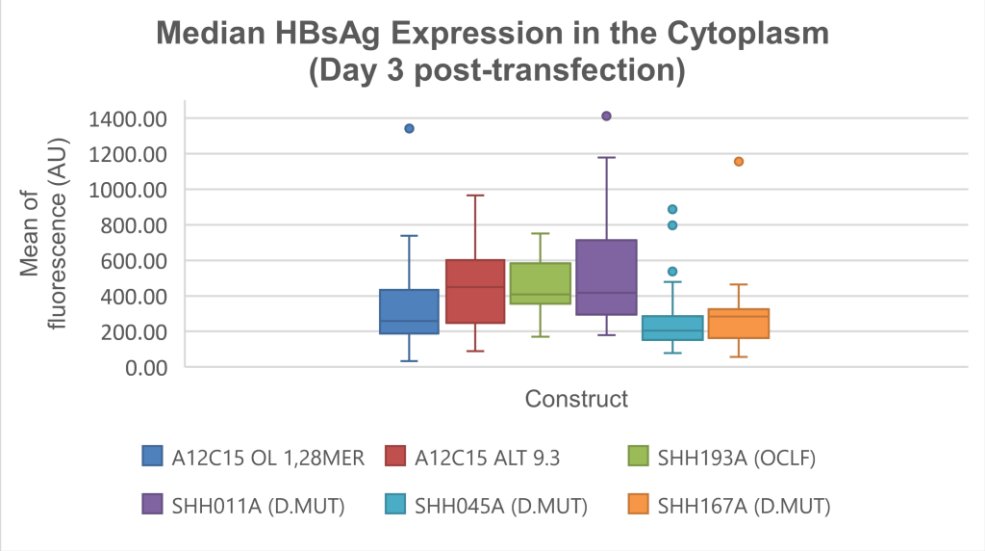

(D)

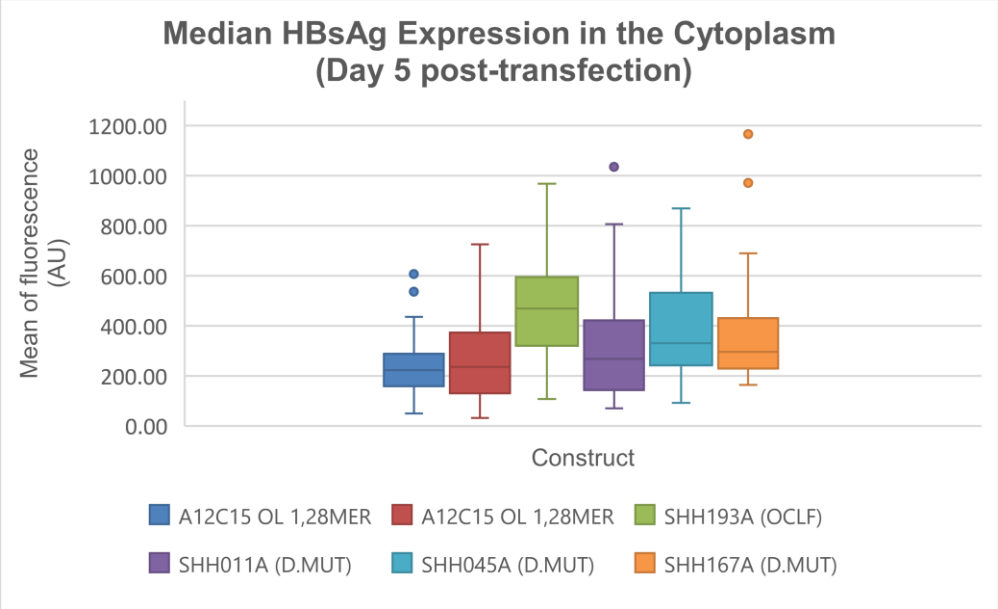

Figure 3.12A-D: Median HBsAg expression in the cytoplasm of transfected Huh7.5 cells.

A. Is a bar graph of showing the HBsAg expression in the cytoplasm of transfected Huh7.5 cells measured by ImageJ software. Different colours represent the three time points post-transfection. The error bars represent the standard deviation of the mean. **B-D.**: box and whisker plots of the same representation than **A.** for the three time points after transfection, respectively. Different colours represent each of the six plasmid construct clones.

3.7 Detection of the expressed envelope proteins using double-staining immunofluorescence technique (both envelope proteins and cellular compartments are stained).

3.7.1 Detection of cellular compartments without HBsAg

Immunofluorescence was done on non-transfected cells with a mouse anti-calnexin antibody (ER), mouse monoclonal anti-ERGIC-53 and mouse anti-giantin antibody (Golgi) individually as primary antibodies and a goat anti-mouse antibody coupled to AlexaFluor 546 fluorophore as the secondary antibody. As a control, non-transfected cells were stained with the rabbit anti-HBsAg antibody and the donkey anti-rabbit antibody coupled with AlexaFluor 488 fluorophore. As expected, no HBsAg expression was recorded as the transfection was done without any HBV plasmid construct, bearing in mind that it was used to negatively control the double-staining immunofluorescence. Figure 3.13 shows the detection of the cellular compartments, the endoplasmic reticulum (ER) (Figure 3.13A), the endoplasmic reticulum intermediate compartment (ERGIC) (Figure 3.13B) and the Golgi apparatus (Figure 3.13C).

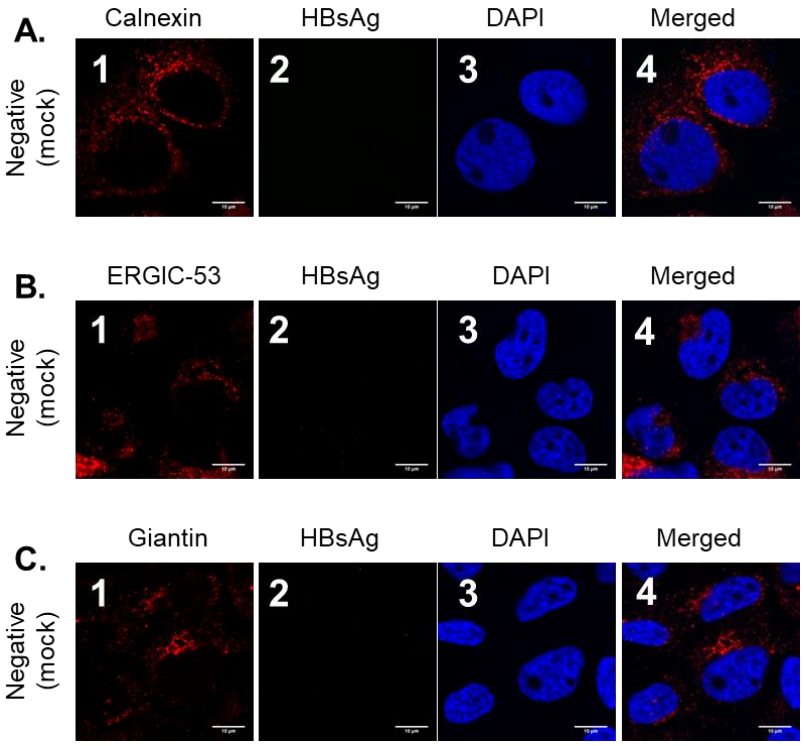

Figure 3.13: Mock transfection for the experimental control

Confocal images of double-staining experiment on non-transfected cells. Image 1A, 1B and 1C: staining of ER with mouse anti-calnexin antibody, ERGIC with mouse monoclonal anti-ERGIC-53 antibody, Golgi with mouse anti-giantin antibody, respectively and all co-stained with goat anti-mouse antibody conjugated to AlexaFluor 546 fluorophore, red. Images 2A, 2B and 2C: staining of HBsAg with rabbit anti-HBsAg, antibody co-stained with donkey anti-rabbit, conjugated with a Alexa Fluor® 488 fluorophore. No HBsAg expression was observed as expected as the cells are not transfected with the HBV DNA. Image 3A, 3B and 3C: staining of Nuclei with DAPI stain. Image 4A, 4B and 4C: shows the merged version ofimages1, 2 and 3. Images were captured on day 3 post-transfection (Scale bar: 10 µm).

3.8 Detection of the expressed envelope proteins using double-staining immunofluorescence technique

Following mono-staining immunofluorescence, we then carried out double-staining immunofluorescence on day 3 post-transfection. Intracellular localization of the expressed envelope proteins in relation to the secretory organelles (ER, ERGIC, and Golgi compartments) was the main objective for the double-staining protocol. The captured images for the intracellularly localized envelope proteins are shown in figures 3.14 - 3.16. The successfully transfected Huh7.5 cells were concurrently stained with rabbit

anti-HBsAg primary antibody and mouse antibodies against an ER marker, Calnexin (Figure 3.14), ERGIC marker (Figure 3.15), as well as Golgi marker, Giantin (Figure 3.16). The anti-HBsAg antibody was detected with a donkey anti-rabbit antibody conjugated with an AlexaFluor 488 fluorophore, green (figures 3.14 -3.16, images B, F, J, N, R, & V) and the antibodies against the markers were detected with a goat anti-mouse antibody coupled with AlexaFluor 546 fluorophore, red (figures 3.14 -3.16, images A, E, I, M, Q, & U). Co-localization of the HBsAg in a secretory organelle can be seen by the yellow colour on the merged images on the three figures (figures 3.14 -3.16, images D, H, L, P, T, & X). Nuclei were stained with DAPI, blue.

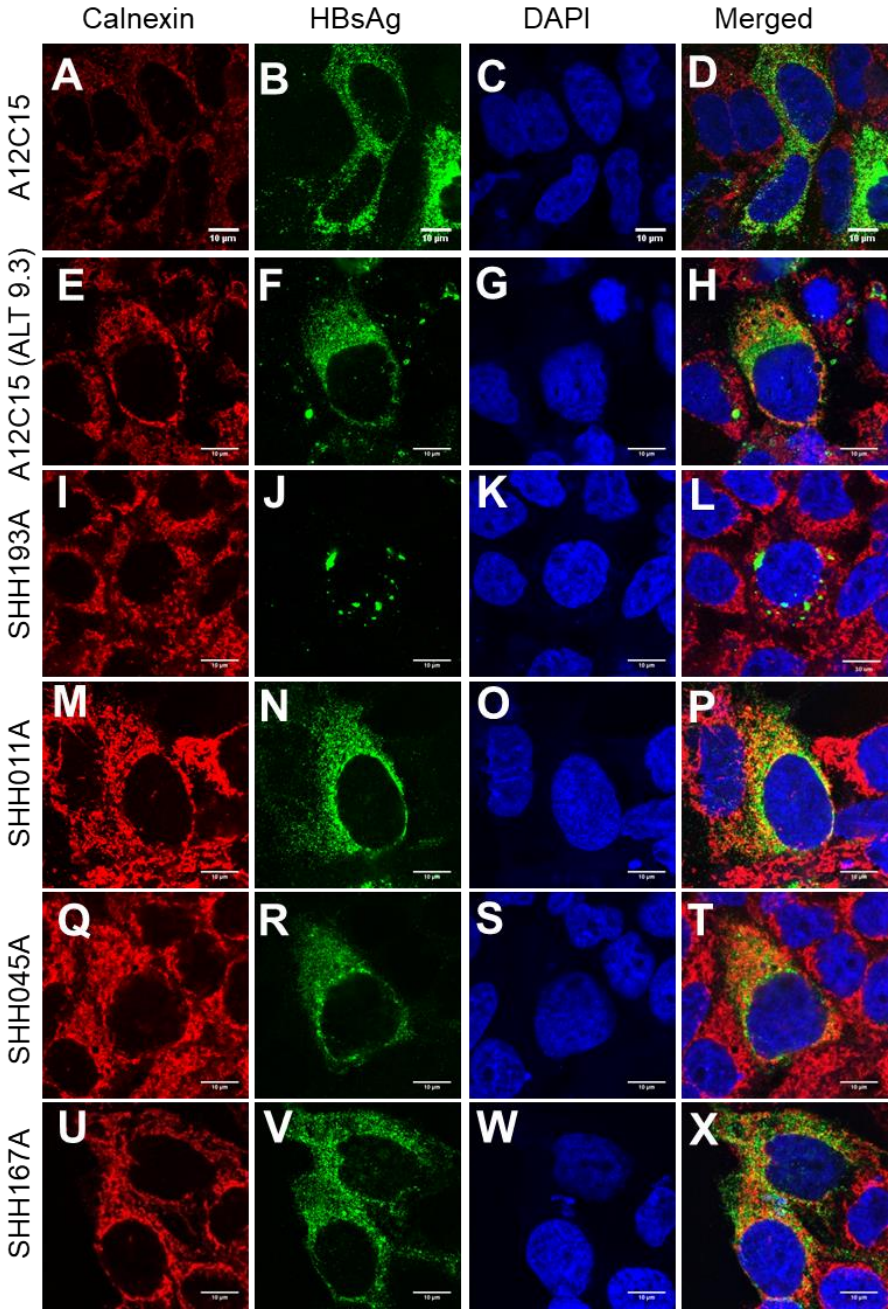

Figure 3.14: Intracellular localization of HBV envelope proteins in relation to ER

Huh7.5 cells were transfected with plasmid constructs (A12C15 OL 1.28MER, A12C15 Altered 9.3 (ALT 9.3), SHH193A, SHH011A, SHH045A, and SHH167A), fixed and then subjected to indirect double immunofluorescence staining and observed with a confocal microscope. Cells were stained with a rabbit anti-HBsAg primary antibody and donkey anti-rabbit secondary antibody conjugated with AlexaFluor 488, green (B, F, J, N, R, & V). The ER was stained with mouse anti-calnexin antibody, which was detected with goat anti-mouse antibody conjugated with AlexaFluor 546 fluorophore, red (A, E, I, M, Q, & U). Co-localization of envelope protein and the ER can be seen by the yellow colour on the merged images (D, H, L, P, T, & X). Nuclei were stained with DAPI, blue. Scale bar, 10 μm.

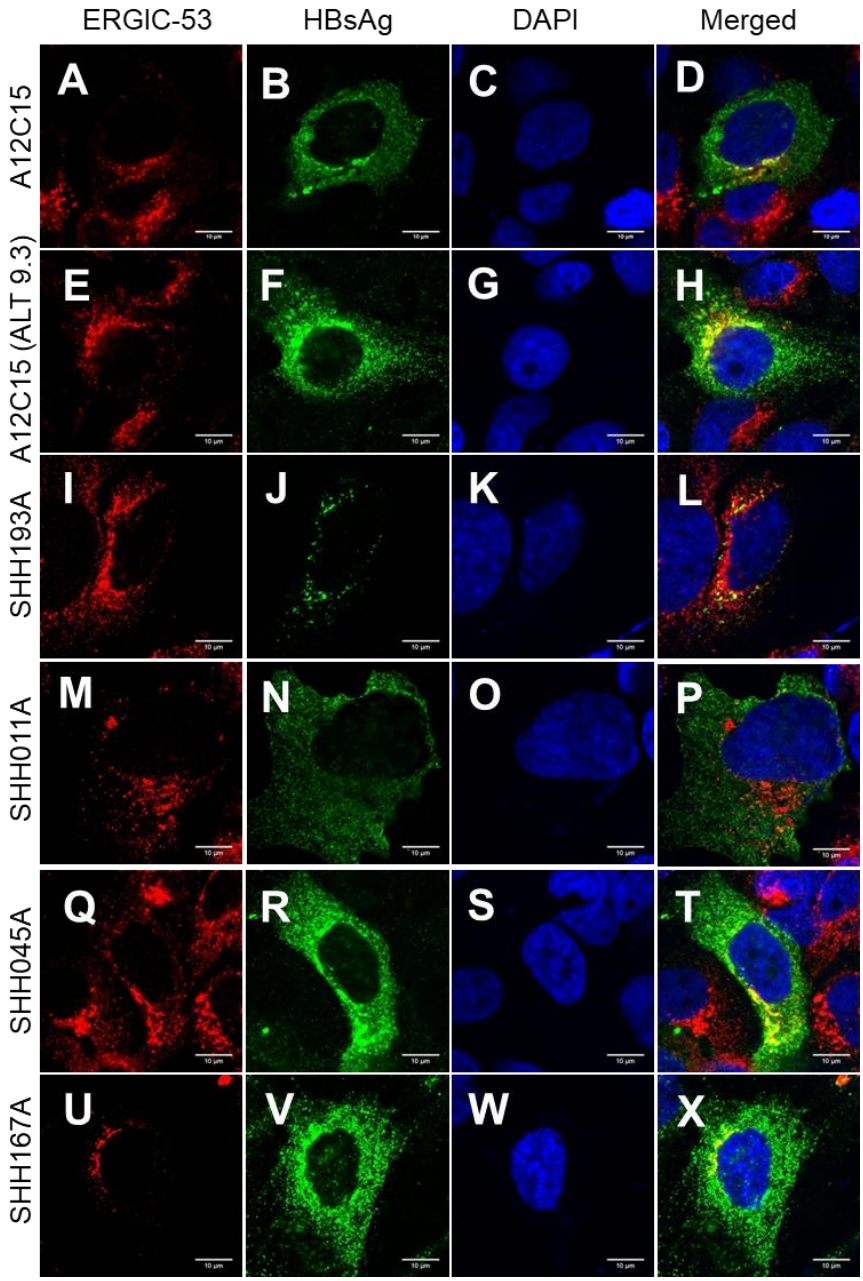

Figure 3.15: Intracellular localization of HBV envelope proteins in relation to ERGIC.

Huh7.5 cells were transfected with plasmid constructs (A12C15 OL 1.28MER, A12C15 Altered 9.3 (ALT 9.3), SHH193A, SHH011A, SHH045A, and SHH167A), fixed and then subjected to indirect double immunofluorescence staining and observed with a confocal microscope. Cells were stained with a rabbit anti-HBsAg primary antibody and donkey anti-rabbit secondary antibody conjugated with AlexaFluor 488, green (B, F, J, N, R, & V). The ERGIC was stained with mouse anti-ERGIC-53 antibody, which was detected with goat anti-mouse antibody conjugated with AlexaFluor 546 fluorophore, red (A, E, I, M, Q, & U). Co-localization of envelope protein and ERGIC can be seen by the yellow colour on the merged images (D, H, L, P, T, & X). Nuclei were stained with DAPI, blue. Scale bar, 10 µm.

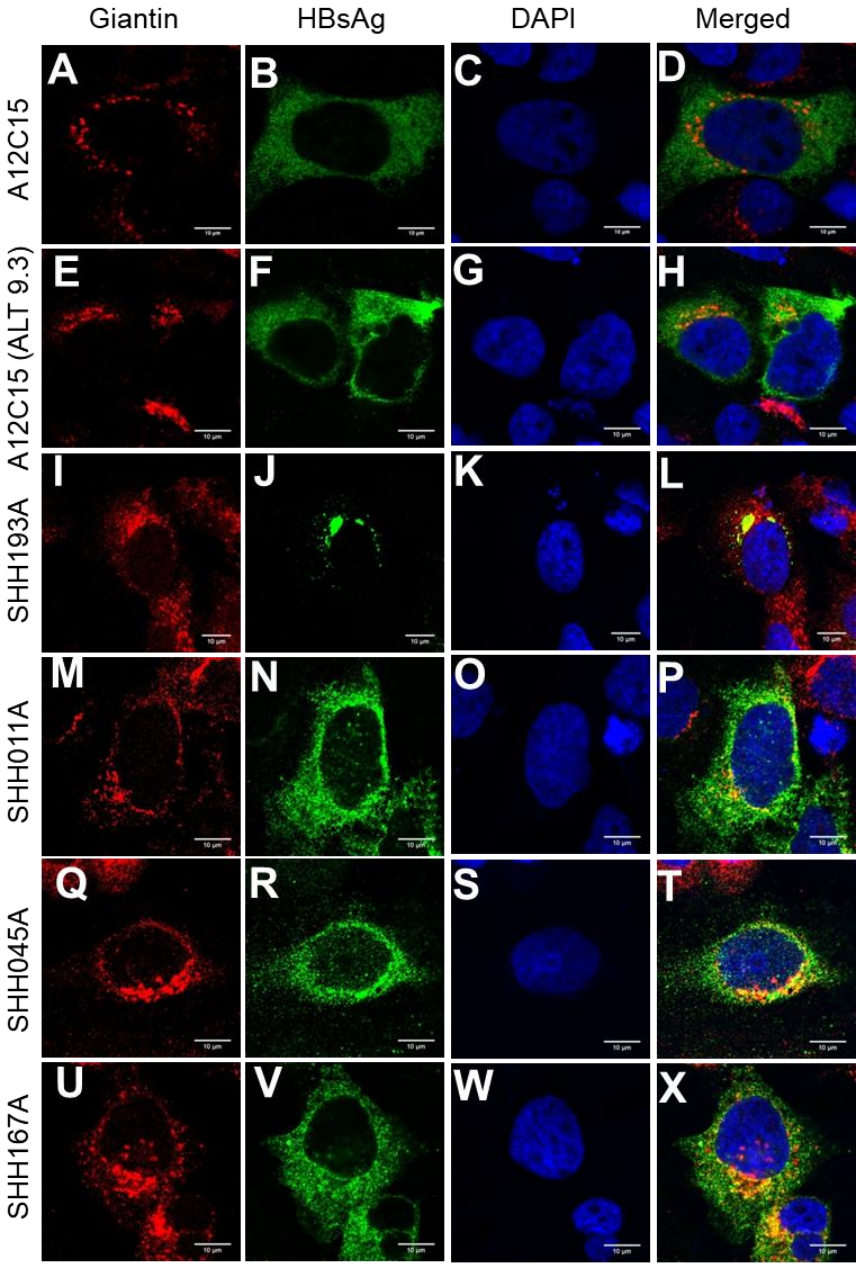

Figure 3.16: Intracellular localization of HBV envelope proteins in relation to Golgi apparatus.

Huh7.5 cells were transfected with plasmid constructs (A12C15 OL 1.28MER, A12C15 Altered 9.3 (ALT 9.3), SHH193A, SHH011A, SHH045A, and SHH167A), fixed and then subjected to indirect double immunofluorescence staining and observed with a confocal microscope. Cells were stained with a rabbit anti-HBsAg primary antibody and donkey anti-rabbit secondary antibody conjugated with AlexaFluor 488, green (B, F, J, N, R, & V). The Golgi was stained with mouse anti-giantin antibody, which was detected with goat anti-mouse antibody conjugated with AlexaFluor 546 fluorophore, red (A, E, I, M, Q, & U). Co-localization of envelope protein and golgi can be seen by the yellow colour on the merged images (D, H, L, P, T, & X). Nuclei were stained with DAPI, blue. Scale bar, 10 µm.

To be able to identify the compartments into which the envelope proteins aggregated, a double staining procedure was carried out where three cell compartments (ER, ERGIC, and Golgi) were concurrently stained with the envelope proteins on day 3 post-transfection. Similarly to the mono-staining immunofluorescence results, all the constructs expressed the envelope proteins. Moreover, the constructs showed the same pattern of envelope protein distribution throughout the transfected cells, which confirm our results. There was a comparable amount of co-localized envelope proteins in all the three compartments (ER, ERGIC and Golgi) between the deletion mutants and the wild-type constructs. For all constructs, the envelope proteins were observed in all compartments with a different pattern of expression, a finding based on the physical observation of the microscope images as shown by figures 3.14-3.16. This finding is qualitative, but it shows that the plasmid construct clones investigated are expressing HBsAg *in vitro*. The strain from the occult infection maintained the same pattern of expression as observed using mono-staining, with envelope protein aggregation at the periphery of the nucleus.

3.9 Co-localization quantification of HBV envelope protein with ER, ERGIC, & Golgi on day 3 post-transfection

In order to have quantitative results, a preliminary co-localization study with quantifications was carried out on the microscopic slides co-stained for HBV envelope proteins and for secretory pathway compartments (ER, ERGIC, & Golgi), for wild-type (A12C15 ALT 9.3), Occult full-length (SHH193A (OCFL)) and deletion mutant constructs on day 3 post-transfection using a confocal microscope. The aim was to determine the distribution of the envelope proteins within the different compartments of the secretory pathway (figure 3.17), for each construct, and to analyse the effect of deletions on the relative localization.

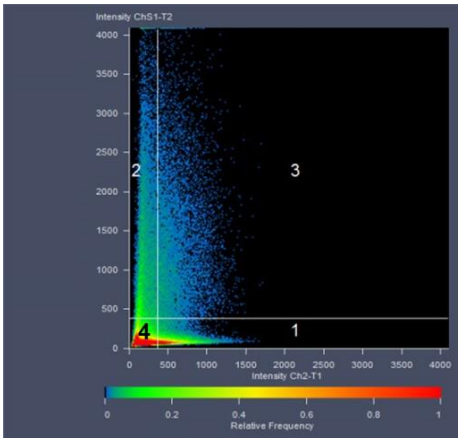

Figure 3.17: Scatter diagram for co-localization

The above diagram is a scatterplot showing different regions of quantification: 1, for pixel of the secretory organelles (red), 2 for pixel of the HBsAg (green), 3 showing co-localization pixels and lastly, 4 showing the background (settings for our quantification). The cross-hair given by the 2 lines on the graph dividing the graph into 4 regions are adjusted when settings are carried out help to determine the background and the actual co-localization pixels of the image under investigation.

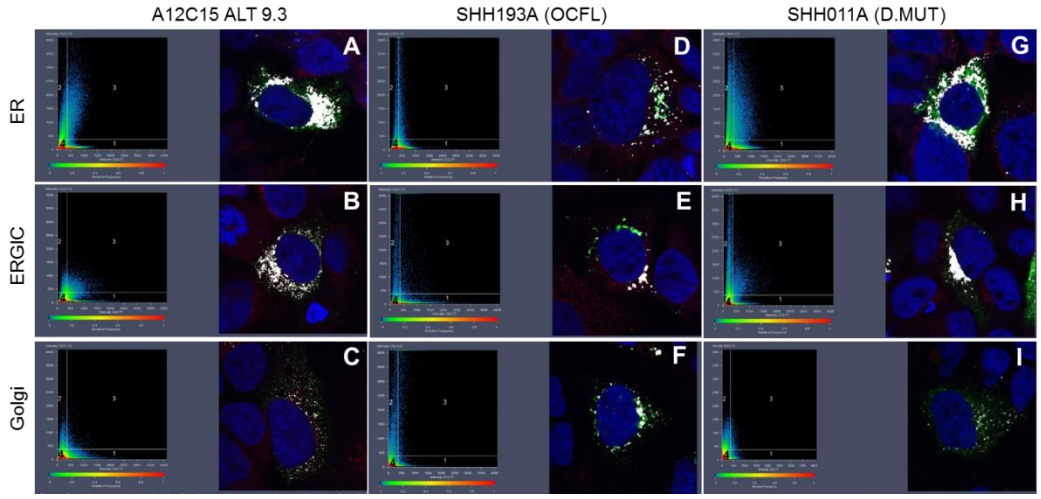

Figure 3.18: Co-localization of the HBsAg on the secretory organelles (ER, ERGIC, & Golgi) on day 3 post-transfection

Following co-staining immunofluorescence, images captured for wild-type (A12C15 ALT 9.3) **A** - **C**, occult full-length (SHH193A) **D** - **F** and deletion mutant (SHH011A) **G** - **I** on day 3 post-transfection for the ER, ERGIC and Golgi cell compartments were used for the co-localization analysis carried out using Zen software. For antibodies used to stain the HBsAg and the secretory compartments, please refer in figure 3.16. The nuclei were stained with DAPI stain, blue. White: co-localization between HBsAg and either ER, ERGIC or Golgi. Left-hand side of each picture: scatterplot of the fluorescence with region 1: pixels in channel 1 only (Red), region 2: pixels in channel 2 only (green), region 3: co-localizing pixels.

The quantification of co-localization was determined with the Zen software (Zeiss), which gives a scatter diagram of fluorescence for each transfected cell. The cross-hair on the diagram was determined to set up the background. The horizontal bar (determining the region 1, only red pixels) was set up with a mono-stained slide in red (slides stained only for ER, ERGIC and Golgi). The vertical bar (determining the region 2, only green pixels) was set up with a mono-stained slide in green (slide stained only for HBsAg). The region 4, next to the point of juncture between the X- and the Y- axes and the intersection of the 2 bars, represents the background. Region 3 shows co-localized pixels in blue (figure 3.17). The data shown in tables 3.17 – 3.18 (Appendix C12 - C13), detailes the average Manders' overlap coefficients for the quantification of the HBsAg co-localization in the secretory pathway (ER, ERGIC & Golgi). From table 3.17 (Appendix: C12), average values were shown in table 3.18 (Appendix: C13) and a bar graph showing the mean of the co-localization coefficients (Manders' overlap coefficient) was drawn (figure 3.19). Quantification was carried out for 5 cells in the ER, ERGIC and Golgi, calculated by the Zen software for cells transfected with plasmid constructs: wild-type (A12C15 ALT 9.3), occult full-length (SHH193A) and deletion mutant (SHH011A). The results are preliminary because only a few quantifications were carried out and this quantification software has only recently been installed, meaning further optimizations may be necessary. Because the plasmid construct clones used for the intracellular co-localization assay against the three cell compartments (ER, ERGIC & Golgi) were the same and the data was almost equally distributed, we carried out a paired samples t-test using SPSS software and the outcomes shown in Appendix C14. A dependent t-test or paired samples t-test compares the means between two related groups on the same continuous, dependent variable.

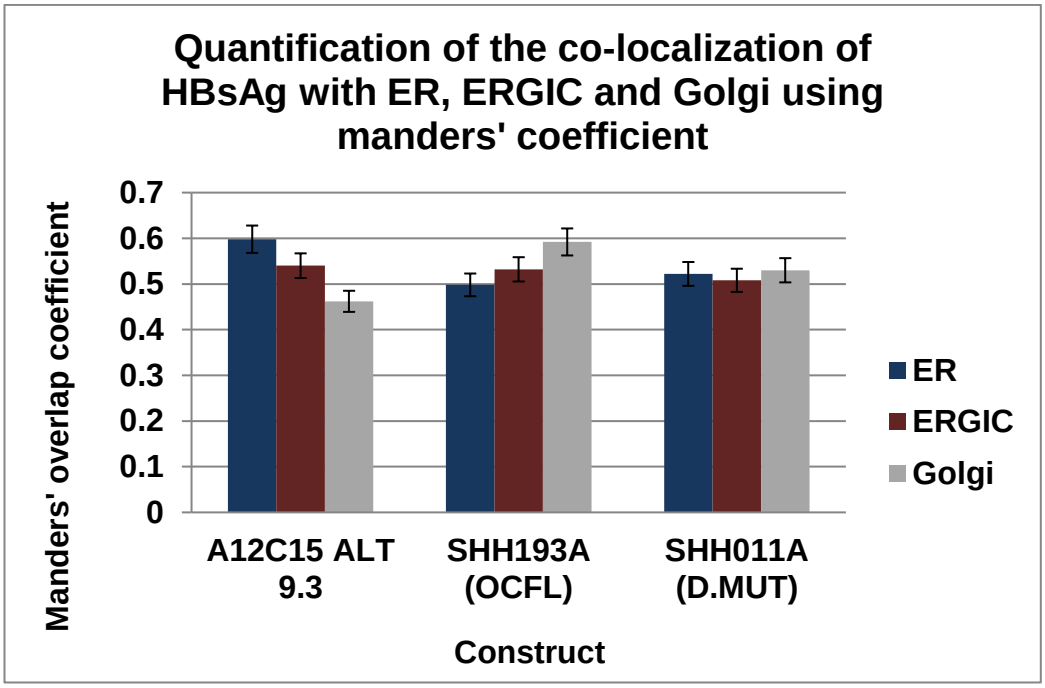

Figure 3.19: Quantification of the co-localization of HBsAg with the secretory organelles (ER, ERGIC, & Golgi) on day 3 post-transfection

This graph is a representation of the quantified HBsAg (overlap coefficiency) in the different cellular compartments. Three Constructs (1 Wild-type, 1 Occult full-length & 1 Deletion mutant) were assessed against three cell compartments of the cellular secretory pathway (ER, ERGIC, & Golgi). Transfected cells with Wild-type (A12C15 ALT 9.3) (n=5), Occult strain (SHH193A) (n=5) and Deletion mutant (SHH011A) (n=5) constructs labelled for ER, ERGIC and Golgi, respectively using data from figure 3.18. The average of the Manders' overlap coefficients was measured by the Zen software.

3.10 Overlap coefficient quantification (Manders)

The Manders' overlap coefficient is one of the parameters used to quantify co-localization in images and it is insensitive to differences in signal intensities between the 2 channels or photo-bleaching. This measurement is given by the Zen software for each image (the pictures were taken in order to have only 1 transfected cell) and where the co-localization analysis was done as described above and figure 3.18. The scale of Manders' coefficient is between 0 and 1 (0 equals no co-localization, while 1 means all pixels are co-localized). When cells were transfected with A12C15 ALT 9.3 (wild-type), a co-localization of the HBsAg of about 60% in the ER, 54% in the ERGIC and 46% in the Golgi compartment was

recorded, thus showing a slightly higher co-localization in the ER than the other compartments (figure 3.19). HBsAg co-localization of about 50% in the ER, 53% in the ERGIC and 59% Golgi was recorded for cells transfected with SHH193A (occult strain), showing a slightly higher co-localization in the Golgi than the other compartments. Lastly, an HBsAg co-localization of about 52% in ER, 51% in the ERGIC and 53% in the Golgi was recorded when cells were transfected with SHH011A (deletion mutant) construct, showing a co-localization that is almost the same throughout the cell compartments.

A paired samples t-test was run to determine if there was a difference in the co-localization of the expressed HBsAg in the cell compartments of the HBsAg secretory pathway when Huh7.5 cells were transfected with either wild-type (A12C15 ALT 9.3), occult strain (SHH193A) or deletion mutant (SHH011A) plasmid construct clones on day 3 after transfection. Through normality check using boxplots and scatter diagrams on Microsoft excel, we found that there were no outliers and with histograms using SPSS our data was found to be equally distributed. Using a paired samples t-test, we showed that there is no statistical significant difference in the co-localized HBsAg amongst the cell compartments (ER, ERGIC & Golgi) when cells were transfected with any of the construct clones (A12C15 ALT 9.3, SHH193A & SHH011A), $t(2) = -0.476$, $p = 0.681$ for HBsAg co-localizations in the ER against HBsAg co-localizations in the ERGIC cell compartment. For the HBsAg co-localizations in the ER against Golgi, the following was found: $t(2) = -0.186$, $p = 0.869$, with $t(2) = 0.000$, $p = 1.000$ for the the HBsAg co-localizations in the Golgi against the ERGIC. The differences reported seem to be occurring by chance.

However, these results have to be interpreted with caution, as they are still preliminary results done on 5 cells. Optimization of the co-localization quantification is in progress in the laboratory, with the selection of a region of interest for each picture. This will allow focusing only on the transfected cells or even the secretory pathway of the transfected cells and eliminating

non-transfected cells, which can bias the results. Although many different coefficients for co-localization analysis exist it seems that Manders' coefficient (figure 3.19) is the best option to quantify our results.

CHAPTER 4: DISCUSSION

Some areas of sub-Saharan Africa are regarded as regions of HBV hyperendemicity, based on the prevalence of the HBsAg carrier rates of greater than 8% (Kramvis and Kew, 2007). It is also the region in the world with the greatest prevalence of HIV infection (Kourtis *et al*., 2012). HBV-HIV co-infection is frequent in the region with an average of 36% (Matthews *et al*., 2014). In a study carried out in Mpumalanga Province, 23.8% of the HIV positive participants, prior to the initiation of anti-retroviral therapy (ART), were found to be co-infected with HBV. About 9% of the co-infected individuals were HBsAg positive (overt infection) and about 15% were HBsAg negative (occult infection) (Bell *et al*., 2012). Molecular analysis from these HIV-infected individuals showed the majority to be infected with subgenotype A1 (Makondo *et al*., 2012). In the same study, pre-S deletion mutants were isolated, four from an overt infection (HBsAg-positive) (SHH011A, SHH167A, SHH274A and SHH300A) and one from an occult (HBsAg-negative) HBV infection (SHH045A). The majority of deletion mutants were pre-S2 deletion mutants (Makondo *et al*., 2012). Similar deletion mutants were also found in HCC patients infected with subgenotype A1 in South Africa (Skelton *et al*., 2012), Kenya (Ochwoto *et al*., 2013) and India (Gopalakrishnan *et al*., 2013) and as shown for other genotypes of HBV, are a risk factor for the development HCC (Liu *et al*., 2009, Chen *et al*., 2007). SHH011A had the pre-S1/pre-S2 deletion mutant, which also leads to the removal of the pre-S2 start codon, which has been shown to lead to the absence of MHBs synthesis and expression (Chen *et al*., 2006, Pollicino *et al*., 1995). MHBs is not required for viral replication and therefore the virus can survive even in the absence of MHBs expression (Pollicino *et al*., 2014).

The three surface proteins are encoded by a single ORF, the S ORF but translated from 2 pre-S mRNAs being with different sizes (2.4 kb and 2.1 kb pre-S mRNAs). The 2.4 kb pre-S1 mRNA transcript encodes for the LHBs and the shorter 2.1 kb pre-S2 transcript for both the MHBs and

HBsAg (Seeger and Mason, 2000). As indicated in the HBV life cycle in chapter 1, the newly synthesized nucleocapsid is transported into the ER, where it acquires the ER membrane containing lipids and embedded SHBs, MHBs and the LHBs proteins forming a mature virion or Dane particle. Envelope protein expression and secretion is through the secretory pathway (through the ER, ERGIC and the Golgi apparatus) (Seeger and Mason, 2000, Lambert *et al*., 2007). SHBs and MHBs are reported to be synthesized in excess when compared to the LHBs protein (10% less) and the ratio is important for viral assembly and secretion. LHBs is important for secretion and all 3 proteins (LHBs, MHBs and SHBs) have different functions for viral morphogenesis and secretion (Huang and Yen, 1993, Pollicino *et al*., 2014). The pre-S deletion mutants (especially pre-S2 mutant LHBs), which were present in the HBV-HIV infected individuals (Makondo *et al*., 2012) and from which the plasmid constructs were generated (S. Wolhuter, MSc: University of the Witwatersrand) have been reported to be a risk factor for chronic liver disease including HCC. The mechanism that leads to HCC is hypothesized to occur as follows: deletion mutations induce protein misfolding, accumulation of the misfolded proteins in the ER, ER stress-dependent DNA damage, leading to apoptosis and then HCC (Chen *et al*., 2007, Chen *et al*., 2013, Yen *et al*., 2018).

Moreover, the pre-S domain of the HBsAg contains overlapping B and T cell epitopes (Neurath *et al*., 1984). Mutations in that region may be associated with alteration of these epitopes and that may lead to host immune recognition impairment, enhanced virulence with increased replication of HBV, escape mutants (Chen *et al*., 2006) and this is advantageous for the virus, leading to its persistence and chronic infection and, as shown by an earlier study, these deletion mutants form the major population of the quasispecies (S. Wolhuter, MSc: University of the Witwatersrand). Chronic HBV infection can ultimately lead to hepatocarcinogenesis.

In order to functionally characterize the deletion mutants detected in the HIV-infected patients (Makondo *et al*., 2012), in a follow up study, plasmid constructs were generated from the HBV isolates (SHH011A, SHH167A, SHH274A, SHH045A and SHH300A) and were found to express HBsAg *in vitro* (S. Wolhuter, MSc: University of the Witwatersrand). In the same study, a plasmid construct from an occult HBV infected HIV positive participant (SHH193A) was generated and post-transfection, this construct replicated the HBsAg negative phenotype seen in the patient (S. Wolhuter, MSc: University of the Witwatersrand).

The aim of the current project was to follow the expression of HBsAg by the deletion mutants (SHH011A, SHH045A and SHH167A) and occult strain (SHH193A) relative to the wild-type subgenotype A1 strains (A12C15 OL 1.28MER, A12C15 Altered 9.3) using immunocytochemistry and confocal microscopy. Although the expression of the deletion mutants has been carried out for other genotypes, such as B and C prevailing in south-east Asia (Kramvis *et al*., 2005), this has never been done for subgenotype A1.

Before carrying out the transfection and immunocytochemistry, the sequences of the subgenotype A1 plasmid constructs were first confirmed before further analysis as highlighted by figure 2.1 in chapter 2.

In the current study, we have shown the expression of the envelope proteins from both the deletion mutant and the wild-type constructs for days 1, 3 and 5 after transfection. Envelope protein expression by the deletion mutant containing deletions in both the pre-S1/pre-S2 (SHH011A) was slightly quicker when compared to that of the wild-type constructs (A12C15_OL and A12C15 ALT 9.3) as well as when compared to the other deletion mutants (SHH045A and SHH167A) (figure 3.12) and that finding is consistent to the finding of Chen et al, on enhanced virulence with increased replication of HBV with such mutations (Chen *et al*., 2006). In general, the deletion mutants expressed envelope proteins, at

comparable amounts to that shown by the wild-type constructs, which is found to be consistent to our previous finding from the ELISA results (Ms. S. Wolhuter, Unpublished). This finding differs to the ELISAs shown by Wang and co-workers, who showed decreased envelope protein expression by 50% for the first deletion mutant (pre-S1 region) and by 22% for the second deletion mutant (pre-S2 region) constructs (genotype not specified) (Wang *et al*., 2003). In a Japanese study, a predominance of genotype C over genotype B in patients with chronic liver disease, chronic hepatitis and HCC patients was reported (Sakugawa *et al*., 2002). Kew et al, showed a 4.5-fold increased risk for developing HCC for genotype A compared to non-A genotypes (Kew *et al*., 2005). HBV genotype A & C have a higher tendency of chronicity than B & D and genotypes C & D have a worse liver cancer and HCC outcomes than genotypes A & B (Allain, 2006, Sunbul, 2014). Sadeghi et al, also showed genotype D pre-S mutants from an occult infection in HIV-positive patients to decrease the envelope protein expression when compared to the wild-type construct clones for both intra- and extra-cellular analysis (Sadeghi *et al*., 2017).

Envelope protein aggregation in perinuclear region of the Huh7.5 cells when transfected with a strain from an occult infection (SHH193A) was observed from images captured on a confocal microscope (figure 3.11; 3.14 - 16). This finding is suggestive of envelope protein retention in the cellular compartments, which prevented secretion leading to the HBsAg-negative phenotype of the patient. The envelope protein aggregation was found to be consistent through the time-points after transfection for both mono- and double-staining immunofluorescence. A slow expression of the envelope proteins in the cytoplasm was recorded on day 1 after transfection when cells were transfected with SHH193A construct, supporting the finding of envelope protein retention within the cell compartments. A similar perinuclear and cytoplasmic fluorescence was also reported by others who investigated HBV strains belonging to genotype D isolated from occult infections (Sadeghi *et al*., 2017) whereas

SHH193A, investigated in the present study, belonged to subgenotype A1. A possible explanation for a similar pattern of expression between the mentioned genotypes could be because an OBI is associated with retention of those HBsAg, hence found at the perinuclear region as explained by Raimondo and co-workers (Raimondo *et al*., 2008). Thus it appears that the retention of the HBsAg in the perinuclear region may contribute to the HBsAg-negative phenotype regardless of the genotype of HBV.

Using the Zen software (Zeiss), we carried out quantification of the envelope proteins co-localized in the cellular secretory pathway (ER, ERGIC and Golgi) using the correlation and overlap coefficient values. As the software had only been recently installed on our system, the quantification analysis was preliminary and was meant to pave the way for future analysis, which will include quantifications for all plasmid constructs and quantifications being carried out on more cells per sample.

Although other groups have shown the expression of the envelope proteins by pre-S deletion mutants of different HBV genotypes, this study is the first to show the expression of the envelope proteins for subgenotype A1 constructs. Immunocytochemistry and high resolution confocal microscopy was successfully used to follow the expression of HBsAg in the secretory pathway. Although the kinetics of expression of the deletion mutants differed from those of the wild-type constructs, the captured images showed the expressed envelope proteins to have a similar pattern of distribution within the cell compartments. The strain isolated from the HIV-positive patient with HBsAg-negative (occult) infection showed a different pattern of expression within the cell, with the accumulation of the protein in the perinuclear region, which can explain the lack of expression of HBsAg in the supernatant *in vitro* and in the serum of the patient *in vivo.* Further optimization of the coefficient analyses will allow for the qualitative observations of the present study to

be measured and quantified, with further comparison of the expression of HBsAg by the wild-type, deletion mutant and occult strains.

CHAPTER 5: CONCLUSION AND FUTURE PLANS

In conclusion, we followed the expression of the envelope proteins for cells transfected with pre-S deletion mutants against the wild-type constructs of HBV subgenotype A1 through Immunofluorescence using a confocal microscope. Deletion mutants of subgenotype A1 have shown almost a similar pattern of HBsAg expression under microscopic examination. The differences in the expressed HBsAg for cells transfected with either pre-S deletion mutants, wild-type and the occult constructs were found not to be statistically significant for expressions of day 1 against 3 and both days 3 against 5 and 1 against 5 post-transfection with Wilcoxon Signed-Rank test. Using Paired Samples T-test, the study also showed no statistical significant difference in the co-localized HBsAg in all three cell compartments (ER, ERGIC, & Golgi) when cells were transfected with any of the construct clones. The strain isolated from the HIV-positive patient with HBsAg-negative (occult) infection showed a different pattern of expression within the cell, with the HBsAg accumulation in the perinuclear region, which can explain the lack of expression of HBsAg in the supernatant *in vitro* and in the serum of the patient *in vivo.*

We can recommend that a co-localization assay on the expressed HBsAg on the cell secretory pathway be carried out with a much bigger sample size. This could give a clearer result in terms of which cell compartment in the secretory pathway the HBsAg is co-localized.

APPENDICES:

Appendix A1: Materials used

1. Primary and Secondary antibodies and DNA Fluorescent stain:

   I. Rabbit Polyclonal HBsAg against the S region (SA8045) antibody was kindly donated by Dr. Dieter Glebe, Institute of Medical Virology, Justus-Liebig University, Giessen, Germany. (Import permit to be attached as appendix B1).
   II. Anti-Calnexin antibody (AF18) ab31290, Abcam (Cambridge, USA).
   III. Monoclonal anti-ERGIC-53 (kindly donated by Prof. H Hauri, Department of Pharmacology, Biozentrum, University of Basel, Switzerland).
   IV. Anti-Giantin antibody (9B6) – Golgi Marker ab37266, Abcam (Cambridge, USA).
   V. Goat anti-Mouse IgG (H+L) Secondary Antibody, Alexa Fluor® 546 conjugate, Thermo Fisher Scientific (Waltham, USA).
   VI. Donkey anti-Rabbit IgG (H+L) Secondary Antibody, Alexa Fluor® 488 conjugate, Thermo Fisher Scientific (Waltham, USA).
   VII. 4′,6-Diamidino-2-Phenylindole, Dihydrocloride (DAPI) was supplied by Thermo Fisher Scientific (Waltham, USA).

2. Antibiotics:

   I. Ampicillin and Kanamycin were supplied by Melford Laboratories Ltd (Ipswich, UK).
   II. 100x Penicillin Streptomycin Glutamine was supplied by GibCo™ by Life Tech Technologies (Paisley, Scotland).

3. Bacterial Strains and Cell line used:

I. SCS110 *Escherichia coli* cell line was acquired from Stratagene-Agilent Technologies (California, USA).
II. The Huh7.5 cell line was kindly donated by Professor Charles M. Rice from the Rockefeller University, NY, USA.

4. Solutions and Liquids:

I. Propan-2-ol, Absolute Ethanol, Methanol, and Glycerol were supplied by Merck (Darmstadt, Germany).
II. Sabax water for injection was supplied by Adcock Ingram (Johannesburg, South Africa).
III. Ethidium Bromide was acquired from Bio Basic Inc. (Ontario, Canada).
IV. 0.25% Trypsin EDTA (10x), DMEM (1X) + GlutaMAX™-1, Minimum Essential Medium Non-Essential Amino Acids (MEM NAA) (100X) were supplied by GibCo™ by Life Tech Technologies (Paisley, Scotland).
V. Foetal Bovine Serum was acquired from Thermo Scientific (Northumberland, UK) and by GibCo™ by Life Tech Technologies (Paisley, Scotland).
VI. *TransIT*® Transfection reagent was obtained from Mirus Bio (Madison, USA).
VII. 6X Blue/Orange Loading Dye was acquired from PROMEGA (WI, USA).
VIII. ProLong™ Gold antifade reagent was supplied by Thermo Fisher Scientific (MA, USA).
IX. 4% Formaldehyde
X. 0.5% Triton

5. Enzymes:

I. Restriction enzymes and their respective buffers were supplied by New England Biolabs (Ipswich, UK) and Thermo Fisher Scientific Inc. (Renfrew, Scotland).

II. HotStarTaq® Polymerase was from Qiagen GmbH (Hilden, Germany).
III. Taq/Tgo Polymerase mix, Roche (Mannheim, Germany).

6. Kits: QIAprep® Spin Miniprep kit, QIAGEN® Plasmid Maxi kit and HotStarTaq® MasterMix Kit, Qiagen GmbH were all from Whitehead Scientific (Pty) Ltd (Hilden, Germany).

7. Molecular Weight Markers:

I. The 1kb DNA Plus GeneRuler™ Ladder, O′GeneRuler™ 1kb DNA Ladder, GeneRuler™ 1kb DNA Ladder and GeneRuler™ 1kb DNA Ladder were supplied by Thermo Fisher Scientific Inc. (Renfrew, Scotland).
II. The 1 kb DNA Ladder was supplied by Promega (Madison, USA).
III. GeneRuler 1Kb Plus DNA Ladder, Ready-to-use, was from Thermo Scientific (Lithuania, EU).

8. Primers: Forward and reverse primers for the complete S-gene was acquired from Integrated DNA Technologies (IDT) of Whitehead Scientific (Cape Town, South Africa).

9. Dry Chemicals:

I. Sodium Cloride, Tris(hydroxymethyl)aminomethane and Bacteriological Agar were supplied by Merck Chemicals (Pty) Ltd (Wadeville, South Africa).
II. Tryptone was obtained from Melford Laboratories Ltd (Ipswich, UK).
III. Yeast extract was acquired from Sigma-Aldrich (St. Louis, USA).
IV. Piperazine-1,2-bis (2-ethanesulfonic acid) (PIPES) were obtained from Merck (Darmstadt, Germany).
V. Magnesium Chloride and Calcium Chloride were supplied by Saarchem (Krugersdorp, South Africa).
VI. Bovine Serum Albumin was supplied by Roche Diagnostics (Indianapolis, USA).

VII. Molecular Grade Agarose was supplied by White Scientific (Cape Town, South Africa).

VIII. Gibco™ Phosphate Buffered Saline tablets were supplied by GibCo™ by Life Tech Technologies (Paisley, Scotland).

IX. Protease Inhibitor Cocktail tablets complete Mini was obtained from Roche (Manheim, Germany).

10. Plastic/Glassware and other consumables:

I. Frosted microscope slides, nitrile and latex gloves were acquired from Lasec (Cape Town, South Africa).

II. 5, 10, 20 and 50 ml pipettes were acquired from Techno Plastic 48 Products® (Trasadingen, Switzerland).

III. 15 ml falcon tubes and 50ml tubes were supplied by Greiner Bio-One (GmbH, Austria).

IV. The 1,5 and 2,0 ml tubes were supplied by Eppendorf (Barkhausenweg, Hamburg).

V. The PCR tubes were acquired from QSP Hoffman-LaRoche (Basel, Switzerland).

VI. 47 mm Petri dishes were acquired from Merck Millipore (Darmstadt, Germany).

VII. Tissue culture 12-well plates, as well as 5, 10, 20 and 50 ml pipettes, were acquired from Techno Plastic Products® (Trasadingen, Switzerland).

VIII. Minisart 0.2 μm filter units were obtained from Sartorius (Goettingen, Germany).

IX. 75 cm^2 cell culture flasks were obtained from Sigma-Aldrich (St. Louis, USA).

Appendix A2: Plasmid construct clones used

Table 2.1: Plasmid construct clones used during this study

Plasmid Name:	Description:	Source/ Reference:
pTZ57R/T	TA cloning vector that allows for blue-white screening and has an ampicillin resistance gene	Thermo Scientific/ Fermentas
pEGFP-C3	A mammalian expression vector containing a fluorescent tag (Green Fluorescent Protein) under the control of the CMV promoter. Contains a Kanamycin resistance gene. Used here to calculate transfection efficiency	Addgene/Clonetech
A12C15_OL A1WTSA1.281MER	1.28 overlength replication-competent Hepatitis B Virus genome of subgenotype A1 within pcDNA4_TO backbone	(Bhoola et al., 2014)
A12C15_OL A1WTSA1.281MER Altered 9.3	The 1.28 overlength replication-competent Hepatitis B Virus genome of subgenotype A1 within pcDNA4_TO backbone, where the third XbaI site present in the backbone was removed and is thus 32 bp shorter than the parent plasmid	Ms S. Wolhuter
OL _DELMUT SHH011A-F	The 1.28 overlength replication-competent subgenotype A1 backbone containing the SHH011A deletion-mutant in the correct orientation	Ms S. Wolhuter
OL _DELMUT SHH045A-F	The 1.28 overlength replication-competent subgenotype A1 backbone containing the SHH045A deletion-mutant in the correct orientation	Ms S. Wolhuter
OL _DELMUT SHH167A-F	The 1.28 overlength replication-competent subgenotype A1 backbone containing the SHH167A deletion-mutant in the correct orientation	Ms S. Wolhuter
OL _OCFL SHH193A-F	The 1.28 overlength replication-competent subgenotype A1 backbone containing the S region of patient SHH193A, which is a occult full-length, sequence in the correct direction	Ms S. Wolhuter

Appendix A3: Bacterial strain and cell line used

Table 2.2: Bacterial strain and cell line used for this study

Bacterial strain or cell line:	Description:	Supplier and Reference:
Escherichia coli SCS110	This is a Dam and Dcm methylation-free strain used for cloning when DNA needs to be restricted with methylation-sensitive enzymes	Stratagene-Agilent Technologies
Huh7.5 human hepatic cell line	A human hepatic cell line generated from the explant of the hepatocellular carcinoma of a male patient in Japan in 1982.	Kindly donated by Professor Charles M. Rice from the Rockefeller University, NY, USA.

Appendix A4: Equipment Used for this Project

Pipettes were either from Gilson Inc. (Middleton, USA), or Finnpipette made by Thermo Fisher Scientific Inc. (Renfrew, Scotland). The Eppendorf Easypet 4221 was from Eppendorf (Barkhausenweg, Hamburg). With other equipment including: centrifuges S810R, 5424, 5417C and 5453, the Thermomixer Comfort with 1.5ml adaptor acquired from Eppendorf (Barkhausenweg, Hamburg). T100™ Thermal Cycler PCR machine was acquired from BioRad (California, USA). Hettich Universal II centrifuge in the tissue culture lab was from DJB Labcare Ltd. (Buckinghamshire, UK). The NanoDrop ND 1000 spectrophotometer was acquired from NanoDrop Technologies-Thermo Fisher Scientific Inc. (Waltham, USA). The Sub-Cell® GT electrophoresis tanks, the PowerPac™ Basic power packs, Geld Doc system and the accompanying software: Quantity-One v4.6.9 were supplied by BioRad (California, USA). The DarkReader Transilluminator DR-45M was from Clare Chemical Research (Dolores, USA). The Heal Force HF90 CO_2 Incubator from Heal Force (Shanghai, China) and the Forma™ Scientific™ Water Jacketed CO_2 Incubator supplied by Thermo

Fisher Scientific Inc. (Renfrew, Scotland) were used in the tissue culture laboratory. The Olympus CK2 inverted microscope was obtained from Olympus Optical Co., Ltd. (Tokyo, Japan). The Erma Optical Works autoclave acquired from Optical Works Inc. (Tokyo, Japan) and the SteriLClav-28 from Raypa® (Barcelona, Spain) were used. The Orion Star™ A111 pH benchtop meter was acquired from Thermo Fisher Scientific Inc. (Renfrew, Scotland). Most chest/upright fridges and freezers were acquired from Defy Appliances (Pty) Ltd (Durban, South Africa). The Heidolph MR1 magnetic stirrer was obtained from Heidolph (Schwabach, Germany). The Prism microcentrifuges and the Accublock Digital Dry bath were acquired from Labnet International Inc. (Edison, USA). The Biosan DNA/RNA UV cleaner hood for PCR and extraction was obtained from BioSan Medical-Biological Research and Technologies (Riga, Latvia). The fume hood (with no UV light), the 37°C shaking incubator and the -70°C chest freezer were supplied by Labcon Air and Vacuum Technologies (Midrand, South Africa). Labotec Bio-Flow laminar flow fume hood used in the tissue culture room was supplied by Labotec (Midrand, South Africa). The Esco Ascent ductless fume hood was acquired from Esco® (Pennsylvania, USA). The stationary 37°C incubator, Jouan EB 53, was obtained from Labexchange® (Burladingen, Germany). The Zeiss LSM 780 multiphoton laser scanning confocal microscope and its ZEM 2.1 software, accessed at the Life Science Imaging Centre (University of the Witwatersrand) was from Carl Zeiss (Oberkochen, Germany).

Appendix A5: Plagiarism declaration report

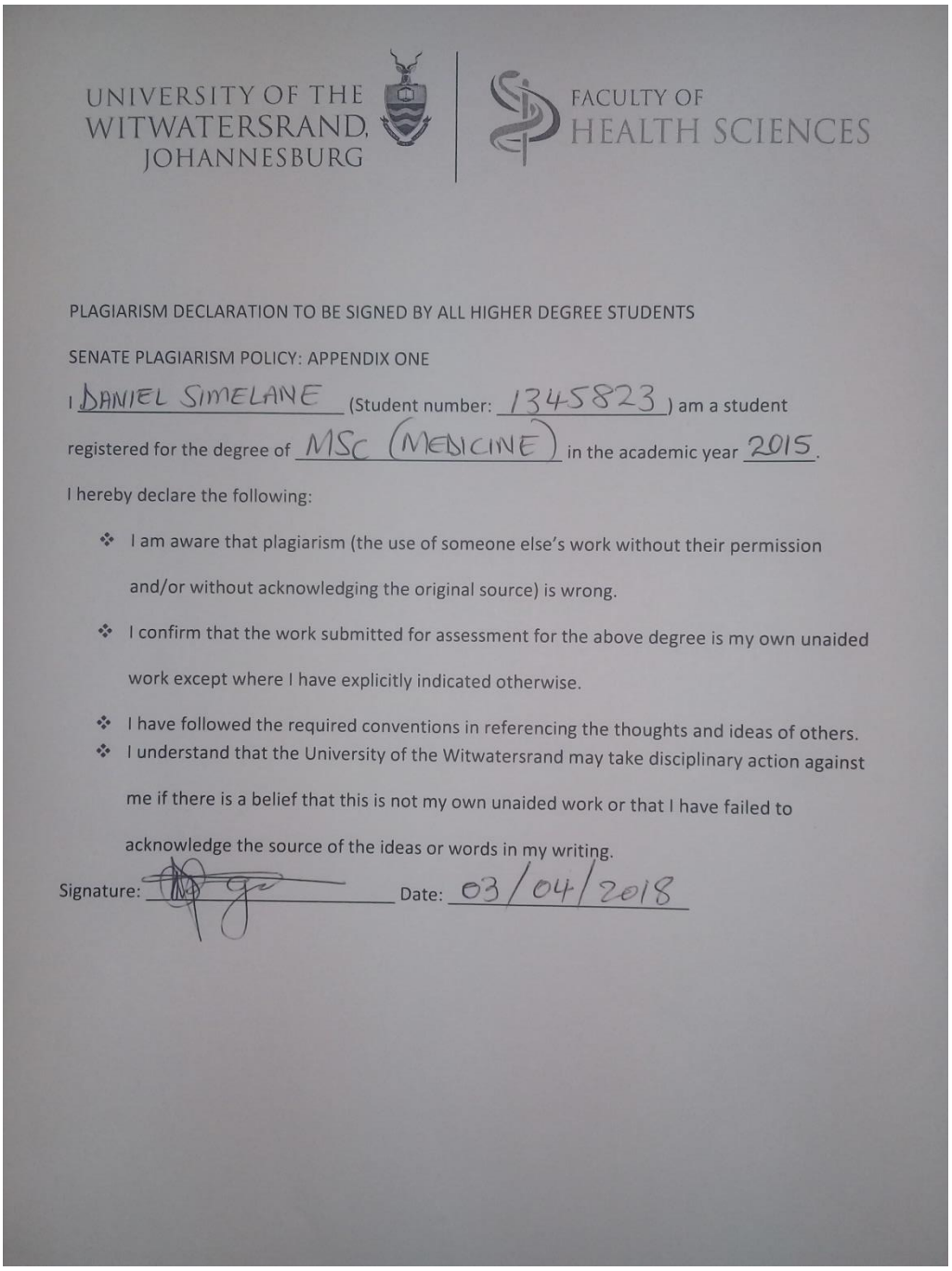

UNIVERSITY OF THE WITWATERSRAND, JOHANNESBURG

FACULTY OF HEALTH SCIENCES

PLAGIARISM DECLARATION TO BE SIGNED BY ALL HIGHER DEGREE STUDENTS

SENATE PLAGIARISM POLICY: APPENDIX ONE

I DANIEL SIMELANE (Student number: 1345823) am a student registered for the degree of MSc (MEDICINE) in the academic year 2015.

I hereby declare the following:

- I am aware that plagiarism (the use of someone else's work without their permission and/or without acknowledging the original source) is wrong.
- I confirm that the work submitted for assessment for the above degree is my own unaided work except where I have explicitly indicated otherwise.
- I have followed the required conventions in referencing the thoughts and ideas of others.
- I understand that the University of the Witwatersrand may take disciplinary action against me if there is a belief that this is not my own unaided work or that I have failed to acknowledge the source of the ideas or words in my writing.

Signature: _____ Date: 03/04/2018

Appendix B1: Antibody import permit

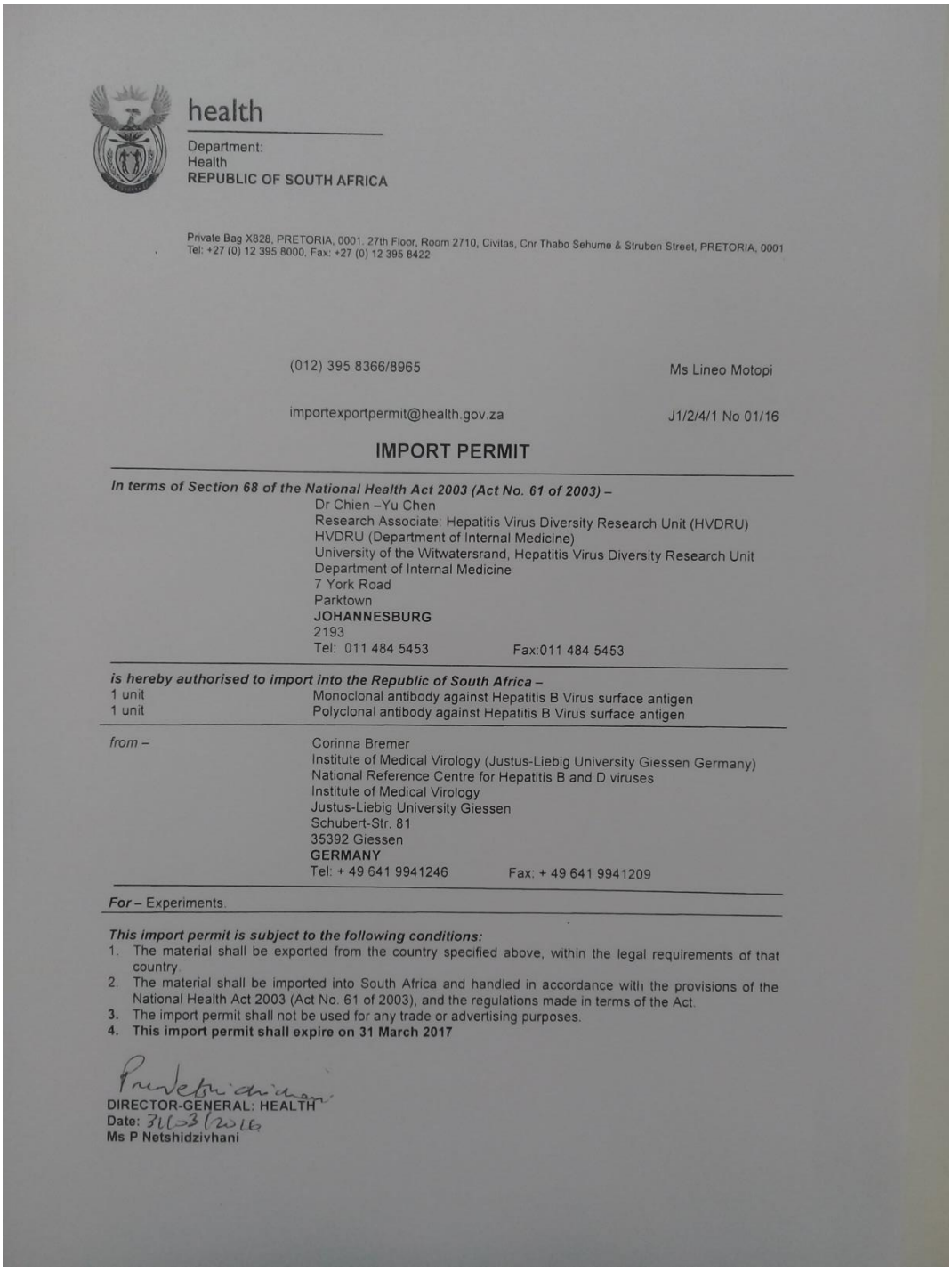

health

Department:
Health
REPUBLIC OF SOUTH AFRICA

Private Bag X828, PRETORIA, 0001. 27th Floor, Room 2710, Civitas, Cnr Thabo Sehume & Struben Street, PRETORIA, 0001
Tel: +27 (0) 12 395 8000, Fax: +27 (0) 12 395 8422

(012) 395 8366/8965 — Ms Lineo Motopi

importexportpermit@health.gov.za — J1/2/4/1 No 01/16

IMPORT PERMIT

In terms of Section 68 of the National Health Act 2003 (Act No. 61 of 2003) –

Dr Chien –Yu Chen
Research Associate: Hepatitis Virus Diversity Research Unit (HVDRU)
HVDRU (Department of Internal Medicine)
University of the Witwatersrand, Hepatitis Virus Diversity Research Unit
Department of Internal Medicine
7 York Road
Parktown
JOHANNESBURG
2193
Tel: 011 484 5453 Fax:011 484 5453

is hereby authorised to import into the Republic of South Africa –

1 unit	Monoclonal antibody against Hepatitis B Virus surface antigen
1 unit	Polyclonal antibody against Hepatitis B Virus surface antigen

from –

Corinna Bremer
Institute of Medical Virology (Justus-Liebig University Giessen Germany)
National Reference Centre for Hepatitis B and D viruses
Institute of Medical Virology
Justus-Liebig University Giessen
Schubert-Str. 81
35392 Giessen
GERMANY
Tel: + 49 641 9941246 Fax: + 49 641 9941209

For – Experiments.

This import permit is subject to the following conditions:

1. The material shall be exported from the country specified above, within the legal requirements of that country
2. The material shall be imported into South Africa and handled in accordance with the provisions of the National Health Act 2003 (Act No. 61 of 2003), and the regulations made in terms of the Act.
3. The import permit shall not be used for any trade or advertising purposes.
4. **This import permit shall expire on 31 March 2017**

DIRECTOR-GENERAL: HEALTH
Date: 31/03/2016
Ms P Netshidzivhani

Appendix B2: Ethics clearance certificate

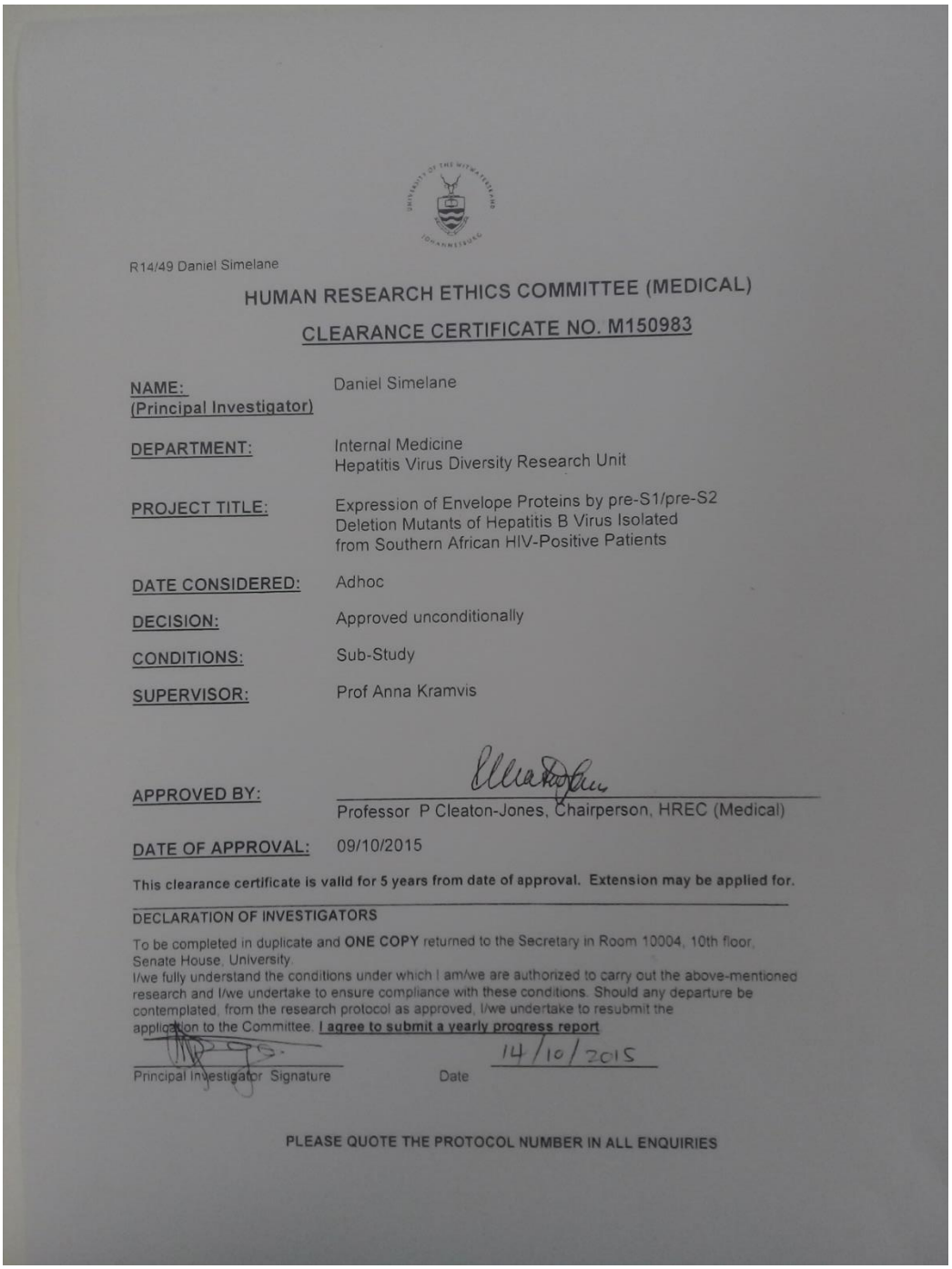

R14/49 Daniel Simelane

HUMAN RESEARCH ETHICS COMMITTEE (MEDICAL)

CLEARANCE CERTIFICATE NO. M150983

NAME: (Principal Investigator)	Daniel Simelane
DEPARTMENT:	Internal Medicine Hepatitis Virus Diversity Research Unit
PROJECT TITLE:	Expression of Envelope Proteins by pre-S1/pre-S2 Deletion Mutants of Hepatitis B Virus Isolated from Southern African HIV-Positive Patients
DATE CONSIDERED:	Adhoc
DECISION:	Approved unconditionally
CONDITIONS:	Sub-Study
SUPERVISOR:	Prof Anna Kramvis
APPROVED BY:	Professor P Cleaton-Jones, Chairperson, HREC (Medical)
DATE OF APPROVAL:	09/10/2015

This clearance certificate is valid for 5 years from date of approval. Extension may be applied for.

DECLARATION OF INVESTIGATORS

To be completed in duplicate and **ONE COPY** returned to the Secretary in Room 10004, 10th floor, Senate House, University.

I/we fully understand the conditions under which I am/we are authorized to carry out the above-mentioned research and I/we undertake to ensure compliance with these conditions. Should any departure be contemplated, from the research protocol as approved, I/we undertake to resubmit the application to the Committee. **I agree to submit a yearly progress report**

Principal Investigator Signature — Date: 14/10/2015

PLEASE QUOTE THE PROTOCOL NUMBER IN ALL ENQUIRIES

Appendix B3: Transient transfection protocol

Transfection of the Huh 7.5 liver cells with 800ng of GFP (Positive control DNA), A12C15, S193A, ALT 9.3 (Wild-type construct clones), S045A, S011A, and S167A (Deletion mutant clones) with 3 µl *TransIT®-LT1* transfection reagent was carried out on both the 01 July (Day 5 Experiment) and 11 August (Day 1 Experiment).

Cell seeding was done a day before the transfection experiment was conducted and 1.8X10^5 cells were plated per well in two 12 well plates for both day 5 and day 1 Experiments, respectively (with a cover slip in each well). The initial DNA concentrations for all the DNA samples were: GFP= 4500.0 ng/µl, A12C15= 3789.5ng/µl, S193A= 4579.5ng/µl, S011A= 4517.9ng/µl, S045A= 3373.0ng/µl, S167A= 4594.1ng/µl, and ALT 9.3= 4337.1ng/µl, respectively. Samples were diluted with a 1:10 dilution factor before use. New concentrations were as follows: GFP= 450ng/µl, A12C15= 380ng/µl, S193A= 458ng/µl, S011A= 452ng/µl, S045A= 337ng/µl, S167A=459ng/µl, and ALT 9.3= 434ng/µl. To determine the volume of the each diluted sample to end up with a DNA quantity of 800ng, the final quantity needed was divided by the concentration of the diluted sample (Example: GFP sample: 800ng divided by 450ng/µl equals 1.7µl). The same calculation was applied to all other samples, and the respective volumes of the diluted samples to be used were as follows:

Table 1

SAMPLE	VOLUME (µl)
A12C15	2.1
S193A	1.8
S045A	2.4
S011A	1.8
S167A	1.7
ALT 9.3	1.8

The experiment was set up as follows (In two 12 well plates):

Plate A:

1. No DNA Transfection+ 3 µl *TransIT* + 1: 800 Rabbit Anti-HBs	2. 800 ng pEGFP-c3 + 3 µl *TransIT* + 1: 800 Rabbit Anti-HBs	3. 800 ng A12C15 + 3 µl *TransIT* + 1: 800 Rabbit Anti-HBs	4. 800 ng S193A +3 µl TransIT + 1: 800 Rabbit Anti-HBs
5. No DNA Transfection+ 3 µl *TransIT* + 1: 800 Rabbit Anti-HBs	6. 800 ng pEGFP-c3 + 3 µl *TransIT* + 1: 800 Rabbit Anti-HBs	7. 800 ng A12C15 + 3 µl *TransIT* + 1: 800 Rabbit Anti-HBs	8. 800 ng S193A +3 µl TransIT + 1: 800 Rabbit Anti-HBs
9. No DNA Transfection+ 3 µl *TransIT* + 1: 800 Rabbit Anti-HBs	10. 800 ng pEGFP-c3 + 3 µl *TransIT* + 1: 800 Rabbit Anti-HBs	11. 800 ng A12C15 + 3 µl *TransIT* + 1: 800 Rabbit Anti-HBs	12. 800 ng S193A +3 µl TransIT + 1: 800 Rabbit Anti-HBs

Plate B:

1. 800 ng A12C15 ALT 9.3 + 3 µl *TransIT* + 1: 800 Rabbit Anti-HBs	2. 800 ng S011A + 3 µl *TransIT* + 1: 800 Rabbit Anti-HBs	3. 800 ng S167A + 3 µl *TransIT* + 1: 800 Rabbit Anti-HBs	4. 800 ng S045A + 3 µl *TransIT* + 1: 800 Rabbit Anti-HBs
5. 800 ng A12C15 ALT 9.3 + 3 µl *TransIT* + 1: 800 Rabbit Anti-HBs	6. 800 ng S011A + 3 µl *TransIT* + 1: 800 Rabbit Anti-HBs	7. 800 ng S167A + 3 µl *TransIT* + 1: 800 Rabbit Anti-HBs	8. 800 ng S045A + 3 µl *TransIT* + 1: 800 Rabbit Anti-HBs
9. 800 ng A12C15 ALT 9.3 + 3 µl *TransIT* + 1: 800 Rabbit Anti-HBs	10. 800 ng S011A + 3 µl *TransIT* + 1: 800 Rabbit Anti-HBs	11. 800 ng S167A + 3 µl *TransIT* + 1: 800 Rabbit Anti-HBs	12. 800 ng S045A + 3 µl *TransIT* + 1: 800 Rabbit Anti-HBs

Protocol

- One day post seeding, twenty-four 1.5 ml Eppendorf tubes were set up, with 100 µl of DMEM medium aliquoted into each tube.
- No DNA with transfection reagent were added into the negative control tubes and the quantity of the DNA (800ng) and the amount of transfection reagent (3 µl) were kept constant for the experiment.
- 1.7 µl of pEGFP-C3 DNA was aliquoted into the positive control tubes (both positive control samples for a successful transfection) with all other volumes as indicated in the table above (Table 1) and

positions as indicated in the two other tables above which represent the two 12 well plates (Plates A and B).

- 3 µl of the transfection reagent was aliquoted into all tubes, including the control tubes respectively with a gently mixing by pippeting up and down in each tube.
- All tubes were incubated at room temperature for 20 minutes to form DNA-Transfection reagent complexes.
- While waiting for the incubation time to elapse, supernatants from the two 12 well plates with the passaged cells were discarded.
- The cells were then washed with 1 ml PBS and then PBS was discarded afterwards.
- 1 ml of complete medium was pippeted into each well, respectively.
- After the incubation time has elapsed, the mixture from the tubes (DNA-Transfection reagent complexes) were pippeted dropwise into the seeded cells on the 12 well plates with the respective same labels as the tubes and incubated at 37ºC in a humidified incubator with 5% CO_2.
- One day post-transfection, positive controls were viewed under a fluorescence microscope to confirm if the experiment was successful or not.
- Supernatants in all wells were changed with 1ml fresh complete growth medium.
- Fixation and Immunofluorescence was carried out on 3 different time-points (days 1, 3 & 5) post-transfection.

Appendix B4: Fixation and Immunofluorescence

- The media was removed from all the wells with the transfected Huh7.5 cells and drying out of cells was avoided while staining.
- Cells were washed 3 times with 1 ml of PBS, respectively.
- One millilitre of 4% Formaldehyde was added into each well and incubate for 10min at room temperature.
- Cells were washed 3 times with 1 ml of PBS, respectively.
- One millilitre of 0.5% Triton in PBS was added into each well and incubated for 8 minutes at room temperature.
- Cells were washed 3 times with 1 ml of PBS, respectively.
- Cells were block in 1 ml of 1% BSA in PBS and incubated for at room temperature for an hour.
- The cover slips were removed from their respective wells into a smooth, sterile surface (cells facing up).
- Then 100µl Rabbit anti-HBs primary antibody (1:800 concentration), drop by drop was added respectively into each cover slip and Incubated for an hour at 37^0C.

  NB: In the case of a double staining procedure, a 1:800 Rabbit anti-HBs primary antibody was prepared in one vial with either 1:1000 of the Mouse anti-Calnexin or 1:100 Mouse anti-ERGIC or 1:100 Mouse anti-Giantin antibodies, respectively and used for staining both the envelope proteins and cell compartment rather than staining only the envelope proteins.

- Cells were washed 3 times with 100µl PBS, respectively.
- Then 100µl Donkey anti-Rabbit secondary antibody (1:1000 concentration), drop by drop was added respectively into each cover slip and Incubated for an hour at 37^0C.

  NB: In the case of a double staining procedure, a 1:1000 Donkey anti-Rabbit secondary antibody was prepared in one vial with a 1:1000 Goat anti-Mouse secondary antibody and used to target both the primary antibodies concurrently.

- Cells were washed 3 times with 100ul PBS, respectively.
- Then 100µl DAPI (1:1000 concentration) was added to the respective cover slips and incubated for 10 minutes at room temperature.
- Cells were washed 3 times with 100ul PBS, respectively.
- Cover slips were then mounted immediately to the microscope slides in 1 drop of the fluorescent mounting medium, respectively.
- Slides were allowed to dry overnight in the dark and images captured under the confocal microscope.

Appendix C1: HBsAg mean of fluorescence in the cytoplasm on Day 1

Table 3.7: Mean of fluorescence of the expressed HBsAg in the cytoplasm on day 1 post-transfection. Twenty-one quantifications per construct.

HBsAg mean of fluorescence in the Cytoplasm (Day 1 post-transfection)						
Cell	A12C15 OL 1,28ME R	A12C15 ALT 9.3	SHH193 A (OCLF)	SHH011 A (D.MUT)	SHH045 A (D.MUT)	SHH167 A (D.MUT)
1	316.15	843.26	29.24	480.29	304.77	497.77
2	1522.13	511.68	157.63	331.63	372.10	323.86
3	430.92	451.16	276.79	591.04	205.32	179.56
4	273.49	191.43	314.41	105.45	251.30	224.11
5	612.21	178.56	344.95	155.69	111.86	241.10
6	152.28	748.89	83.83	701.29	133.33	230.63
7	126.22	619.91	118.16	509.37	245.05	191.58
1	199.88	639.55	123.44	174.65	234.17	170.16
2	192.29	114.88	102.38	249.81	637.48	128.82
3	156.43	164.72	244.85	466.21	769.69	342.75
4	492.53	185.13	154.29	375.89	583.87	525.21
5	322.88	165.53	627.03	271.29	287.02	245.87
6	141.30	183.48	613.79	557.99	248.24	197.70
7	223.48	273.21	238.97	337.70	297.72	1463.68
1	349.61	327.96	299.29	429.62	365.72	477.88
2	312.13	257.84	350.32	739.59	380.53	361.23
3	184.10	218.75	439.15	543.99	178.07	315.13
4	351.87	314.52	353.90	342.48	441.72	303.86
5	195.97	341.30	282.83	376.75	528.56	290.69
6	209.57	149.42	323.56	394.38	486.57	211.80
7	371.66	103.82	219.05	328.75	129.51	361.64

Appendix C2: HBsAg mean of fluorescence in the cytoplasm on Day 3

Table 3.8: Mean of fluorescence of the expressed HBsAg in the cytoplasm on day 3 post-transfection. Twenty-one quantifications per construct.

HBsAg mean of fluorescence in the Cytoplasm (Day 3 post-transfection)						
Cell	A12C15 OL 1,28ME R	A12C15 ALT 9.3	SHH193 A (OCLF)	SHH011 A (D.MUT)	SHH045 A (D.MUT)	SHH167 A (D.MUT)
1	150.49	476.57	328.52	493.25	337.82	480.00
2	1394.17	706.28	436.15	257.34	212.11	377.49
3	486.00	436.88	416.70	316.16	234.24	320.08
4	307.22	492.00	420.95	478.44	279.36	1208.40
5	447.09	682.25	389.55	368.30	280.94	337.95
6	487.61	653.78	340.44	437.90	530.55	215.85
7	534.90	235.40	527.87	387.03	221.79	372.53
1	294.10	267.50	818.87	1240.99	206.87	363.90
2	79.78	383.72	669.39	777.06	335.58	398.47
3	377.68	242.99	589.96	946.65	149.97	147.85
4	530.45	555.19	428.63	242.27	133.65	124.51
5	235.24	719.43	476.58	659.51	852.47	120.15
6	184.86	842.93	237.51	252.89	941.93	107.44
7	165.49	543.19	597.83	469.69	140.16	515.74
1	164.40	511.34	657.45	533.11	201.20	242.41
2	292.05	1027.98	712.52	959.32	585.81	414.85
3	663.42	540.07	414.48	645.53	333.30	336.30
4	792.76	309.80	594.47	785.98	254.19	328.76
5	397.93	152.57	642.10	357.08	202.24	225.30
6	312.98	293.50	666.47	1472.23	225.50	359.54
7	285.71	613.63	277.19	282.14	605.23	208.49

Appendix C3: HBsAg mean of fluorescence in the cytoplasm on Day 5

Table 3.9: Mean of fluorescence of the expressed HBsAg in the cytoplasm on day 5 post-transfection. Twenty-one quantifications per construct.

HBsAg mean of fluorescence in the Cytoplasm (Day 5 post-transfection)						
Cell	A12C15 OL 1,28ME R	A12C15 ALT 9.3	SHH193 A (OCLF)	SHH011 A (D.MUT)	SHH045 A (D.MUT)	SHH167 A (D.MUT)
1	215.12	410.98	1014.86	370.24	577.43	480.00
2	337.87	504.77	375.30	430.99	316.20	377.49
3	491.75	387.13	515.09	320.41	184.42	320.08
4	662.59	793.62	599.60	195.68	287.00	1208.40
5	301.83	598.04	689.22	859.35	808.53	337.95
6	592.39	530.19	588.74	431.90	228.31	215.85
7	420.68	642.16	545.09	166.50	471.99	372.53
1	273.92	224.15	212.38	1102.98	594.45	343.31
2	174.79	230.25	161.79	842.44	324.46	381.59
3	196.10	331.57	236.93	209.87	355.93	248.65
4	325.44	136.20	541.26	309.63	563.10	217.96
5	233.77	109.35	402.84	488.20	927.08	1025.82
6	221.55	324.10	345.08	256.46	679.29	537.21
7	148.22	269.75	951.56	776.71	876.21	744.79
1	354.34	127.74	374.97	128.20	561.69	238.17
2	433.24	138.66	742.59	167.06	385.53	337.70
3	289.28	195.44	474.44	153.44	396.59	358.42
4	116.23	300.46	741.92	563.43	336.52	331.30
5	118.60	437.96	649.71	343.22	187.18	236.59
6	239.16	147.70	214.12	200.76	155.89	229.12
7	287.92	159.58	476.19	258.55	147.22	478.60

Appendix C4: Background Intensities on Day 1

Table 3.10: Background intensities of the none-expressing regions of the images taken on days 1 post-transfection (Twenty-one quantifications per construct).

Background intensities (Day 1 post-transfection)						
Cell	A12C15 OL 1,28MER	A12C15 ALT 9.3	SHH193A (OCLF)	SHH011A (D.MUT)	SHH045A (D.MUT)	SHH167A (D.MUT)
1	35.98	33.98	39.44	37.36	39.08	38.50
2	37.45	42.88	35.54	47.98	25.59	33.78
3	35.79	44.91	47.31	60.51	29.35	51.95
4	29.24	42.82	49.04	56.78	29.86	41.79
5	36.86	39.69	37.36	59.04	30.37	56.35
6	32.36	42.75	32.71	30.36	41.93	60.76
7	33.41	30.20	39.49	37.73	35.48	51.72
Average	34.44	39.60	40.12	47.11	33.09	47.83
1	27.94	33.94	34.78	34.78	33.92	42.24
2	48.48	57.78	34.87	36.37	37.19	47.94
3	45.57	45.63	37.04	29.86	45.43	36.25
4	33.95	64.80	42.17	39.80	48.55	42.05
5	45.72	52.02	42.93	32.79	51.63	40.55
6	45.65	50.07	41.14	34.92	49.66	38.42
7	44.75	50.57	48.97	38.06	45.40	42.08
Average	41.72	50.69	40.27	35.23	44.54	41.36
1	41.81	47.29	47.69	40.81	40.40	42.03
2	45.24	44.97	42.09	47.67	54.82	40.65
3	46.28	50.38	46.49	52.48	53.76	41.80
4	43.17	47.85	43.07	49.03	33.70	39.31
5	47.54	43.17	35.56	49.84	40.50	38.43
6	39.23	53.85	37.19	46.64	43.04	38.91
7	45.08	43.72	37.85	49.98	46.04	39.68
Average	44.05	47.32	41.42	48.06	44.61	40.12

Appendix C5: Background Intensities on Day 3

Table 3.11: Background intensities of the none-expressing regions of the images taken on days 3 post-transfection (Twenty-one quantifications per construct).

Background intensities (Day 3 post-transfection)						
Cell	A12C15 OL 1,28MER	A12C15 ALT 9.3	SHH193A (OCLF)	SHH011A (D.MUT)	SHH045A (D.MUT)	SHH167A (D.MUT)
1	48.26	48.52	44.38	65.34	40.68	43.93
2	70.04	47.17	61.91	64.35	60.94	48.13
3	55.45	56.16	64.89	46.99	63.38	49.65
4	50.30	62.39	49.98	65.89	55.51	56.43
5	48.13	53.45	55.31	56.24	50.12	61.23
6	53.42	46.83	61.15	61.65	46.31	46.03
7	50.77	54.20	47.97	66.17	49.17	62.27
Average	53.77	52.67	55.08	60.95	52.30	52.53
1	46.98	56.26	64.60	61.60	74.78	55.60
2	48.92	55.88	53.30	60.86	54.12	52.00
3	49.04	56.20	52.03	57.11	48.78	52.52
4	49.42	53.28	55.50	51.11	43.49	60.25
5	43.04	63.87	53.89	65.17	54.33	48.95
6	44.45	61.25	90.16	76.75	66.51	46.15
7	47.77	66.09	107.54	71.97	44.48	45.13
Average	47.09	58.98	68.14	63.51	55.21	51.51
1	55.05	57.61	53.13	53.58	33.37	40.55
2	47.08	32.20	92.63	99.58	54.34	49.82
3	50.94	74.60	88.06	58.39	48.60	51.94
4	49.50	75.33	56.98	54.08	49.52	52.52
5	55.01	60.69	49.20	57.36	53.24	56.60
6	57.74	65.32	42.79	50.97	57.16	57.08
7	71.11	72.71	33.62	57.85	49.05	57.02
Average	55.20	62.64	59.49	61.68	49.33	52.22

Appendix C6: Background Intensities on Day 5

Table 3.12: Background intensities of the none-expressing regions of the images taken on days 5 post-transfection (Twenty-one quantifications per construct).

Background intensities (Day 5 post-transfection)						
Cell	A12C15 OL 1,28MER	A12C15 ALT 9.3	SHH193A (OCLF)	SHH011A (D.MUT)	SHH045A (D.MUT)	SHH167A (D.MUT)
1	49.13	48.77	35.46	70.47	29.36	62.44
2	48.89	76.58	44.37	49.63	56.20	37.06
3	62.46	77.34	49.62	39.92	47.00	39.72
4	62.16	70.89	45.88	42.90	38.10	36.47
5	51.08	71.61	53.46	47.99	46.09	36.53
6	51.71	74.82	49.98	67.79	62.48	35.66
7	67.09	54.83	45.65	52.71	39.51	44.28
Average	56.07	67.83	46.35	53.06	45.53	41.74
1	57.03	46.17	72.30	62.15	64.32	63.09
2	52.45	64.81	51.39	58.59	42.20	62.29
3	57.29	93.61	51.12	71.30	51.27	54.90
4	46.04	103.60	43.86	96.35	53.71	52.90
5	55.67	66.14	47.86	58.55	73.27	55.51
6	59.69	92.34	52.73	63.21	44.24	46.88
7	72.47	74.04	58.31	59.21	72.25	47.82
Average	57.23	77.24	53.94	67.05	57.32	54.77
1	61.45	64.03	50.13	46.65	56.26	39.02
2	58.95	62.20	51.40	55.13	66.02	49.76
3	93.35	62.11	53.89	77.51	52.63	47.71
4	66.83	75.95	40.53	75.18	54.23	57.02
5	72.99	70.40	62.83	41.68	50.48	45.31
6	57.74	53.12	62.58	67.45	56.56	46.51
7	53.22	66.16	60.52	42.15	50.17	53.39
Average	66.36	64.85	54.55	57.96	55.19	48.39

Appendix C7: HBsAg mean of fluorescence in the cytoplasm for Day 1

Table 3.13: Mean of fluorescence of the expressed HBsAg in the cytoplasm on day 1 post-transfection (Background intensity subtracted).

HBsAg mean of fluorescence in the Cytoplasm (Day 1 post-transfection)						
Cell	A12C15 OL 1,28MER	A12C15 ALT 9.3	SHH193A (OCLF)	SHH011A (D.MUT)	SHH045A (D.MUT)	SHH167A (D.MUT)
1	91.78	56.50	-10.89	58.34	78.77	87.46
2	99.58	64.19	43.71	108.59	84.90	128.80
3	114.71	102.10	62.11	139.43	100.24	131.73
4	117.84	114.03	78.04	214.59	133.46	143.74
5	140.05	114.85	83.17	236.06	172.23	156.34
6	150.56	132.80	114.02	280.69	189.63	171.69
7	151.92	134.45	117.51	284.52	203.71	176.28
1	158.16	138.95	177.63	294.42	211.95	182.79
2	165.52	151.82	198.70	302.47	218.21	193.27
3	181.76	171.43	204.58	328.68	242.49	204.51
4	239.04	210.52	236.66	340.66	253.18	250.57
5	268.08	222.52	241.41	346.32	271.68	263.75
6	281.16	267.20	257.87	381.56	321.11	275.01
7	281.71	280.64	274.28	430.98	335.93	276.03
1	305.56	293.98	282.14	433.18	339.01	301.39
2	307.82	411.56	304.82	462.26	397.11	321.11
3	327.61	472.08	308.90	495.92	441.97	321.53
4	396.48	580.31	312.48	522.77	483.96	437.76
5	450.80	588.86	397.73	543.94	539.33	449.93
6	577.77	709.28	573.52	654.18	592.94	483.85
7	1487.69	803.66	586.76	691.52	725.15	1422.32
Median	239.04	210.52	236.66	340.66	253.18	250.57
Q1	145.31	123.82	98.59	258.37	180.93	164.01
Q3	317.71	441.82	306.86	479.09	419.54	321.32
IQR	317.71 - 145.31	441.82 - 123.82	306.86 - 98.59	479.09 - 258.37	419.54 - 180.93	321.32 - 164.01

Q1=Lower Quartile; Q3=Upper Quartile; IQR= Interquartile Range

Appendix C8: HBsAg mean of fluorescence in the cytoplasm for Day 3

Table 3.14: Mean of fluorescence of the expressed HBsAg in the cytoplasm on day 3 post-transfection (Background intensity subtracted).

HBsAg mean of fluorescence in the Cytoplasm (Day 3 post-transfection)						
Cell	A12C15 OL 1,28MER	A12C15 ALT 9.3	SHH193A (OCLF)	SHH011A (D.MUT)	SHH045A (D.MUT)	SHH167A (D.MUT)
1	32.69	89.93	169.36	178.76	78.44	55.92
2	96.72	182.73	217.71	189.38	84.95	68.63
3	109.20	184.01	273.44	196.40	94.76	72.99
4	118.40	208.52	285.35	220.45	151.66	96.33
5	137.77	230.86	334.47	255.22	151.87	156.27
6	188.15	247.16	354.99	295.40	152.92	163.32
7	230.51	324.75	360.49	307.36	159.81	173.08
1	236.85	384.20	361.61	326.08	169.49	190.19
2	247.01	423.90	365.87	376.96	176.17	267.55
3	253.45	439.33	381.06	406.18	181.94	276.54
4	257.78	448.70	408.43	417.50	204.87	284.08
5	330.59	477.43	472.79	432.30	227.06	285.43
6	342.72	484.22	521.82	471.43	228.64	307.32
7	393.32	496.21	529.68	583.84	280.37	312.38
1	432.23	550.99	534.98	596.00	283.98	320.01
2	433.84	601.11	582.61	713.55	285.52	324.96
3	481.14	629.58	597.96	724.30	478.25	346.95
4	483.36	653.61	601.25	883.14	536.49	362.63
5	608.22	660.45	606.99	897.64	555.90	427.47
6	737.56	783.95	653.03	1177.48	797.26	464.23
7	1340.40	965.34	750.72	1410.54	886.72	1155.88
Median	257.78	448.70	408.43	417.50	204.87	284.08
Q1	162.96	239.01	344.73	275.31	152.39	159.80
Q3	457.49	615.34	590.29	718.92	381.88	335.96
IQR	457.49 - 162.96	615.34 - 239.01	590.29 - 344.73	718.92 - 275.31	381.88 - 152.39	335.96 - 159.80

Q1=Lower Quartile; Q3=Upper Quartile; IQR= Interquartile Range

Appendix C9: HBsAg mean of fluorescence in the cytoplasm for Day 5

Table 3.15: Mean of fluorescence of the expressed HBsAg in the cytoplasm on day 5 post-transfection (Background intensity subtracted).

HBsAg mean of fluorescence in the Cytoplasm (Day 5 post-transfection)						
Cell	A12C15 OL 1,28MER	A12C15 ALT 9.3	SHH193A (OCLF)	SHH011A (D.MUT)	SHH045A (D.MUT)	SHH167A (D.MUT)
1	49.87	32.11	107.86	70.23	92.02	163.19
2	52.24	58.95	158.44	95.48	131.98	174.11
3	90.99	62.89	182.99	109.10	138.89	188.20
4	117.56	73.80	214.12	113.45	155.89	189.79
5	138.87	94.73	291.15	142.62	182.78	193.88
6	159.05	130.58	320.42	142.81	241.46	229.12
7	164.32	146.90	328.95	189.41	267.14	278.34
1	176.54	147.70	348.91	200.59	270.66	282.91
2	216.69	153.01	419.89	200.76	281.32	288.54
3	221.56	192.51	421.64	242.58	298.61	289.31
4	222.92	235.61	468.74	267.36	330.34	296.22
5	239.16	246.86	487.32	285.25	341.40	310.03
6	245.76	254.32	498.75	317.18	426.45	326.82
7	268.21	319.30	542.39	377.93	505.78	330.80
1	281.80	343.15	553.26	378.84	506.50	335.75
2	287.98	373.11	595.15	421.14	531.89	430.21
3	364.61	436.93	642.88	505.46	537.13	438.26
4	366.87	462.35	687.37	709.66	621.97	482.44
5	435.68	530.20	688.03	775.39	763.00	690.02
6	536.31	574.32	897.62	806.29	818.89	971.05
7	606.52	725.78	968.51	1035.93	869.75	1166.66
Median	222.92	235.61	468.74	267.36	330.34	296.22
Q1	148.96	112.66	305.78	142.72	212.12	211.50
Q3	326.29	405.02	619.01	463.30	534.51	434.24
IQR	326.29 - 148.96	405.02 - 112.66	619.01 - 305.78	463.30 - 142.72	534.51 - 212.12	434.24 - 211.50

Q1=Lower Quartile; Q3=Upper Quartile; IQR= Interquartile Range

Appendix C10: Median HBsAg mean of fluorescence in the cytoplasm for days 1, 3, & 5

Table 3.16: Meadian HBsAg mean of fluorescence in the cytoplasm (background intensity subtracted) for days 1, 3, & 5 post-transfection.

Mean of fluorescence in the Cytoplasm			
Construct	Day 1	Day 3	Day 5
A12C15 OL 1,28MER	239.04	257.78	222.92
A12C15 ALT 9.3	210.52	448.70	235.61
SHH193A (OCLF)	236.66	408.43	468.74
SHH011A (D.MUT)	340.66	417.50	267.36
SHH045A (D.MUT)	253.18	204.87	330.34
SHH167A (D.MUT)	250.57	284.08	296.22

Appendix C11: Additional statistical information for Mono-staining experiments

Non-Parametric Tests

Descriptive Statistics

	N	Mean	Std. Deviation	Minimum	Maximum	Percentiles 25th	50th (Median)	75th
Mean_of_fluorescence_on_day3	6	336.8933	100.59223	204.87	448.70	244.5525	346.2550	425.3000
Mean_of_fluorescence_on_day5	6	303.5317	89.98436	222.92	468.74	232.4375	281.7900	364.9400
Mean_of_fluorescence_on_day1	6	255.1050	44.56468	210.52	340.66	230.1250	244.8050	275.0500

Wilcoxon Signed Ranks Test

		N	Mean Rank	Sum of Ranks
Mean_of_fluorescence_on_day1 - Mean_of_fluorescence_on_day3	Negative Ranks	5[a]	3.60	18.00
	Positive Ranks	1[b]	3.00	3.00
	Ties	0[c]		
	Total	6		
Mean_of_fluorescence_on_day1 - Mean_of_fluorescence_on_day5	Negative Ranks	4[d]	4.00	16.00
	Positive Ranks	2[e]	2.50	5.00
	Ties	0[f]		
	Total	6		
Mean_of_fluorescence_on_day3 - Mean_of_fluorescence_on_day5	Negative Ranks	3[g]	2.67	8.00
	Positive Ranks	3[h]	4.33	13.00
	Ties	0[i]		
	Total	6		

a. Mean_of_fluorescence_on_day1 < Mean_of_fluorescence_on_day3

b. Mean_of_fluorescence_on_day1 > Mean_of_fluorescence_on_day3

c. Mean_of_fluorescence_on_day1 = Mean_of_fluorescence_on_day3

d. Mean_of_fluorescence_on_day1 < Mean_of_fluorescence_on_day5

e. Mean_of_fluorescence_on_day1 > Mean_of_fluorescence_on_day5

f. Mean_of_fluorescence_on_day1 = Mean_of_fluorescence_on_day5

g. Mean_of_fluorescence_on_day3 < Mean_of_fluorescence_on_day5

h. Mean_of_fluorescence_on_day3 > Mean_of_fluorescence_on_day5

i. Mean_of_fluorescence_on_day3 = Mean_of_fluorescence_on_day5

Test Statistics[a]

	Mean_of_fluorescence_on_day1 - Mean_of_fluorescence_on_day3	Mean_of_fluorescence_on_day1 - Mean_of_fluorescence_on_day5	Mean_of_fluorescence_on_day3 - Mean_of_fluorescence_on_day5
Z	-1.572[b]	-1.153[b]	-.524[c]
Asymp. Sig. (2-tailed)	.116	.249	.600

a. Wilcoxon Signed Ranks Test

b. Based on positive ranks.

c. Based on negative ranks.

The descriptive statistics table shows the median and quartile ranges for the 6 intensity quantifications of all the constructs for the three time point days 1, 3 & 5 post-transfection. The ranks table shows a comparison of the median HBsAg mean of fluorescence of the constructs of one time point against the other. The test statistics table shows the statistical significant difference of the quantified median HBsAg mean of fluorescence for the different constructs between the time points.

Appendix C12: Manders' overlap co-efficiency (MOC) of the expressed HBsAg on cell compartments on day 3

Table 3.17: Manders' overlap co-efficiency of the expressed HBsAg on cell compartments on day 3 post-transfection.

Manders' overlap coefficiency of the expressed HBsAg on the secretory organelles (ER, ERGIC, & Golgi) on day 3 post-transfection									
	ER			ERGIC			Golgi		
MOC	A12C15 ALT 9.3	SHH193A (OCFL)	SHH011A (D.MUT)	A12C15 ALT 9.3	SHH193A (OCFL)	SHH011A (D.MUT)	A12C15 ALT 9.3	SHH193A (OCFL)	SHH011A (D.MUT)
1	0.47	0.43	0.43	0.43	0.48	0.41	0.38	0.48	0.50
2	0.51	0.45	0.44	0.52	0.50	0.44	0.42	0.57	0.50
3	0.59	0.50	0.52	0.57	0.51	0.53	0.44	0.61	0.52
4	0.65	0.51	0.61	0.59	0.52	0.58	0.50	0.65	0.53
5	0.77	0.60	0.61	0.59	0.65	0.58	0.57	0.65	0.60
Mean	0.60	0.50	0.52	0.54	0.53	0.51	0.46	0.59	0.53

Appendix C13: Median of the Manders' overlap co-efficiency of the expressed HBsAg on cell compartments on day 3

Table 3.18: Median Manders' overlap co-efficiency of the expressed HBsAg on cell compartments on day 3 post-transfection.

Median Manders' overlap coefficiency of the expressed HBsAg on the cell compartments (Day 3 post-transfection)			
	A12C15 ALT 9.3	SHH193A (OCFL)	SHH011A (D.MUT)
ER	0.60	0.50	0.52
ERGIC	0.54	0.53	0.51
Golgi	0.46	0.59	0.53

Appendix C14: Additional statistical information for Co-staining experiments

Paired Samples T-Test

Paired Samples Statistics

		Mean	N	Std. Deviation	Std. Error Mean
Pair 1	MOC_of_HBsAg_in_ERGIC	.5267	3	.01528	.00882
	MOC_of_HBsAg_in_ER	.5393	3	.05368	.03099
Pair 2	MOC_of_HBsAg_in_Golgi	.5267	3	.06506	.03756
	MOC_of_HBsAg_in_ER	.5393	3	.05368	.03099
Pair 3	MOC_of_HBsAg_in_Golgi	.5267	3	.06506	.03756
	MOC_of_HBsAg_in_ERGIC	.5267	3	.01528	.00882

Paired Samples Correlations

		N	Correlation	Sig.
Pair 1	MOC_of_HBsAg_in_ERGIC & MOC_of_HBsAg_in_ER	3	.606	.586
Pair 2	MOC_of_HBsAg_in_Golgi & MOC_of_HBsAg_in_ER	3	-.963	.174
Pair 3	MOC_of_HBsAg_in_Golgi & MOC_of_HBsAg_in_ERGIC	3	-.369	.759

Paired Samples Test

		Paired Differences					t	df	Sig. (2-tailed)
		Mean	Std. Deviation	Std. Error Mean	95% Confidence Interval of the Difference Lower	Upper			
Pair 1	MOC_of_HBsAg_in_ERGIC - MOC_of_HBsAg_in_ER	-.01267	.04606	.02659	-.12708	.10175	-.476	2	.681
Pair 2	MOC_of_HBsAg_in_Golgi - MOC_of_HBsAg_in_ER	-.01267	.11765	.06792	-.30492	.27959	-.186	2	.869
Pair 3	MOC_of_HBsAg_in_Golgi - MOC_of_HBsAg_in_ERGIC	.00000	.07211	.04163	-.17913	.17913	.000	2	1.000

MOC = Manders' overlap co-efficiency

The paired samples test table shows the results of the dependent t-test and the information in this table give details of the differences between the two pairs investigated (labelled "Paired Differences"). The Paired Differences' columns show the mean, standard deviation, standard error mean and 95% confidence interval of the difference that in our case refers to the mean difference of the MOC of HBsAg co-localized between the two cell compartments of a pair and the standard deviation, standard error and 95% confidence interval of this mean difference, respectively. The other result on the table are: *t*-value (t), the degrees of freedom (df) and the significance level (Sig. (2-tailed)).

REFERENCES

ALLAIN, J.-P. 2006. Epidemiology of Hepatitis B virus and genotype. *Journal of clinical virology,* 36**,** S12-S17.

ALTER, M. J. 2003. Epidemiology of hepatitis B in Europe and worldwide. *Journal of hepatology,* 39**,** 64-69.

ALTER, M. J. 2006. Epidemiology of viral hepatitis and HIV co-infection. *Journal of hepatology,* 44**,** S6-S9.

ARANKALLE, V., GANDHE, S., BORKAKOTY, B., WALIMBE, A., BISWAS, D. & MAHANTA, J. 2010. A novel HBV recombinant (genotype I) similar to Vietnam/Laos in a primitive tribe in eastern India. *Journal of viral hepatitis,* 17**,** 501-510.

ARAUZ-RUIZ, P., NORDER, H., ROBERTSON, B. H. & MAGNIUS, L. O. 2002. Genotype H: a new Amerindian genotype of hepatitis B virus revealed in Central America. *Journal of general virology,* 83**,** 2059-2073.

ARAUZ-RUIZ, P., NORDER, H., VISONÁ, K. A. & MAGNIUS, L. O. 1997. Genotype F prevails in HBV infected patients of hispanic origin in Central America and may carry the precore stop mutant. *Journal of medical virology,* 51**,** 305-312.

BAPTISTA, M., KRAMVIS, A. & KEW, M. C. 1999. High prevalence of 1762T 1764A mutations in the basic core promoter of hepatitis B virus isolated from black Africans with hepatocellular carcinoma compared with asymptomatic carriers. *Hepatology,* 29**,** 946-953.

BEASLEY, R. P., GEORGE, C.-Y. L., ROAN, C.-H., HWANG, L.-Y., LAN, C.-C., HUANG, F.-Y. & CHEN, C.-L. 1983. Prevention of perinatally transmitted hepatitis B virus infections with hepatitis B immune globulin and hepatitis B vaccine. *The Lancet,* 322**,** 1099-1102.

BECK, J. & NASSAL, M. 2007. Hepatitis B virus replication. *World journal of gastroenterology: WJG,* 13**,** 48.

BELL, T. G. & KRAMVIS, A. 2013. Fragment merger: an online tool to merge overlapping long sequence fragments. *Viruses,* 5**,** 824-833.

BELL, T. G., MAKONDO, E., MARTINSON, N. A. & KRAMVIS, A. 2012. Hepatitis B virus infection in human immunodeficiency virus infected southern African adults: occult or overt–that is the question. *PloS one,* 7**,** e45750.

BHOOLA, N. H., REUMANN, K., KEW, M. C., WILL, H. & KRAMVIS, A. 2014. Construction of replication competent plasmids of hepatitis B virus subgenotypes A1, A2 and D3 with authentic endogenous promoters. *Journal of virological methods,* 203**,** 54-64.

BLUMBERG, B. S., ALTER, H. J. & VISNICH, S. 2000. A “new” antigen in leukemia sera. *Hepatitis B And The Prevention Of Primary Cancer Of The Liver: Selected Publications of Baruch S Blumberg.* World Scientific.

BODSWORTH, N. J., COOPER, D. A. & DONOVAN, B. 1991. The influence of human immunodeficiency virus type 1 infection on the development of the hepatitis B virus carrier state. *Journal of Infectious Diseases,* 163**,** 1138-1140.

BOWYER, S. M., VAN STADEN, L., KEW, M. C. & SIM, J. 1997. A unique segment of the hepatitis B virus group A genotype identified in isolates from South Africa. *Journal of General Virology,* 78**,** 1719-1729.

BRUSS, V. 2007. Hepatitis B virus morphogenesis. *World journal of gastroenterology: WJG,* 13**,** 65.

CATTANEO, R., WILL, H. & SCHALLER, H. 1984. Hepatitis B virus transcription in the infected liver. *The EMBO journal,* 3**,** 2191-2196.

CHEN, B. F., LIU, C. J., JOW, G. M., CHEN, P. J., KAO, J. H. & CHEN, D. S. 2006. High prevalence and mapping of pre-S deletion in hepatitis B virus carriers with progressive liver diseases. *Gastroenterology,* 130**,** 1153-1168.

CHEN, C.-H., LEE, C.-M., WANG, J.-H., HU, T.-H., HUNG, C.-H., CHANGCHIEN, C.-S. & LU, S.-N. 2013. Combination and evolution of HBV mutant strains in the HBeAg-positive status predict clinical outcomes after HBeAg seroconversion. *Hepatology international,* 7**,** 477-488.

CHEN, C. H., HUNG, C. H., LEE, C. M., HU, T. H., WANG, J. H., WANG, J. C., LU, S. N. & CHANGCHIEN, C. S. 2007. Pre-S deletion and complex mutations of hepatitis B virus related to advanced liver disease in HBeAg-negative patients. *Gastroenterology,* 133**,** 1466-1474.

CHEN, Y., DELBROOK, K., DEALWIS, C., MIMMS, L., MUSHAHWAR, I. K. & MANDECKI, W. 1996. Discontinuous epitopes of hepatitis B surface antigen derived from a filamentous phage peptide library. *Proceedings of the National Academy of Sciences,* 93**,** 1997-2001.

CHOUTEAU, P., LE SEYEC, J., CANNIE, I., NASSAL, M., GUGUEN-GUILLOUZO, C. & GRIPON, P. 2001. A short N-proximal region in the large envelope protein harbors a determinant that contributes to the species specificity of human hepatitis B virus. *Journal of virology,* 75**,** 11565-11572.

COLIN, J. F., CAZALS-HATEM, D., LORIOT, M. A., MARTINOT-PEIGNOUX, M., PHAM, B. N., AUPERIN, A., DEGOTT, C., BENHAMOU, J. P., ERLINGER, S. & VALLA, D. 1999. Influence of human immunodeficiency virus infection on chronic hepatitis B in homosexual men. *Hepatology,* 29**,** 1306-1310.

DANE, D., CAMERON, C. & BRIGGS, M. 1970. Virus-like particles in serum of patients with Australia-antigen-associated hepatitis. *The lancet,* 295**,** 695-698.

DAVIS, G. L., DEMPSTER, J., MELER, J. D., ORR, D. W., WALBERG, M. W., BROWN, B., BERGER, B. D., O'CONNOR, J. K. & GOLDSTEIN, R. M. Hepatocellular carcinoma: management of an increasingly common problem. Baylor University Medical Center Proceedings, 2008. Taylor & Francis, 266-280.

EL–SERAG, H. B. & RUDOLPH, K. L. 2007. Hepatocellular carcinoma: epidemiology and molecular carcinogenesis. *Gastroenterology,* 132**,** 2557-2576.

FAN, Y. F., LU, C. C., CHEN, W. C., YAO, W. J., WANG, H. C., CHANG, T. T., LEI, H. Y., SHIAU, A. L. & SU, I. J. 2001. Prevalence and significance of hepatitis B virus (HBV) pre-S mutants in serum and liver at different replicative stages of chronic HBV infection. *Hepatology,* 33**,** 277-286.

FRANÇOIS, G., KEW, M., VAN DAMME, P., MPHAHLELE, M. J. & MEHEUS, A. 2001. Mutant hepatitis B viruses: a matter of academic interest only or a problem with far-reaching implications? *Vaccine,* 19**,** 3799-3815.

GANEM, D. 1991. Assembly of hepadnaviral virions and subviral particles. *Hepadnaviruses.* Springer.

GANEM, D. & VARMUS, H. 1987. The molecular biology of the hepatitis B viruses. *Annual review of biochemistry,* 56**,** 651-693.

GERLICH, W. H. & ROBINSON, W. S. 1980. Hepatitis B virus contains protein attached to the 5′ terminus of its complete DNA strand. *Cell,* 21**,** 801-809.

GOPALAKRISHNAN, D., KEYTER, M., SHENOY, K. T., LEENA, K. B., THAYUMANAVAN, L., THOMAS, V., VINAYAKUMAR, K., PANACKEL, C., KORAH, A. T. & NAIR, R. 2013. Hepatitis B virus subgenotype A1 predominates in liver disease patients from Kerala, India. *World Journal of Gastroenterology: WJG,* 19**,** 9294.

GREENBERG, H. B., POLLARD, R. B., LUTWICK, L. I., GREGORY, P. B., ROBINSON, W. S. & MERIGAN, T. C. 1976. Effect of human leukocyte interferon on hepatitis B virus infection in patients with chronic active hepatitis. *New England Journal of Medicine,* 295**,** 517-522.

GRETHE, S., HECKEL, J.-O., RIETSCHEL, W. & HUFERT, F. T. 2000. Molecular epidemiology of hepatitis B virus variants in nonhuman primates. *Journal of virology,* 74**,** 5377-5381.

GROB, P., JILG, W., BORNHAK, H., GERKEN, G., GERLICH, W., GÜNTHER, S., HESS, G., HÜDIG, H., KITCHEN, A. & MARGOLIS, H. 2000. Serological pattern “anti-HBc alone”: Report on a workshop. *Journal of medical virology,* 62**,** 450-455.

HANNOUN, C., NORDER, H. N. & LINDH, M. 2000. An aberrant genotype revealed in recombinant hepatitis B virus strains from Vietnam. *Journal of General Virology,* 81**,** 2267-2272.

HEERMANN, K., GOLDMANN, U., SCHWARTZ, W., SEYFFARTH, T., BAUMGARTEN, H. & GERLICH, W. 1984. Large surface proteins of hepatitis B virus containing the pre-s sequence. *Journal of virology,* 52**,** 396-402.

HOFER, M., JOLLER-JEMELKA, H., GROB, P., LÜTHY, R., OPRAVIL, M. & STUDY, S. H. C. 1998. Frequent chronic hepatitis B virus infection in HIV-infected patients positive for antibody to hepatitis B core antigen only. *European Journal of Clinical Microbiology and Infectious Diseases,* 17**,** 6-13.

HOU, J., LIU, Z. & GU, F. 2005. Epidemiology and prevention of hepatitis B virus infection. *International journal of medical sciences,* 2**,** 50.

HSIEH, C.-C., TZONOU, A., ZAVITSANOS, X., KAKLAMANI, E., LAN, S.-J. & TRICHOPOULOS, D. 1992. Age at first establishment of chronic hepatitis B virus infection and hepatocellular carcinoma risk: a birth order study. *American journal of epidemiology,* 136**,** 1115-1121.

HSIEH, Y.-H., SU, I.-J., WANG, H.-C., CHANG, W.-W., LEI, H.-Y., LAI, M.-D., CHANG, W.-T. & HUANG, W. 2004. Pre-S mutant surface antigens in chronic hepatitis B virus infection induce oxidative stress and DNA damage. *Carcinogenesis,* 25**,** 2023-2032.

HU, K. Q. 2002. Occult hepatitis B virus infection and its clinical implications. *Journal of viral hepatitis,* 9**,** 243-257.

HUANG, Z. & YEN, T. 1993. Dysregulated surface gene expression from disrupted hepatitis B virus genomes. *Journal of virology,* 67**,** 7032-7040.

HUY, T. T. T., NGOC, T. T. & ABE, K. 2008. New complex recombinant genotype of hepatitis B virus identified in Vietnam. *Journal of virology,* 82**,** 5657-5663.

HWANG, L., LEE, C. & BEASLEY, R. 1991. Five year follow-up of HBV vaccination with plasma-derived vaccine in neonates. Evaluation of immunogenicity and efficacy against perinatal transmission. *Viral hepatitis and liver disease. Baltimore: Williams & Wilkins***,** 759-61.

HYAMS, K. C. 1995. Risks of chronicity following acute hepatitis B virus infection: a review. *Clinical Infectious Diseases,* 20**,** 992-1000.

KEW, M. 1996. Progress towards the comprehensive control of hepatitis B in Africa: a view from South Africa. *Gut,* 38**,** S31-S36.

KEW, M. C. 2013. Epidemiology of hepatocellular carcinoma in sub-Saharan Africa. *Ann Hepatol,* 12**,** 173-82.

KEW, M. C., KRAMVIS, A., YU, M. C., ARAKAWA, K. & HODKINSON, J. 2005. Increased hepatocarcinogenic potential of hepatitis B virus genotype A in Bantu-speaking sub-saharan Africans. *Journal of medical virology,* 75**,** 513-521.

KOURTIS, A. P., BULTERYS, M., HU, D. J. & JAMIESON, D. J. 2012. HIV–HBV coinfection—A global challenge. *New England Journal of Medicine,* 366**,** 1749-1752.

KOZIEL, M. J. & PETERS, M. G. 2007. Viral hepatitis in HIV infection. *New England Journal of Medicine,* 356**,** 1445-1454.

KRAMVIS, A. 2013. Genotypes and genetic variability of hepatitis B virus. *Intervirology,* 57**,** 141-150.

KRAMVIS, A. 2014. Genotypes and genetic variability of hepatitis B virus. *Intervirology,* 57**,** 141-150.

KRAMVIS, A., ARAKAWA, K., YU, M. C., NOGUEIRA, R., STRAM, D. O. & KEW, M. C. 2008. Relationship of serological subtype, basic core promoter and precore mutations to genotypes/subgenotypes of hepatitis B virus. *Journal of medical virology,* 80**,** 27-46.

KRAMVIS, A. & KEW, M. 2005. Relationship of genotypes of hepatitis B virus to mutations, disease progression and response to antiviral therapy. *Journal of viral hepatitis,* 12**,** 456-464.

KRAMVIS, A., KEW, M. & FRANÇOIS, G. 2005. Hepatitis B virus genotypes. *Vaccine,* 23**,** 2409-2423.
KRAMVIS, A. & KEW, M. C. 2007. Epidemiology of hepatitis B virus in Africa, its genotypes and clinical associations of genotypes. *Hepatology research,* 37**,** S9-S19.
KRAMVIS, A. & PARASKEVIS, D. 2013. Subgenotype A1 of HBV–tracing human migrations in and out of Africa. *Antivir Ther,* 18**,** 513-521.
KRAMVIS, A., WEITZMANN, L., OWIREDU, W. K. & KEW, M. C. 2002. Analysis of the complete genome of subgroup A′ hepatitis B virus isolates from South Africa. *Journal of general virology,* 83**,** 835-839.
LAMBERT, C., DÖRING, T. & PRANGE, R. 2007. Hepatitis B virus maturation is sensitive to functional inhibition of ESCRT-III, Vps4, and γ2-adaptin. *Journal of virology,* 81**,** 9050-9060.
LANFORD, R. E., CHAVEZ, D., BRASKY, K. M., BURNS, R. B. & RICO-HESSE, R. 1998. Isolation of a hepadnavirus from the woolly monkey, a New World primate. *Proceedings of the National Academy of Sciences,* 95**,** 5757-5761.
LAURE, F., ZAGURY, D., SAIMOT, A., GALLO, R. C., HAHN, B. & BRECHOT, C. 1985. Hepatitis B virus DNA sequences in lymphoid cells from patients with AIDS and AIDS-related complex. *Science,* 229**,** 561-563.
LAVANCHY, D. 2004. Hepatitis B virus epidemiology, disease burden, treatment, and current and emerging prevention and control measures. *Journal of viral hepatitis,* 11**,** 97-107.
LIANG, T. J. 2009. Hepatitis B: the virus and disease. *Hepatology,* 49.
LIN, C.-M., WANG, G.-M., JOW, G.-M. & CHEN, B.-F. 2012. Functional analysis of hepatitis B virus pre-s deletion variants associated with hepatocellular carcinoma. *J Biomed Sci,* 19**,** 17.
LINDH, M., ANDERSSON, A.-S. & GUSDAL, A. 1997. Genotypes, nt 1858 variants, and geographic origin of hepatitis B virus—large-scale analysis using a new genotyping method. *The Journal of infectious diseases,* 175**,** 1285-1293.
LIU, S., ZHANG, H., GU, C., YIN, J., HE, Y., XIE, J. & CAO, G. 2009. Associations between hepatitis B virus mutations and the risk of hepatocellular carcinoma: a meta-analysis. *Journal of the National Cancer Institute,* 101**,** 1066-1082.
LOCARNINI, S. Molecular virology of hepatitis B virus. Seminars in liver disease, 2004. 3-10.
LÜRMAN, A. 1885. Eine icterusepidemie. *Ber Klin Wochenschr,* 22**,** 20-23.
MACCALLUM, F. 1972. 1971 International Symposium on Viral Hepatitis. Historical perspectives. *Canadian Medical Association Journal,* 106**,** 423.
MAHONEY, F. J. 1999. Update on diagnosis, management, and prevention of hepatitis B virus infection. *Clinical microbiology reviews,* 12**,** 351-366.
MAKONDO, E., BELL, T. G. & KRAMVIS, A. 2012. Genotyping and molecular characterization of hepatitis B virus from human

immunodeficiency virus-infected individuals in southern Africa. *PLoS One,* 7**,** e46345.
MARION, P., SALAZAR, F., ALEXANDER, J. & ROBINSON, W. 1980. State of hepatitis B viral DNA in a human hepatoma cell line. *Journal of virology,* 33**,** 795-806.
MAST, E. E., ALTER, M. J. & MARGOLIS, H. S. 1999. Strategies to prevent and control hepatitis B and C virus infections: a global perspective. *Vaccine,* 17**,** 1730-1733.
MATTHEWS, P. C., GERETTI, A. M., GOULDER, P. J. & KLENERMAN, P. 2014. Epidemiology and impact of HIV coinfection with hepatitis B and hepatitis C viruses in Sub-Saharan Africa. *Journal of clinical virology,* 61**,** 20-33.
MCMAHON, B. J., ALWARD, W. L., HALL, D. B., HEYWARD, W. L., BENDER, T. R., FRANCIS, D. P. & MAYNARD, J. E. 1985. Acute hepatitis B virus infection: relation of age to the clinical expression of disease and subsequent development of the carrier state. *Journal of infectious diseases,* 151**,** 599-603.
MOOLLA, N., KEW, M. & ARBUTHNOT, P. 2002. Regulatory elements of hepatitis B virus transcription. *Journal of viral hepatitis,* 9**,** 323-331.
MPHAHLELE, M. J., LUKHWARENI, A., BURNETT, R. J., MOROPENG, L. M. & NGOBENI, J. M. 2006. High risk of occult hepatitis B virus infection in HIV-positive patients from South Africa. *Journal of clinical virology,* 35**,** 14-20.
NAUMANN, H., SCHAEFER, S., YOSHIDA, C. F. T., GASPAR, A. M. C., REPP, R. & GERLICH, W. H. 1993. Identification of a new hepatitis B virus (HBV) genotype from Brazil that expresses HBV surface antigen subtype adw4. *Journal of General Virology,* 74**,** 1627-1632.
NEURATH, A. R., KENT, S. & STRICK, N. 1984. Location and chemical synthesis of a pre-S gene coded immunodominant epitope of hepatitis B virus. *Science,* 224**,** 392-395.
NORDER, H., COUROUCÉ, A.-M., COURSAGET, P., ECHEVARRIA, J. M., LEE, S.-D., MUSHAHWAR, I. K., ROBERTSON, B. H., LOCARNINI, S. & MAGNIUS, L. O. 2004. Genetic diversity of hepatitis B virus strains derived worldwide: genotypes, subgenotypes, and HBsAg subtypes. *Intervirology,* 47**,** 289-309.
NORDER, H., COUROUCÉ, A.-M. & MAGNIUS, L. O. 1994. Complete genomes, phylogenetic relatedness, and structural proteins of six strains of the hepatitis B virus, four of which represent two new genotypes. *Virology,* 198**,** 489-503.
NORDER, H., EBERT, J. W., FIELDS, H. A., MUSHAHWAR, I. K. & MAGNIUS, L. O. 1996. Complete sequencing of a gibbon hepatitis B virus genome reveals a unique genotype distantly related to the chimpanzee hepatitis B virus. *Virology,* 218**,** 214-223.
NORDER, H., HAMMAS, B., LEE, S.-D., BILE, K., COUROUCÉ, A.-M., MUSHAHWAR, I. K. & MAGNIUS, L. O. 1993. Genetic relatedness of hepatitis B viral strains of diverse geographical origin and natural variations in the primary structure of the surface antigen. *Journal of General Virology,* 74**,** 1341-1348.

NORDER, H., HAMMAS, B., LÖFDAHL, S., COUROUCÉ, A.-M. & MAGNIUS, L. O. 1992. Comparison of the amino acid sequences of nine different serotypes of hepatitis B surface antigen and genomic classification of the corresponding hepatitis B virus strains. *Journal of General Virology,* 73**,** 1201-1208.

OCHWOTO, M., CHAUHAN, R., GOPALAKRISHNAN, D., CHEN, C.-Y., OKOTH, F., KIOKO, H., KIMOTHO, J., KAIGURI, P. & KRAMVIS, A. 2013. Genotyping and molecular characterization of hepatitis B virus in liver disease patients in Kenya. *Infection, Genetics and Evolution,* 20**,** 103-110.

OKAMOTO, H., TSUDA, F., SAKUGAWA, H., SASTROSOEWIGNJO, R. I., IMAI, M., MIYAKAWA, Y. & MAYUMI, M. 1988. Typing hepatitis B virus by homology in nucleotide sequence: comparison of surface antigen subtypes. *J Gen Virol,* 69**,** 2575-2583.

OLINGER, C. M., JUTAVIJITTUM, P., HÜBSCHEN, J. M., YOUSUKH, A., SAMOUNTRY, B., THAMMAVONG, T., TORIYAMA, K. & MULLER, C. P. 2008. Possible new hepatitis B virus genotype, southeast Asia. *Emerging infectious diseases,* 14**,** 1777.

POLLACK, J. R. & GANEM, D. 1994. Site-specific RNA binding by a hepatitis B virus reverse transcriptase initiates two distinct reactions: RNA packaging and DNA synthesis. *Journal of virology,* 68**,** 5579-5587.

POLLICINO, T., CACCIOLA, I., SAFFIOTI, F. & RAIMONDO, G. 2014. Hepatitis B virus PreS/S gene variants: Pathobiology and clinical implications. *Journal of hepatology,* 61**,** 408-417.

POLLICINO, T., CAMPO, S. & RAIMONDO, G. 1995. PreS and core gene heterogeneity in hepatitis B virus (HBV) genomes isolated from patients with long-lasting HBV chronic infection. *Virology,* 208**,** 672-677.

POLLICINO, T., ZANETTI, A. R., CACCIOLA, I., PETIT, M. A., SMEDILE, A., CAMPO, S., SAGLIOCCA, L., PASQUALI, M., TANZI, E. & LONGO, G. 1997. Pre-S2 defective hepatitis B virus infection in patients with fulminant hepatitis. *Hepatology,* 26**,** 495-499.

POWNALL, B. 1999. Genomes. *Heredity,* 83**,** 500.

PRINCE, A. 1968. Relation of Australia and SH antigens. *The Lancet,* 292**,** 462-463.

PRINCE, A., HARGROVE, R., SZMUNESS, W., CHERUBIN, C., FONTANA, V. & JEFFRIES, G. 1970. Immunologic distinction between infectious and serum hepatitis. *New England Journal of Medicine,* 282**,** 987-991.

QU, L.-S., LIU, J.-X., LIU, T.-T., SHEN, X.-Z., CHEN, T.-Y., NI, Z.-P. & LU, C.-H. 2014. Association of hepatitis B virus pre-s deletions with the development of hepatocellular carcinoma in qidong, china. *PloS one,* 9**,** e98257.

RAIMONDO, G., ALLAIN, J.-P., BRUNETTO, M. R., BUENDIA, M.-A., CHEN, D.-S., COLOMBO, M., CRAXÌ, A., DONATO, F., FERRARI, C. & GAETA, G. B. 2008. Statements from the Taormina expert

meeting on occult hepatitis B virus infection. *Journal of hepatology,* 49**,** 652-657.

SADEGHI, A., SHIRVANI-DASTGERDI, E., TACKE, F., YAGMUR, E., POORTAHMASEBI, V., POOREBRAHIM, M., MOHRAZ, M., HAJABDOLBAGHI, M., RASOOLINEJAD, M. & ABBASIAN, L. 2017. HBsAg mutations related to occult hepatitis B virus infection in HIV-positive patients result in a reduced secretion and conformational changes of HBsAg. *Journal of medical virology,* 89**,** 246-256.

SAKUGAWA, H., NAKASONE, H., NAKAYOSHI, T., ORITO, E., MIZOKAMI, M., YAMASHIRO, T., MAESHIRO, T., KINJO, F., SAITO, A. & MIYAGI, Y. 2002. Preponderance of hepatitis B virus genotype B contributes to a better prognosis of chronic HBV infection in Okinawa, Japan. *Journal of medical virology,* 67**,** 484-489.

SEEFF, L. B., BEEBE, G. W., HOOFNAGLE, J. H., NORMAN, J. E., BUSKELL-BALES, Z., WAGGONER, J. G., KAPLOWITZ, N., KOFF, R. S., PETRINI JR, J. L. & SCHIFF, E. R. 1987. A serologic follow-up of the 1942 epidemic of post-vaccination hepatitis in the United States Army. *New England Journal of Medicine,* 316**,** 965-970.

SEEGER, C., GANEM, D. & VARMUS, H. E. 1986. Biochemical and genetic evidence for the hepatitis B virus replication strategy. *Science,* 232**,** 477-484.

SEEGER, C. & MASON, W. S. 2000. Hepatitis B virus biology. *Microbiology and molecular biology reviews,* 64**,** 51-68.

SKELTON, M., KEW, M. C. & KRAMVIS, A. 2012. Distinct mutant hepatitis B virus genomes, with alterations in all four open reading frames, in a single South African hepatocellular carcinoma patient. *Virus research,* 163**,** 59-65.

SNOWBERGER, N., CHINNAKOTLA, S., LEPE, R., PEATTIE, J., GOLDSTEIN, R., KLINTMALM, G. & DAVIS, G. 2007. Alpha fetoprotein, ultrasound, computerized tomography and magnetic resonance imaging for detection of hepatocellular carcinoma in patients with advanced cirrhosis. *Alimentary pharmacology & therapeutics,* 26**,** 1187-1194.

STUYVER, L., DE GENDT, S., VAN GEYT, C., ZOULIM, F., FRIED, M., SCHINAZI, R. F. & ROSSAU, R. 2000. A new genotype of hepatitis B virus: complete genome and phylogenetic relatedness. *Journal of general virology,* 81**,** 67-74.

SU, T.-S., LAI, C.-J., HUANG, J., LIN, L.-H., YAUK, Y., CHANG, C., LO, S. & HAN, S. 1989. Hepatitis B virus transcript produced by RNA splicing. *Journal of virology,* 63**,** 4011-4018.

SUMMERS, J., O'CONNELL, A. & MILLMAN, I. 1975. Genome of hepatitis B virus: restriction enzyme cleavage and structure of DNA extracted from Dane particles. *Proceedings of the National Academy of Sciences,* 72**,** 4597-4601.

SUMMERS, J., SMOLEC, J. M. & SNYDER, R. 1978. A virus similar to human hepatitis B virus associated with hepatitis and hepatoma in woodchucks. *Proceedings of the National Academy of Sciences,* 75**,** 4533-4537.

SUNBUL, M. 2014. Hepatitis B virus genotypes: global distribution and clinical importance. *World journal of gastroenterology: WJG,* 20**,** 5427.

SUNG, J., TSOI, K., WONG, V., LI, K. & CHAN, H. 2008. Meta-analysis: treatment of hepatitis B infection reduces risk of hepatocellular carcinoma. *Alimentary pharmacology & therapeutics,* 28**,** 1067-1077.

TANAKA, Y., MUKAIDE, M., ORITO, E., YUEN, M.-F., ITO, K., KURBANOV, F., SUGAUCHI, F., ASAHINA, Y., IZUMI, N. & KATO, M. 2006. Specific mutations in enhancer II/core promoter of hepatitis B virus subgenotypes C1/C2 increase the risk of hepatocellular carcinoma. *Journal of hepatology,* 45**,** 646-653.

TATEMATSU, K., TANAKA, Y., KURBANOV, F., SUGAUCHI, F., MANO, S., MAESHIRO, T., NAKAYOSHI, T., WAKUTA, M., MIYAKAWA, Y. & MIZOKAMI, M. 2009. A genetic variant of hepatitis B virus divergent from known human and ape genotypes isolated from a Japanese patient and provisionally assigned to new genotype J. *Journal of virology,* 83**,** 10538-10547.

TESTUT, P., RENARD, C.-A., TERRADILLOS, O., VITVITSKI-TREPO, L., TEKAIA, F., DEGOTT, C., BLAKE, J., BOYER, B. & BUENDIA, M. A. 1996. A new hepadnavirus endemic in arctic ground squirrels in Alaska. *Journal of virology,* 70**,** 4210-4219.

THIO, C. L. 2009. Hepatitis B and human immunodeficiency virus coinfection. *Hepatology,* 49.

TIOLLAIS, P., POURCEL, C. & DEJEAN, A. 1985. The hepatitis B virus. *Nature,* 317**,** 489.

TORBENSON, M. & THOMAS, D. L. 2002. Occult hepatitis B. *The Lancet infectious diseases,* 2**,** 479-486.

TUTTLEMAN, J. S., POURCEL, C. & SUMMERS, J. 1986. Formation of the pool of covalently closed circular viral DNA in hepadnavirus-infected cells. *Cell,* 47**,** 451-460.

UTAMA, A., SIBURIAN, M. D., FANANY, I., INTAN, M. D. B., DHENNI, R., KURNIASIH, T. S., LELOSUTAN, S. A., ACHWAN, W. A., LUKITO, B. & YUSUF, I. 2011. Low prevalence of hepatitis B virus pre-s deletion mutation in Indonesia. *Journal of medical virology,* 83**,** 1717-1726.

VAUDIN, M., WOLSTENHOLME, A. J., TSIQUAYE, K. N., ZUCKERMAN, A. J. & HARRISON, T. J. 1988. The complete nucleotide sequence of the genome of a hepatitis B virus isolated from a naturally infected chimpanzee. *Journal of General Virology,* 69**,** 1383-1389.

VERMEULEN, M., DICKENS, C., LELIE, N., WALKER, E., COLEMAN, C., KEYTER, M., REDDY, R., CROOKES, R. & KRAMVIS, A. 2012. Hepatitis B virus transmission by blood transfusion during 4 years of

individual-donation nucleic acid testing in South Africa: estimated and observed window period risk. *Transfusion,* 52**,** 880-892.

WANG, G. & SEEGER, C. 1993. Novel mechanism for reverse transcription in hepatitis B viruses. *Journal of virology,* 67**,** 6507-6512.

WANG, H.-C., WU, H.-C., CHEN, C.-F., FAUSTO, N., LEI, H.-Y. & SU, I.-J. 2003. Different types of ground glass hepatocytes in chronic hepatitis B virus infection contain specific pre-S mutants that may induce endoplasmic reticulum stress. *The American journal of pathology,* 163**,** 2441-2449.

WARREN, K. S., HEENEY, J. L., SWAN, R. A. & VERSCHOOR, E. J. 1999. A new group of hepadnaviruses naturally infecting orangutans (Pongo pygmaeus). *Journal of virology,* 73**,** 7860-7865.

WATANABE, T., SORENSEN, E. M., NAITO, A., SCHOTT, M., KIM, S. & AHLQUIST, P. 2007. Involvement of host cellular multivesicular body functions in hepatitis B virus budding. *Proceedings of the National Academy of Sciences,* 104**,** 10205-10210.

WHITE, D. L., KANWAL, F., JIAO, L. & EL-SERAG, H. B. 2016. Epidemiology of hepatocellular carcinoma. *Hepatocellular Carcinoma.* Springer.

WILL, H., REISER, W., WEIMER, T., PFAFF, E., BÜSCHER, M., SPRENGEL, R., CATTANEO, R. & SCHALLER, H. 1987. Replication strategy of human hepatitis B virus. *Journal of Virology,* 61**,** 904-911.

XU, Z., JENSEN, G. & YEN, T. 1997. Activation of hepatitis B virus S promoter by the viral large surface protein via induction of stress in the endoplasmic reticulum. *Journal of virology,* 71**,** 7387-7392.

YAN, H., ZHONG, G., XU, G., HE, W., JING, Z., GAO, Z., HUANG, Y., QI, Y., PENG, B. & WANG, H. 2012. Sodium taurocholate cotransporting polypeptide is a functional receptor for human hepatitis B and D virus. *elife,* 1.

YEN, C. J., AI, Y. L., TSAI, H. W., CHAN, S. H., YEN, C. S., CHENG, K. H., LEE, Y. P., KAO, C. W., WANG, Y. C. & CHEN, Y. L. 2018. Hepatitis B virus surface gene pre-S2 mutant as a high-risk serum marker for hepatoma recurrence after curative hepatic resection. *Hepatology*.

YEUNG, P., WONG, D. K.-H., LAI, C.-L., FUNG, J., SETO, W.-K. & YUEN, M.-F. 2011. Association of hepatitis B virus pre-S deletions with the development of hepatocellular carcinoma in chronic hepatitis B. *Journal of Infectious Diseases,* 203**,** 646-654.

YU, H., YUAN, Q., GE, S.-X., WANG, H.-Y., ZHANG, Y.-L., CHEN, Q.-R., ZHANG, J., CHEN, P.-J. & XIA, N.-S. 2010. Molecular and phylogenetic analyses suggest an additional hepatitis B virus genotype “I”. *PloS one,* 5**,** e9297.

ZHANG, Y.-Y., ZHANG, B.-H., THEELE, D., LITWIN, S., TOLL, E. & SUMMERS, J. 2003. Single-cell analysis of covalently closed circular DNA copy numbers in a hepadnavirus-infected liver.

Proceedings of the National Academy of Sciences, 100**,** 12372-12377.

Reference link:

WORLD HEALTH ORGANIZATION. Guidelines for the prevention, care and treatment of persons with chronic hepatitis B infection. 2015. (http://www.who.int/hiv/pub/hepatitis/hepatitis-b-guidelines/en/)